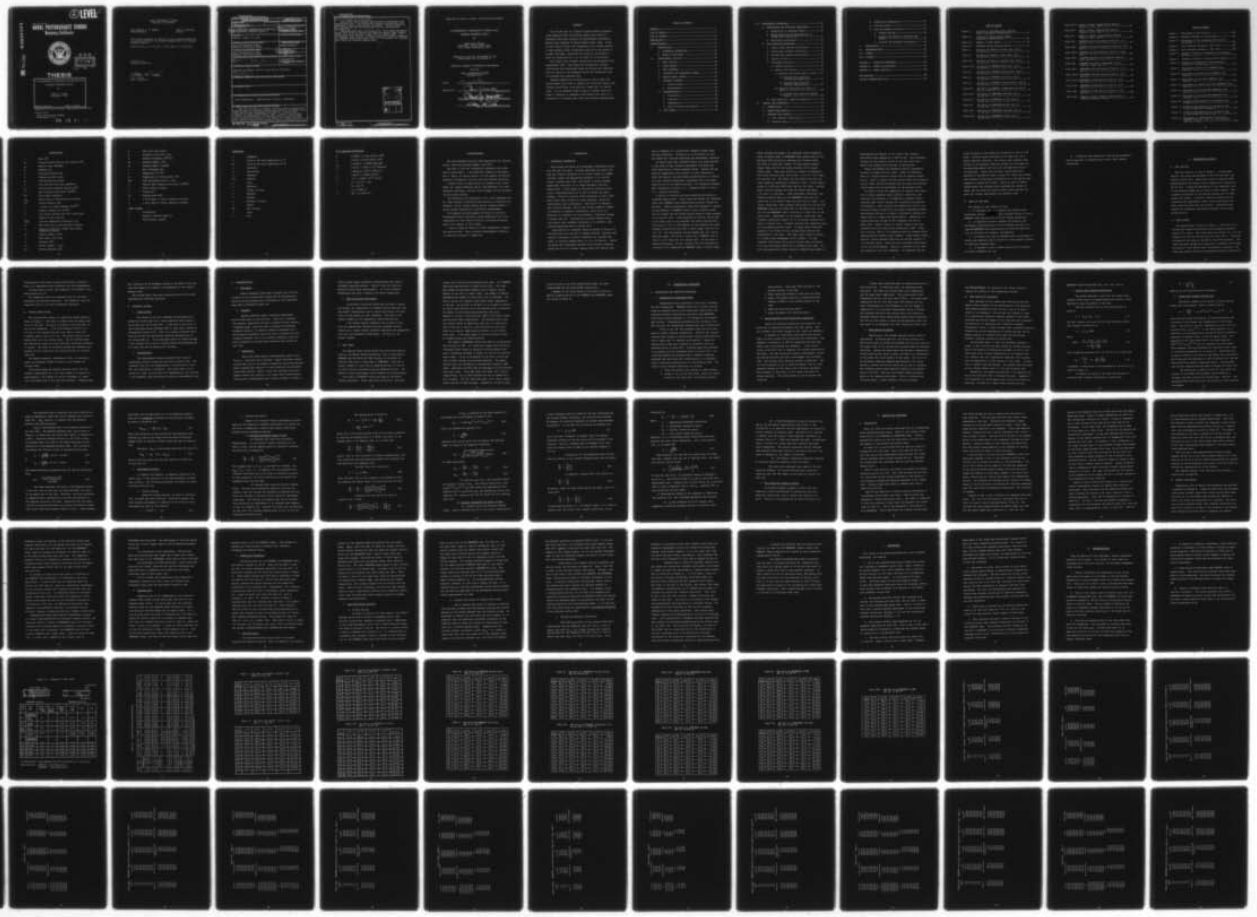
AD-A062 204 NAVAL POSTGRADUATE SCHOOL MONTEREY CALIF F/G 13/11
AN EXPERIMENTAL COMPARISON OF ENHANCED HEAT TRANSFER CONDENSER --ETC(U)
SEP 78 J H FENNER
UNCLASSIFIED NPS69-78-015 NL

1 OF 2
AD A062204



(2) LEVEL II

AD A062204

DDC FILE COPY

NPS 69-78-015

NAVAL POSTGRADUATE SCHOOL

Monterey, California



DDC
RECEIVED
DEC 18 1978
B

THESIS

AN EXPERIMENTAL COMPARISON OF ENHANCED HEAT TRANSFER CONDENSER TUBING

by

James H. Fenner
September 1978

Thesis Advisor: Paul J. Marto

Approved for public release; distribution unlimited.

Prepared for:

Naval Sea Systems Command
Washington, D. C.

78 12 11 187

NAVAL POSTGRADUATE SCHOOL
Monterey, California

Rear Admiral T. F. Dedman
Superintendent

Jack R. Borsting
Provost

This thesis prepared in conjunction with research supported in part by the Naval Sea Systems Command under work request N0002477-WR74134.

Reproduction of all or part of this report is authorized.

Released as a
Technical Report by:

William M. Tolles

W. M. Tolles
Dean of Research

UNCLASSIFIED

SECURITY CLASSIFICATION OF THIS PAGE (When Data Entered)

REPORT DOCUMENTATION PAGE	READ INSTRUCTIONS BEFORE COMPLETING FORM
1. REPORT NUMBER (14) NPS 69-78-015 / 2. GOVT ACCESSION NO.	3. RECIPIENT'S CATALOG NUMBER
4. TITLE (and Subtitle) (6) AN EXPERIMENTAL COMPARISON OF ENHANCED HEAT TRANSFER CONDENSER TUBING	5. TYPE OF REPORT & PERIOD COVERED (9) Master's Thesis, September 1978
	6. PERFORMING ORG. REPORT NUMBER
7. AUTHOR(s) James H. Fenner, LT, USN	8. CONTRACT OR GRANT NUMBER(s)
9. PERFORMING ORGANIZATION NAME AND ADDRESS Naval Postgraduate School Monterey, California 93940	10. PROGRAM ELEMENT, PROJECT, TASK AREA & WORK UNIT NUMBERS N0002477-WR74134
11. CONTROLLING OFFICE NAME AND ADDRESS (11) Naval Postgraduate School Monterey, California 93940	12. REPORT DATE September 1978
	13. NUMBER OF PAGES 177
14. MONITORING AGENCY NAME & ADDRESS(if different from Controlling Office) (10) James Henry / Fenner	15. SECURITY CLASS. (of this report) UNCLASSIFIED
	15a. DECLASSIFICATION/DOWNGRADING SCHEDULE

16. DISTRIBUTION STATEMENT (of this Report)

Approved for public release; distribution unlimited.

(12) 178 p.

17. DISTRIBUTION STATEMENT (of the abstract entered in Block 20, if different from Report)

18. SUPPLEMENTARY NOTES

19. KEY WORDS (Continue on reverse side if necessary and identify by block number)

Film Condensation, Enhanced Heat Transfer, Condensers

20. ABSTRACT (Continue on reverse side if necessary and identify by block number)

Ten 15.9 mm (5/8 in.) nominal outside diameter geometrically enhanced tubes of different metals were tested to determine their heat transfer and hydrodynamic performance. Results were compared to smooth copper-nickel tubes. Steam at about 21kPa (3 psia) was condensed on the outside surface of each enhanced tube, horizontally mounted in the center of a dummy tube bank. Each tube was cooled on the inside by water at velocities of

DD FORM 1 JAN 73 1473 EDITION OF 1 NOV 68 IS OBSOLETE S/N 0102-014-6601

78 12 1

UNCLASSIFIED

SECURITY CLASSIFICATION OF THIS PAGE (When Data Entered)

2.7 to 7.6 m/sec (3 to 25 ft/sec).

The overall heat transfer coefficient was determined from experimental data. The inside heat transfer coefficients were determined using the Wilson plot technique. Friction factor in the enhanced section was determined from the cooling water pressure drop.

Enhanced geometries (utilizing pitch, helix angle and groove depth) were found to improve the corrected overall heat transfer coefficient by as much as 2 times that for smooth tubes. Use of enhanced tubes in place of smooth tubes will permit a decrease in condenser tube surface area from 17 to 53 percent for constant heat loads and constant pumping power.

ACCESSION for
NTIS White Section ☑
DDC Buff Section ☐
UNANNOUNCED ☐
JUSTIFICATION
BY
DISTRIBUTION/AVAILABILITY CODES
Dist. AVAIL. and/or SPECIAL
A

Approved for public release; distribution unlimited

AN EXPERIMENTAL COMPARISON OF ENHANCED HEAT TRANSFER CONDENSER TUBING

by

James Henry Fenner
Lieutenant, United States Navy
B.S., Miami University, 1973

Submitted in partial fulfillment of the
requirements for the degree of

MASTER OF SCIENCE IN MECHANICAL ENGINEERING

from the

NAVAL POSTGRADUATE SCHOOL
September 1978

Author James H. Fenner

Approved by: Paul J. Marto
Thesis Advisor

Paul J. Marto
Chairman, Department of Mechanical Engineering

William M. Tolles
Dean of Science and Engineering

ABSTRACT

Ten 15.9 mm (5/8 in.) nominal outside diameter geometrically enhanced tubes of different metals were tested to determine their heat transfer and hydrodynamic performance. Results were compared to smooth copper-nickel tubes. Steam at about 21kPa (3 psia) was condensed on the outside surface of each enhanced tube, horizontally mounted in the center of a dummy tube bank. Each tube was cooled on the inside by water at velocities of 2.7 to 7.6 m/sec (3 to 25 ft/sec).

The overall heat transfer coefficient was determined from experimental data. The inside and outside heat transfer coefficients were determined using the Wilson plot technique. Friction factor in the enhanced section was determined from the cooling water pressure drop.

Enhanced geometries (utilizing pitch, helix angle and groove depth) were found to improve the corrected overall heat transfer coefficient by as much as 2 times that for smooth tubes. Use of enhanced tubes in place of smooth tubes will permit a decrease in condenser tube surface area from 17 to 53 percent for constant heat loads and constant pumping power.

TABLE OF CONTENTS

ABSTRACT---------- 4

LIST OF TABLES---------- 8

LIST OF FIGURES----------10

NOMENCLATURE----------13

ACKNOWLEDGEMENT----------17

I. INTRODUCTION----------18

A. BACKGROUND INFORMATION----------18

B. GOALS OF THIS WORK----------22

II. EXPERIMENTAL FACILITY----------24

A. TEST FACILITY----------24

B. STEAM SYSTEM----------24

C. TEST CONDENSER----------25

D. CONDENSATE AND FEEDWATER SYSTEMS----------26

E. COOLING WATER SYSTEM----------27

F. SECONDARY SYSTEMS----------28

1. Vacuum System----------28

2. Desuperheater----------28

G. INSTRUMENTATION----------29

1. Flow Rates----------29

2. Pressure----------29

3. Temperature----------29

4. Data Collection and Display----------30

H. TEST TUBES----------30

III. EXPERIMENTAL PROCEDURES---------- 33

A. INSTALLATION AND OPERATION PROCEDURES---------- 33

1. Preparation of Condenser Tubes---------- 33

2. System Operation and Determination of Steady State Conditions---------- 34

3. Maintenance Procedures---------- 35

B. DATA REDUCTION PROCEDURES---------- 36

1. Overall Heat Transfer Coefficient---------- 37

2. Inside Heat Transfer Coefficient---------- 38

3. Outside Heat Transfer Coefficient---------- 40

4. Friction Factor---------- 40

5. Performance Criteria---------- 42

a. Colburn Analogy---------- 42

b. Surface Area Ratios---------- 43

(1) External Resistance Equal to Zero.--- 43

(a) Constant Heat Load with Increasing Pumping Power.-------- 43

(b) Constant Heat Load with Constant Pumping Power.---------- 43

(2) External Resistance Not Equal to Zero.---------- 45

(a) Constant Heat Load and Pumping Power---------- 45

6. Data Reduction Computer Program---------- 48

IV. RESULTS AND DISCUSSION---------- 49

A. INTRODUCTION---------- 49

B. SMOOTH TUBE RESULTS---------- 52

C. ENHANCED TUBE RESULTS---------- 54

1. Heat Transfer Coefficient---------- 54

2. Pressure Drop---------- 56

3. Sieder-Tate Parameters---------- 57

4. Friction Factor---------- 57

5. Tube Performance Criteria---------- 58

a. Colburn Analogy---------- 58

b. Surface Area Ratios at Constant Heat Loads---------- 59

c. Internal and External Performance------- 60

V. CONCLUSIONS---------- 63

VI. RECOMMENDATIONS---------- 65

VII. TABLES---------- 67

VIII. FIGURES----------105

APPENDIX A: OPERATING PROCEDURES---------- 146

APPENDIX B: SAMPLE CALCULATIONS---------- 154

APPENDIX C: ERROR ANALYSIS---------- 162

BIBLIOGRAPHY---------- 172

INITIAL DISTRIBUTION LIST---------- 174

LIST OF TABLES

Table I. Location of Stainless Steel Sheathed Copper Constantan Thermocouples---------- 67

Table II. Location of Teflon Coated Copper Constantan Thermocouples---------- 68

Table III. Summary of Test Tubes---------- 69

Table IV. Enhanced Tubing Characteristics---------- 70

Table V. Raw Data for Smooth "fouled" CuNi, Run 2, 11 MAY 78---------- 71

Table VI. Raw Data for Smooth "clean" CuNi, Run 7, 11 JUL 78---------- 71

Table VII. Raw Data for Smooth "rippled" CuNi, Run 8, 12 JUL 78---------- 72

Table VIII. Raw Data for TURBOTEC High Pitch, Run 4, 12 JUN 78---------- 72

Table IX. Raw Data for TURBOTEC Medium Pitch, Run 5, 13 JUN 78---------- 73

Table X. Raw Data for TURBOTEC Low Pitch, Run 6, 14 JUN 78---------- 73

Table XI. Raw Data for TURBOTEC Variable Pitch, Run 15, 28 JUL 78---------- 74

Table XII. Raw Data for TURBOTEC "supported" Low Pitch, Run 17, 6 AUG 78---------- 74

Table XIII. Raw Data for KORODENSE CuNi-LPD, Run 9, 13 JUL 78---------- 75

Table XIV. Raw Data for KORODENSE Aℓ-LPD, Run 13, 18 JUL 78---------- 75

Table XV. Raw Data for KORODENSE Aℓ-MHT, Run 11, 16 JUL 78---------- 76

Table XVI. Raw Data for KORODENSE CuNi-MHT, Run 12, 17 JUL 78---------- 76

Table XVII. Raw Data for KORODENSE Ti-MHT, Run 14, 19 JUL 78---------- 77

Table XVIII. Smooth "fouled" Copper-Nickel Results, (Tube No. S-1a), Run 2---------- 78

Table XIX. Smooth "Clean" Copper-Nickel Results, (Tube No. S-1b), Run 7---------- 80

Table XX. Smooth "rippled" Copper-Nickel Results, (Tube No. S-2), Run 8---------- 82

Table XXI. TURBOTEC High Pitch Results (Tube No. T-1) Run 4---------- 84

Table XXII. TURBOTEC Medium Pitch Results (Tube No. T-2) Run 5---------- 86

Table XXIII. TURBOTEC Low Pitch Results (Tube No. T-3a) Run 6---------- 88

Table XXIV. TURBOTEC Variable Pitch Results (Tube No. T-4), Run 15---------- 90

Table XXV. TURBOTEC Low Pitch "supported" Results (Tube No. T-3b), Run 17---------- 92

Table XXVI. KORODENSE CuNi-LPD Results (Tube No. K-1) Run 9---------- 94

Table XXVII. KORODENSE CuNi-MHT Results (Tube No. K-2) Run 12---------- 96

Table XXVIII. KORODENSE Aℓ-LPD Results (Tube No. K-3) Run 13---------- 98

Table XXIX. KORODENSE Aℓ-MHT Results (Tube No. K-4) Run 11----------100

Table XXX. KORODENSE Ti-MHT Results (Tube No. K-5) Run 14----------102

Table XXXI. Summary of Heat Transfer Capabilities of Enhanced Condenser Tubing----------104

LIST OF FIGURES

Figure 1. Photograph of Test Facility----------105

Figure 2. Schematic Diagram of Steam System----------106

Figure 3. Photograph of Test Condenser with Partial Insulation----------107

Figure 4. Test Condenser Schematic, Front View----------108

Figure 5. Test Condenser Schematic, Side View----------109

Figure 6. Schematic Diagram of Condensate and Feedwater System----------110

Figure 7. Schematic Diagram of Cooling Water System------111

Figure 8. Enhanced Tube Schematic Drawing Showing Location of Pressure Taps----------112

Figure 9. Photograph of High Pitch TURBOTEC Tube (Tube No. T-1)----------113

Figure 10. Photograph of Medium Pitch TURBOTEC Tube (Tube No. T-2)----------114

Figure 11. Photograph of Low Pitch TURBOTEC Tube (Tube No. T-3)----------115

Figure 12. Photograph of Copper-Nickel-MHT KORODENSE Tube (Tube No. K-2)----------116

Figure 13. Photograph of Aluminum-MHT KORODENSE Tube (Tube No. K-4)----------117

Figure 14. Photograph of Titanium-MHT KORODENSE Tube (Tube No. K-5)----------118

Figure 15. Schematic Representation of Procedure Used to Find U_n----------119

Figure 16. Schematic Representation of Procedure Used to Find Sieder-Tate Parameter----------120

Figure 17. Schematic Representation of Procedure Used to Find Sieder-Tate Coefficient C_i, h_i and h_o--121

Figure 18. Photograph of Condensation on Low Pitch TURBOTEC Tube (No. T-3a) at a Cooling Water Velocity of 3m/s----------122

Figure 19. Photograph of Condensation on Low Pitch TURBOTEC Tube (No. T-3a) Showing Effect of Tube Vibration at a Cooling Water Velocity of 4m/s----------123

Figure 20. Corrected Overall Heat Transfer Coefficient Versus Cooling Water Mass Flow Rate for Smooth Tubes----------124

Figure 21. Corrected Pressure Drop Versus Cooling Water Mass Flow Rate for Smooth Tubes----------125

Figure 22. Wilson Plot for Smooth Tubes----------126

Figure 23. Inside Nusselt Number Correlation Versus Reynolds Number for Smooth Tubes----------127

Figure 24. Fanning Friction Factor Versus Reynolds Number for Smooth Tubes----------128

Figure 25. Tube Performance Factor, 2j/f, Versus Reynolds Number for Smooth Tubes----------129

Figure 26. Corrected Overall Heat Transfer Coefficient, U_c, Versus Cooling Water Mass Flow Rate for TURBOTEC Tubes----------130

Figure 27. Corrected Overall Heat Transfer Coefficient, U_c, Versus Cooling Water Mass Flow Rate for KORODENSE Tubes----------131

Figure 28. Uncorrected Overall Heat Transfer Coefficient, U_n, Versus Cooling Water Velocity for Tube K-5 Compared with Data of Cunningham and Milne [26]----------132

Figure 29. Corrected Pressure Drop Versus Cooling Water Mass Flow Rate for TURBOTEC Tubes----------133

Figure 30. Corrected Pressure Drop Versus Cooling Water Mass Flow Rate for KORODENSE Tubes----------134

Figure 31. Wilson Plot for TURBOTEC Tubes----------135

Figure 32. Wilson Plot for KORODENSE Tubes----------136

Figure 33. Inside Nusselt Number Correlation Versus Reynolds Number for TURBOTEC Tubes----------137

Figure 34. Inside Nusselt Number Correlation Versus Reynolds Number for KORODENSE Tubes----------138

Figure 35. Fanning Friction Factor versus Reynolds Number for TURBOTEC Tubes----------139

Figure 36. Fanning Friction Factor Versus Reynolds Number for KORODENSE Tubes----------140

Figure 37. Tube Performance Factor, 2j/f, Versus Reynolds Number for TURBOTEC Tubes----------141

Figure 38. Tube Performance Factor, 2j/f, Versus Reynolds Number for KORODENSE Tubes----------142

Figure 39. Augmented to Smooth Tube Surface Area Ratio ($R_{ext} = 0$) Versus Reynolds Number----------143

Figure 40. Augmented to Smooth Tube Surface Area Ratio ($R_{ext} \neq 0$) Versus Reynolds Number----------144

Figure 41. Comparative Effect of Tube Pitch (Helix Angle) on Both Inside and Outside Heat Transfer Coefficients (for Constant Groove Depth)----------145

NOMENCLATURE

A	Area (m^2)
Ac	Cross sectional area of test section (m^2)
c_p	Specific heat (kJ/kg^oC)
D	Diameter (m)
e	Tube groove depth (mm)
f	Fanning friction factor
Fc	Flow calibration factor
G	Flow rate per unit area (kg/m^2sec)
g_c	Gravitational constant ($kg\ m/N\ sec^2$)
h	Heat transfer coefficient ($W/m^{2o}C$)
HA	Helix Angle (degrees)
h_{fg}	Latent heat of vaporization (W sec/kg)
ID	Inside diameter (mm)
j	j factor in Colburn Analogy ($StPr^{2/3}$)
k	Thermal conductivity (W/m^oC)
K	Flow abrupt entrance and exit coefficient
L	Length of test tube (m)
LMTD	Log mean temperature difference (^oC)
$\dot{m}$	Mass flow rate of cooling water (kg/sec)
M	Slope of Wilson Plot output from linear regression program
Nu	Nusselt number = hD/k
p	Tube spiral pitch (mm)
P	Pressure (kPa)
Pr	Prandtl number = $\mu c_p/k$
Pw	Wetted perimeter (mm)

Q	Heat flow rate (W/sec)
$\dot{Q}$	Volumetric flow rate (ℓ/m)
R	Thermal resistance ($m^{2o}C/W$)
Re	Reynolds number = DG/μ
St	Stanton number = Nu/RePr
t	Wall thickness (mm)
T	Temperature ($^oC, ^oK$)
Tc	Temperature of cooling water (^oC)
TPF	Tube performance factor = 2j/f
U	Overall heat transfer coefficient ($W/m^{2o}C$)
v	Water velocity (m/sec)
V	Volume (m^3)
Wp	Pumping power (kW)
X	x axis input to linear regression program
Y	y axis input to linear regression program

GREEK SYMBOLS

Δ	Differential
μ	Dynamic viscosity (kg/m hr)
ρ	Fluid density (kg/m^3)

Subscripts

a	Augmented
b	Fluid at the bulk temperature in ^{o}C
br	Fluid at the bulk temperature in ^{o}K
c	Corrected
cn	Contraction
e	Expansion
ext	External
f	Film
h	Hydraulic
i	Inside, or inlet
m	Measured
n	Nominal
o	Outside, or outlet
s	Smooth
TS	Test section
v	vapor
w	wall

SI to English Conversions

h	1 $W/m^{2o}C$ = 0.1761 $BTU/hr\ ft^{2o}F$
k	1 $W/m^{o}C$ = 0.5778 $BTU/hr\ ft^{o}F$
c_p	1 $kJ/kg^{o}C$ = 0.23884 $BTU/lbm^{o}F$
Q	1 W/sec = 9.4781 x 10^{-4} BTU/sec^2
μ	1 kg/m hr = 2419.2 lbm/ft hr
ρ	1 kg/m^3 = 0.06243 lbm/ft^3
P	Pa = 1.45038 x 10^{-4} lbf/in^2
T	$^{o}C = 5/9\ (^{o}F - 32)$
	$^{o}K = 5/9\ ^{o}R$
L	1 m = 3.2808 ft
A	1 m^2 = 10.7639 ft^2

ACKNOWLEDGEMENT

The work presented here has been supported by Mr. Charles Miller, Naval Sea Systems Command, Code 0331.

Any work of this sort necessarily represents the influence of many people. I am especially indebted to Professor Paul J. Marto, my thesis advisor, for his support and patient guidance in helping me overcome even the smallest obstacles.

A special note of appreciation is extended to Mr. James Selby, Mr. Thomas Christian and Mr. Ken Mothersell for their technical assistance, and Mrs. Marty Delgado for her deciphering and typing talents.

The assistance and cooperation of Mr. Bruce Henderson and Mr. James Withers of Wolverine Tube Division of Universal Oil Products, and Mr. Robert Perkins and Mr. Richard Siebers of Spiral Tubing Corporation is gratefully acknowledged.

The Graphics and Photographic Divisions of the Naval Postgraduate School Educational Media Department are to be recognized for their special efforts in helping me produce many of the figures in this thesis.

I wish to thank my family for their enthusiastic support and understanding. Their constant encouragement allowed me to bring this project to completion.

I. INTRODUCTION

A. BACKGROUND INFORMATION

Ship design has become an increasingly integrated process over the past few years. Systems approaches are being utilized that require attention to the entire complex of communications, combat and engineering equipment to be carried within a desired hull form. The desire to obtain maximum operational efficiency is no longer dependent upon hull design alone. Every system is reviewed for possible reductions in manufacturing costs as well as weight and space savings. Efforts to achieve these reductions in naval steam power plants must include the steam condenser, which has traditionally been overdesigned. Application of enhanced heat transfer methods, such as tube surface geometry changes or promotion of dropwise condensation, would allow for reduction in condenser size with perhaps a resulting savings in weight and cost. Enhanced heat transfer methods would also permit lower condenser pressures to be achieved, thus reducing operating costs by saving fuel.

Investigation of condenser design processes by Search [1], indicated that with the use of computer methods, enhanced heat transfer techniques in marine condensers can increase heat loads, at constant pumping power, by up to 50 percent. Search concluded that enhancement methods could decrease condenser weight and cost for constant pumping power and constant heat

load as compared to a conventional condenser design under the same conditions. Savings of up to 40 percent in size and weight were reported depending upon enhancement technique.

In recent years many research efforts have been directed to the study of heat transfer enhancement techniques and their application to heat exchanger design. Bergles [2] has recently summarized a wide variety of tests conducted to study the behavior and performance characteristics of convective heat transfer enhancement techniques both with single phase as well as two phase processes. He categorized enhancement techniques as passive (i.e., enhanced tubes) or active (i.e., surface vibration).

A variety of studies have been conducted pertaining to condenser applications. Palen, Cham and Taborek [3] conducted tests with TURBOTEC tubes manufactured by Spiral Tubing Corporation. Bundle configuration tests were designed to compare the performance of TURBOTEC tubes to that of smooth tubes. The test bundle had 196 25.4 mm outside diameter tubes arranged in 16 vertical rows. Steam pressures of 379 kPa and 724 kPa on the shell side of the condenser and bundle cooling water flow rates of 47.9 to 100.8 kg/sec on the tubeside were used. Average cooling water bulk temperatures ranged from 118.3 to 171.1 ^{o}C. The experimental results showed that for a given Reynolds number, the friction factor for a TURBOTEC tube is from 10 to 15 times that of a smooth tube. On the basis of bundle performance, the heat transfer rate was increased by a factor of 2.5 comparing the TURBOTEC tubes to smooth tubes.

Young, Withers and Lampert [4] conducted bundle comparison tests of smooth tubes to KORODENSE tubes manufactured by the Wolverine Tube Division of Universal Oil Products (UOP). Two sizes of tubes were tested: 15.9 mm outside diameter copper tubes and 25.4 mm outside diameter 90-10 copper-nickel tubes. Tubes were tested in a bundle configuration with three vertical rows, with either 1 to 9 or 1 to 7 tubes per vertical row. The middle row was offset such that the tubes formed an equilateral triangular pitch. Steam temperatures of 37.8°C and 100°C were used for the tests. Cooling water velocity through each tube was varied from about 0.91 m/sec to 1.98 m/sec. Under isothermal conditions, the tubeside pressure drop for the KORODENSE tubes was five times that of the smooth tubes for both sizes of tubes. The inside, water-side, heat transfer coefficient for the 25.4 mm KORODENSE tube was 2.2 times that of the smooth tube, while the 15.9 mm KORODENSE tube's value was 2.7 times that of the smooth tube. Enhancement of the outside, steam-side, heat transfer coefficient showed a 30 to 40 percent increase over that of a smooth tube. Catchpole and Drew [5] conducted tests on five radially grooved tubes. In these tests, steam was supplied at 13.79 kPa and the cooling water velocity was maintained at 3.05 m/sec. The tubes could either be tested in a single tube arrangement or as a bundle. All heat transfer coefficients and friction factors were calculated as if the tube being tested were a standard plain tube. All five tube geometries tested yielded a combined improvement of

approximately 40 percent in the overall heat transfer coefficient when compared to a smooth tube. The percentage increase in the friction factor of the test tubes over a smooth tube ranged from 33 percent to 264 percent.

Newson and Hodgson [6] condensed steam at atmospheric pressure on single vertical tubes. Combs [7] conducted tests on a single vertical fluted tube for ammonia condensation. Tests on single vertical fluted tubes were conducted also by Combs, Mailen and Murphy [8] utilizing six different fluorocarbons and one hydrocarbon as the working fluids.

In order to allow for comparison of enhanced tube types with a single apparatus under identical conditions, and alleviate the confusion of attempting to compare results obtained under widely varying test procedures and physical environments, a test facility was designed and initial construction begun by Beck [9] at the Naval Postgraduate School that permits testing of a single, horizontally mounted condenser tube in a dummy tube bundle matrix. Completion of construction and testing of this condenser was done by Pence [10]. Pence's tests on a smooth copper-nickel tube indicated that the facility was technically sound. Using this facility, Reilly [11] conducted tests on enhanced tubes manufactured by General Atomic Company. Three General Atomic spirally fluted aluminum tubes with an outside diameter of 15.9 mm were tested. Each tube had a different helix angle of 30, 45 and 60 degrees. Steam at a pressure of 20.7 kPa was supplied to the test condenser. The enhanced tube was

cooled by water on the inside at velocities of 0.91 to 7.62 m/sec. Friction factor increases of 10 times that for a smooth tube were observed. The overall heat transfer coefficient of the enhanced tubes was as much as 1.75 times the corresponding smooth tube value for the same mass flow of cooling water. Inside heat transfer coefficients were observed to increase by about a factor of 3 while the outside heat transfer coefficients decreased by 10 to 29 percent when compared to smooth tube values. Reilly's tests of smooth copper-nickel and aluminum tubes confirmed the results of Pence, and his work with General Atomic tubes provided the basis for further experiments with enhanced tubes.

B. GOALS OF THIS WORK

The purpose of this thesis was then:

1. to determine the heat transfer and pressure drop performance characteristics of four different spirally fluted TURBOTEC tubes manufactured by Spiral Tubing Corporation,

2. to determine the heat transfer and pressure drop performance characteristics of five different spirally corrugated KORODENSE tubes manufactured by Wolverine Tube Division of Universal Oil Products, Incorporated,

3. to compare each type of enhanced tube's performance to smooth tube operation and to results of other research efforts on similarly enhanced tubes,

4. to estimate if any of these tubes would be suitable for naval condenser use, and

5. to identify what geometrical tube design parameters may be important in enhancing the overall heat transfer coefficient.

II. EXPERIMENTAL FACILITY

A. TEST FACILITY

The test facility is seen in Figure 1. As mentioned earlier, the layout was designed by Beck [9] and built and tested by Pence [10]. Operational tests of enhanced tubes manufactured by the General Atomic Company were conducted by Reilly [11]. A detailed description of the components used in the various systems may be found in these reports. Only a general description of the various systems will be found within this report. Particular attention however will be focused on the experimental tubes, their construction and their location within the test section. Calibration procedures for components requiring calibration are outlined by Reilly [11].

B. STEAM SYSTEM

The steam system is shown in Figure 2. The boiler is an electrically heated Fulton Boiler which produces saturated steam at 45.4 kg/hr. The steam leaves the boiler via a 19.1 mm diameter line and the boiler-isolation valve (MS-1). The water contained in the steam is removed by the steam separator. The steam continues through the system past a flowmeter and through the throttle valve (MS-3) where the pressure is reduced. The steam next passes through the desuperheater wherein water from

the feed system is injected in order to remove some of the sensible heat from the steam. The steam continues into the test condenser where part of it is condensed on the test tube. The steam not condensed is collected in the vapor outlet and sent to the secondary condenser wherein the latent heat of vaporization is removed. If the boiler fails, steam may be provided via the house-steam-cross-connect valve (MS-2). Steam could be routed around the test condenser to the secondary condenser via the bypass valve (MS-4). All steam lines (except the section downstream of MS-3, see [10]) were insulated with 25.4 mm thick fiberglass insulation.

C. TEST CONDENSER

The test condenser is shown in Figures 3, 4, and 5. Steam enters via the top. It then passes through the expansion section over the baffle separators, and through three layers of 150 mesh screen and a flow straightener into the tube bundle. The condensate collects at the bottom of the test condenser where it flows through two 12.7 mm diameter lines to the hotwell.

The viewing windows, shown in Figure 3 and Figure 4, allow viewing of the condensation process. Two types of pyrex glass windows were used. One type was a standard pyrex glass plate 12.7 mm thick. The second type of window was an Owens-Corning pyrex glass with a transparent electrically conducting coating applied over one surface. A Lambda power supply set at 20 VDC

and 2.2 Amp was used with this window to supply power to the electrically conducting surface to minimize fogging effects.

The tube sheet arrangement is as seen in Figure 5. There are eight 15.9 mm OD, 18 gauge, 90-10 copper-nickel tubes arranged in a typical condenser configuration, with a spacing to diameter ratio (S/D) of 1.5, around a single test tube. The test tube is the only tube with water passing through it. This arrangement was selected to best simulate the steam flow conditions in an actual condenser.

The test condenser is insulated with a 51 mm thick sheet of Johns-Manville Aerotube insulation.

D. CONDENSATE AND FEEDWATER SYSTEMS

The condensate and feedwater systems are shown in Figure 6. The test condenser hotwell collects the condensate from the test tube, while the secondary condenser hotwell collects the condensate from the secondary condenser. Valve C-1 allows isolation of the test condenser hotwell so the condensate mass from the test condenser may be measured. Valve C-4 is a vent valve between the test condenser hotwell and the test condenser. The condensate is pumped from the hotwells to the feedwater tank by the condensate pump. The feed pump routes the water from the feed tank to the boiler via the solenoid-controlled valve FW-3, a hot-water filter, and the boiler-isolation valve, FW-4.

The feedwater temperature is maintained between 54.4^{o}C and 60.0^{o}C by thermostat controlled heaters. This reduces

fluctuations in the boiler output and provides a source of water at a temperature near saturation for the desuperheater.

If house steam is used, the condensate is returned to the house system via C-3.

The condensate lines are insulated with 19.1 mm thick Johns-Manville Aerotube insulation. The feedwater lines are insulated with 12.7 mm thick fiberglass insulation.

E. COOLING WATER SYSTEM

The cooling water system is a partially-closed system as shown in Figure 7. The water is pumped from the supply tank via a 5.6 kw pump. The water is routed to the test tube via one of two rotameters. A low flow rotameter allows up to 5.6 ℓ/m to flow through the test tube, while a high flow rotameter permits up to 71.2 ℓ/m. The water returns to the supply tank via a dry cooling tower. The dry cooling tower was constructed using four large plate/fin radiators connected in series. The water was directed through the radiators and outside air was forced over the cooling surface by a centrifugal fan.

The bypass-rotameter, downstream of CW-C, is provided to permit an increased volume of water to flow through the cooling tower.

The system piping was reduced from 25.4 mm to 15.9 mm diameter (approximate OD of all test tubes) at a distance of approximately 0.76 m ahead of the test condenser to insure fully developed flow at the test-tube entrance. Pressure taps

were installed in the permanent piping at the ends of the test tube (see Figure 8) to permit the measurement of the overall pressure drop.

The cooling water lines were insulated with 25.4 mm thick Johns-Manville Aerotube insulation.

F. SECONDARY SYSTEMS

1. Vacuum System

The vacuum in the test condenser is maintained by a mechanical vacuum pump and a vacuum regulator which induces an air leak into the vacuum line. A cold trap at the inlet of the vacuum pump forces incoming vapor to pass over a system of refrigerated copper coils. This is to remove entrained water from the vacuum line and prevent moisture contamination of the vacuum pump oil. The vacuum pump outlet is vented through a roof exhaust fan to avoid a health hazard from breathing any oil vapor that may be exhausted by the pump.

2. Desuperheater

The desuperheater removes sensible heat from the superheated steam by injecting feed water at about 60°C. The feedwater flow into the desuperheater is controlled by valve DS-1 and measured by a rotameter. The excess water is collected in a tank, located below the desuperheater, and returned to the feedwater tank periodically during the experimental runs.

G. INSTRUMENTATION

1. Flow Rates

Fulton rotameters were used to measure the flow rate of water in the cooling water system and the desuperheater, while an Ellison Annubar and a differential water manometer were used to determine steam flow.

2. Pressure

Several different types of pressure measurement devices were used in this facility. They were: a Bourdon tube pressure gauge which was used to measure boiler pressure, a compound gauge which was used to measure the secondary condenser pressure, an absolute pressure transducer and a 760 mm mercury manometer which were used to measure the test condenser pressure, and a 3.6 m mercury manometer which was used to measure the cooling water pressure drop across the test tube.

3. Temperature

There were three types of thermocouples used in this facility. Stainless steel sheathed, copper-constantan thermocouples were used as the primary temperature monitoring devices. Eleven temperatures required for data reduction were measured using these devices. Table I lists the locations monitored. Figure 2 shows the location of six vapor space thermocouples. Cooling water thermocouples were located as shown in Figure 7.

Teflon coated copper-constantan thermocouples were used as secondary measuring devices. Table II lists the locations monitored using these thermocouples. An iron-constantan thermocouple was used to measure the boiler temperature.

4. Data Collection and Display

An autodata collection system was utilized to record and display the temperatures in degrees Celsius obtained from the primary thermocouples and to record and display the pressure in cm Hg inside the test condenser. See Table I for channel numbers of the temperature monitoring devices.

A 28 channel digital pyrometer uas utilized to display the temperatures obtained from the secondary thermocouples and a single channel pyrometer displayed the temperature from the iron-constantan thermocouple. See Table II for channel numbers.

H. TEST TUBES

The enhanced tubes tested during this study were manufactured by the Spiral Tubing Corporation, with a trade name of TURBOTEC, and the Wolverine Tube Division of Universal Oil Products (UOP), with a trade name of KORODENSE. Each had an overall length of 1.22 m and an enhanced section of 0.914 m. All were helically spiraled along the enhanced section. The method of spiral development varied however with manufacturer.

Four types of TURBOTEC tubing were made by the Spiral Tubing Corporation. These tubes were three-start, helically

fluted, with flute pitch determining tube type. All TURBOTEC tubes were manufactured of copper (Alloy 122). The tubes were formed by externally making a set of equally spaced dimples at one end of a smooth tube. The number of dimples determines the number of flutes that will be produced. The tube is placed in a mandrel lathe under slight compression at one end. As the tube is twisted, it is allowed to draw-in on itself (self-shorten) until the desired pitch is obtained. The amount of self-shortening determines tube pitch. Figures 9, 10 and 11 show close-up views of the High, Medium and Low pitch tubes respectively. The Variable pitch tube (not shown) varies in appearance from that of a High pitch tube at one end to that of a Low pitch tube at the other. There is no special significance attached to the Variable pitch tube. It was made simply to see if tube pitch could be changed during the forming process.

Two types of KORODENSE tubing were made by the Wolverine Tube Division of UOP. All tubes were single-start helically corrugated tubes formed by passing a rotating smooth tube under a mechanism designed to indent the tube to the desired groove depth. Pitch is determined by the rate at which the tube is drawn through the grooving mechanism. The deeper grooved tubes are designated as Maximum Heat Transfer (MHT) tubes. Shallower grooved tubes are designated as Low Pressure Drop (LPD) tubes. Three MHT tubes were made: one of 90/10 Copper-Nickel, one of 3003-Aluminum and one of commercially pure Titanium. Two LPD tubes were made: one of 90/10 Copper-Nickel and one of 3003-Aluminum. Figures 12, 13 and 14 show

close-up views of the 90/10 Copper-Nickel-MHT, the 3003-Aluminum-MHT and the Titanium-MHT respectively.

A summary of all tubes tested is provided in Table III. Special characteristics of the TURBOTEC and KORODENSE tubes are listed in Table IV.

III. EXPERIMENTAL PROCEDURES

A. INSTALLATION AND OPERATING PROCEDURES

1. Preparation of Condenser Tubes

Thermocouples were installed on each tube to measure the wall temperature. TURBOTEC tubes have a larger diameter along the enhanced section than along their smooth ends, and required different installation procedures than KORODENSE tubes whose outside diameter is not changed by the enhancement process. Standardized procedures given by Reilly [11] were followed for thermocouple mounting and tube installation.

Prior to any run, the condenser tubes had to be prepared to insure filmwise condensation. Exterior and interior surfaces were cleaned to insure proper wetting characteristics and to insure that all deposits were removed. Copper and copper-nickel tubes were prepared in accordance with the procedure given in Pence [10]. Aluminum tubes were prepared in accordance with the procedure given in Reilly [11]. To clean and prepare the titanium tube, a chemical cleaning procedure was used which was a modification of a procedure used in descaling titanium prior to acid pickling [12]. The steps in this cleaning process are as follows:

a. Swab tube surface with acetone to remove grease.

b. Using a 1.91 cm test tube brush, brush the inside surface of the tube with a 50 percent sulfuric

acid solution. Also apply this solution to the outside surface of the tube.

c. Rinse inside and outside of tube with tap water.

d. Apply a 50 percent solution of sodium hydroxide (heated to 95°C) to the outside surface of the tube.

e. Rinse the tube with tap water.

f. Rinse thoroughly with distilled water.

2. System Operation and Steady State Conditions

Pence [10] developed and Reilly [11] modified a detailed set of operating procedures for this system. They are included, with minor changes, in this report as Appendix A.

In general it takes about three hours from initial light off until steady state conditions are established. The feedwater is heated up to 60°C by energizing the feed tank heaters and recirculating the feedwater. After installation of the test tube is complete, the vacuum system can be activated. The data collection system is programmed, including setting the date and time in accordance with reference [13]. The cooling water system is placed in operation. The 71.2 ℓ/m rotameter is set at about 50 percent flow to allow adequate venting of both legs of the 3.66 meter manometer. The rotameter is then reset to the lowest flow point for system operation. The steam system can now be placed into operation.

Steady state conditions must be established prior to data collection. To determine this, two parameters were monitored. They were the cooling water inlet temperature and the steam vapor temperature. The cooling water inlet temperature did not rise more than 0.6°C/hr. The steam vapor temperature did not vary more than 3.3°C between the six vapor thermocouples in the condenser or did the change in temperature at an individual thermocouple exceed 0.3°C/min. The steaming conditions and cooling water flow conditions remained constant while establishing steady state conditions. The time for the system to stabilize was generally about one hour which is in agreement with that reported by Reilly [11].

3. Maintenance Procedures

Periodically, the systems required various forms of maintenance. Following each run, the boiler received two bottom blow downs to remove any sediment that may have settled. The supply tank in the cooling water system required occasional refilling. Treated tap water which ran through a commercially rented resin bed was used to reduce the amount of contaminants in the water that could deposit on the tubes. The filter in the feedwater required changing approximately every three months to prevent low boiler levels due to lack of feedwater. The condenser glass window required cleaning after approximately five runs. This was true whether using the heated glass or the standard pyrex glass. Prior to reinstalling the pyrex glass, a light coating of Glycerol Reagent

ACS $HOCH_2CHOHOH_2OH$, was applied to the inside surface to enhance the viewing of the condensation process.

B. DATA REDUCTION PROCEDURES

Data obtained in this thesis were evaluated using the smooth inside diameter as the characteristic flow dimension. This method presents the data in such a way as to make it useful to the designer. The data was not reduced in terms of a conventional hydraulic diameter because of the widely different geometrical shapes of the tubes and the corresponding difficulty in measuring such a hydraulic diameter. Furthermore, there is recent evidence that a modified hydraulic diameter may be more appropriate in describing heat and momentum transfer in turbulent flow than the conventional hydraulic diameter defined as 4 Ac/Pw [14].

As mentioned above, to meet the condenser designer's needs, it was felt that the data should be reduced using the smooth end diameter following the procedure of Reilly [11]. This would allow a direct substitution of an enhanced tube for a smooth tube and is especially important when considering the comparison of a wide variety of tube types. In addition, a nominal area was defined. The nominal area was based on the outside surface area of a 15.9 mm OD smooth tube.

Appendix B, the sample calculations, is a complete listing of the equations used to evaluate the data. Appendix C is a derivation of the probable error in the data reduction equations, followed by a sample error analysis for the

KORODENSE Copper-Nickel-MHT tube, (No. K-2), Run 12.

1. Overall Heat Transfer Coefficient

The method employed to arrive at the overall heat transfer coefficient is straightforward and similar to that employed by many researchers in the past.

The heat transfer rate to the cooling water is given by

$$Q = \dot{m}\, c_p\, (Tc_o - Tc_i) \quad . \tag{1}$$

The heat transfer rate can also be found from the overall heat transfer coefficient by

$$Q = U_n\, A_n\, LMTD \quad , \tag{2}$$

where

$$LMTD = \frac{(T_v - Tc_i) - (T_v - Tc_o)}{\ln\left(\frac{T_v - Tc_i}{T_v - Tc_o}\right)} \quad . \tag{3}$$

After combining equations (1), (2) and (3) it is found that

$$U_n = \frac{\dot{m}\, c_p}{A_n} \ln\left(\frac{T_v - Tc_i}{T_v - Tc_o}\right) \quad . \tag{4}$$

A schematic illustration of the procedures to arrive at U_n is shown in Figure 15.

To remove the effect of the tube wall material, a corrected heat transfer coefficient is found from

$$U_c = \frac{1}{\frac{1}{U_n} - \frac{1}{R_w}} \quad , \tag{5}$$

where R_w is the calculated wall resistance.

2. Inside Heat Transfer Coefficient

The Nusselt number on the inside is found from the Sieder Tate relationship, found in Holman [15] as:

$$Nu = \frac{h_i D_i}{k_b} = C_i \, Re^{0.8} \, Pr^{1/3} \, (\mu/\mu_w)^{0.14}. \tag{6}$$

With this well-known correlation, all fluid properties are evaluated at the average bulk temperature of the cooling water. The effect of the wall temperature is only felt by a viscosity ratio $(\mu/\mu_w)^{0.14}$. In the above equation, C_i is referred to as the Sieder Tate coefficient which is normally expressed as between 0.023 - 0.027 for smooth tubes. The remainder of the right hand side of the above equation $(Re^{0.8} \, Pr^{1/3} (\mu/\mu_w)^{0.14})$ will be referred to as the Sieder Tate parameter, and the procedure for arriving at this value is illustrated schematically in Figure 16. The Wilson plot is used to arrive at the value of the Sieder Tate coefficient. The Wilson plot was developed in 1915 by Wilson [16], and has been modified by several researchers since. The procedure used in this research was developed by Briggs and Young [17].

The Wilson plot is merely a plot of $1/U_n$ versus the inverse of the Sieder Tate parameter which should be a straight line when varying the cooling water velocity. The reasoning behind the Wilson plot can be seen in the following development.

The overall heat transfer coefficient can be written as:

$$U_n = \frac{1}{\frac{D_o}{D_i h_i} + R_w + \frac{1}{h_o}} \quad . \tag{7}$$

The inverse of equation (7) is:

$$\frac{1}{U_n} = \frac{D_o}{D_i h_i} + R_w + \frac{1}{h_o} \quad . \tag{8}$$

If $(R_w + \frac{1}{h_o})$ is assumed to be constant, and equation (6) is solved for h_i in terms of the Sieder Tate parameter, equation (8) can be rewritten as:

$$\frac{1}{U_n} = \frac{D_o}{C_i k_b} \, Re^{-0.8} \, Pr^{-1/3} \, (\mu/\mu_w)^{-0.14} + B \quad , \tag{9}$$

where $B = R_w + \frac{1}{h_o}$ = constant.

The form of equation (9) is then exactly that of a straight line,

$$Y = MX + B \quad , \tag{10}$$

where:

$$Y = \frac{1}{U_n} \quad , \tag{10a}$$

$$X = \frac{1}{\text{Sieder Tate parameter}} \quad , \text{ and} \tag{10b}$$

$$M = \frac{D_o}{C_i k_b} \quad . \tag{10c}$$

The values of $1/U_n$ and the Sieder Tate parameter are obtained by varying the water velocity and holding the other parameters, such as water temperatures, steam vapor

temperatures and condenser tube wall temperature, nearly constant. When $1/U_n$ is plotted versus $Re^{-0.8}\ Pr^{-1/3}\ (\mu/\mu_w)^{-0.14}$, a linear regression subroutine [18] fits these points to a straight line and then solves for the slope, M, and the intercept, B. Knowing the slope, M, the Sieder Tate coefficient C_i can be found from equation (10c). The inside heat transfer coefficient, h_i, is then found from equation (6).

Once the inside heat transfer coefficient, h_i, is known, then the Nusselt number can be solved for in equation (6), to find the Stanton number,

$$St = \frac{Nu}{RePr} = \frac{h}{c_p G} \quad . \tag{11}$$

The cooling water properties (ρ, μ, k, c_p, and Pr) are solved for as shown in Appendix B. Appendix B also demonstrates the procedure for arriving at the water viscosity evaluated at the condenser tube wall, μ_w.

3. Outside Heat Transfer Coefficient

The outside heat transfer coefficient, h_o, can now be found from equation (7) knowing U_n, h_i and R_w. Figure 17 schematically illustrates the various steps outlined above.

4. Friction Factor

The friction factor for the test tube is found from:

$$f_a = \frac{(\rho_b)(\Delta P_{TS})(2g_c)}{4(L_{TS}/D_i)\ G^2} \quad . \tag{12}$$

The variables used in equation (12) are solved for as shown in Appendix B, while the inside diameters are listed in Table III. ΔP_{TS}, however, is reduced from the measured pressure drop outlined below.

ΔP_{TS} is the pressure drop in the enhanced section of the test tube. The measured pressure drop, ΔP_m as seen in Figure 8, is taken over the entire tube length, a distance of 1.299 m. Since the enhanced section is only 0.914 m long, the pressure drop over each of the smooth ends must be subtracted off of the measured pressure drop. This is done by calculating the friction factor in the smooth ends using:

$$f_s = \frac{0.079}{Re^{0.25}} \quad \text{for } Re < 30{,}000 \quad , \tag{13}$$

or

$$f_s = \frac{0.046}{Re^{0.2}} \quad \text{for } Re > 30{,}000 \quad . \tag{14}$$

The smooth-end-section pressure drops can then be calculated from,

$$\Delta P_s = \frac{(f_s)(4)(L_S/D_i)(G^2)}{(\rho_b)(2g_c)} \tag{15}$$

The cross sectional flow area of the enhanced section of the test tube is less than the cross sectional flow area of the smooth end of the tube. Therefore, the water undergoes an expansion and a contraction at the exit and entrance to the enhanced section of the tube. Associated with the expansion and contraction processes are certain irreversible losses which cause additional pressure drops to occur. These pressure

drops must also be subtracted off of the measured pressure drop and are estimated following the calculational procedure as shown in reference [19]:

$$\Delta P_{e/cn} = \rho v_{TS}^2 (K_e + K_{cn}) \quad . \tag{16}$$

Since the variations in the contraction and expansion coefficients K_{cn} and K_e are slight over the range of Reynolds numbers used, an average of these values was used in equation (16).

Therefore, ΔP_{TS} is found using equations (15) and (16):

$$\Delta P_{TS} = \Delta P_m - \Delta P_s - \Delta P_{e/cn} \quad , \tag{17}$$

and the friction factor for the test section is solved for in equation (12).

5. Performance Criteria

To compare the enhanced, or augmented tubes with the smooth tube, it was necessary to use some meaningful performance criteria. The following procedures are similar to those outlined by Reilly [11].

a. Colburn Analogy

Using the Colburn Analogy, as found in reference [20], provided one such criterion. Using this analogy, the heat transfer performance is compared to the friction factor performance as seen by the relation:

$$j = StPr^{2/3} = f/2 \quad . \tag{18}$$

b. Surface Area Ratios

Bergles [21] outlines several performance criteria based on the inside heat transfer coefficients by solving for the ratio of augmented to smooth tube surface areas while holding various parameters constant.

(1) External Resistance Equal to Zero.

(a) Constant Heat Load with Increasing Pumping Power. If the external thermal resistance is set equal to zero, and the pumping power is allowed to increase, one such ratio is defined by

$$\frac{A_a}{A_s} = \frac{h_s}{h_a} = \frac{Nu_s/Pr^{1/3}(\mu/\mu_w)^{0.14}}{Nu_a/Pr^{1/3}(\mu/\mu_w)^{0.14}} \quad . \qquad (19)$$

This assumes that Q, $\dot{m}$, D_i, T_b and LMTD are constant, and $R_{ext} = R_w + 1/h_o = 0$. In equation (19) the augmented heat transfer coefficient h_a is the value h_i referred to earlier. In this situation, the flow velocities for the smooth and augmented tubes are the same.

(b) Constant Heat Load and Constant Pumping Power. The area ratio defined by equation (19) does not, however, take into account the increase in pressure drop and hence the increase in friction factor caused by enhancement techniques. The increase in pressure drop can be included when evaluating the performance of an enhanced tube compared to that of a smooth tube. Bergles [21] shows this by defining an area ratio for constant pumping power as well as for the conditions defined earlier.

The pumping power is given by:

$$Wp = (\rho\ v\ \frac{\pi}{4} D^2)\ 4\ f\ (\frac{L}{D})\ (\frac{v^2}{2g_c}) \qquad (20)$$

$$= (\frac{\rho}{2g_c})\ (\pi DL)\ fv^3 \quad ,$$

where πDL is the inside surface area for the tube in question. By setting the pumping power of a smooth tube equal to the pumping power of an enhanced tube, it is found that:

$$\frac{A_a}{A_s} = \frac{v_s^3\ f_s}{v_a^3\ f_a} = \frac{Re_s^3\ f_s}{Re_a^3\ f_a} \quad . \qquad (21)$$

Notice, that in this situation of constant pumping power, the flow velocities and hence Reynolds numbers are different for the smooth and the augmented tube.

The heat flow rate is given by:

$$Q = h_i\ A_i\ LMTD_i \quad . \qquad (22)$$

Since the heat flow is also assumed to be constant in both the enhanced and smooth tubes, the area ratio can be found

$$\frac{A_a}{A_s} = \frac{h_s}{h_a} = \frac{Nu_s/Pr^{1/3}(\mu/\mu_w)^{0.14}}{Nu_a/Pr^{1/3}(\mu/\mu_w)^{0.14}} \quad . \qquad (23)$$

Equation (21) can now be set equal to equation (23) to show:

$$\frac{A_a}{A_s} = \frac{Nu_s/Pr^{1/3}(\mu/\mu_w)^{0.14}}{Nu_a/Pr^{1/3}(\mu/\mu_w)^{0.14}} = \frac{Re_s^3\ f_s}{Re_a^3\ f_a} \quad . \qquad (24)$$

If Nu_s is replaced in the above equation by the Sieder-Tate relationship as found in [15]:

$$Nu_s = 0.027\ Re_s^{0.8}\ Pr^{1/3}(\mu/\mu_w)^{0.14} \quad , \qquad (25)$$

and f_s is replaced by equation (14)

$$f_s = \frac{.046}{Re_s^{0.2}} \quad , \qquad (14)$$

equation (24) can be solved for the smooth tube Reynolds number in terms of the augmented conditions:

$$Re_s = \sqrt{\frac{0.027\ f_a\ Re_a^3}{0.046\ Nu_a/Pr^{1/3}(\mu/\mu_w)^{0.14}}} \quad . \qquad (26)$$

In these expressions,

$$Re_s = \frac{G_s D_i}{\mu} = \frac{\rho D_i v_s}{\mu} \quad , \text{ and} \qquad (27a)$$

$$Re_a = \frac{G_a D_i}{\mu} = \frac{\rho D_i v_a}{\mu} \quad . \qquad (27b)$$

To find the area ratio, the procedure begins by choosing a value of Re_a. The related quantities f_a and $Nu_a/Pr^{1/3}(\mu/\mu_w)^{0.14}$ are then found from experimental data. Equation (26) is solved for Re_s, and knowing Re_s and f_s from equation (14), equation (24) can be solved for the resulting area ratio.

(2) External Resistance Not Equal to Zero.

(a) Constant Heat Load Constant Pumping Power. Since a sizeable portion of the overall resistance in

a naval condenser could be caused by the wall resistance and the outside thermal resistance, the area ratios as defined by Bergles [21] should be expanded to include these external resistances. If the heat flow is written by equation (2):

$$Q = U_n A_n \text{ LMTD} \quad , \tag{2}$$

and a thin wall thickness is assumed, then the external resistance effects on the area ratio can be included in the analysis. The wall thickness must be assumed to be small since the nominal area is based on an outside diameter of 15.9 mm.

Invoking all of the assumptions made earlier, then the results of the constant pumping power case are again:

$$\frac{A_a}{A_s} = \frac{v_s^3 f_s}{v_a^3 f_a} \quad . \tag{21}$$

In addition, constant heat flow results in:

$$\frac{A_a}{A_s} = \frac{U_s}{U_a} \quad . \tag{28}$$

As before, these two area ratios can be set equal, and it is found that:

$$\frac{A_a}{A_s} = \frac{U_s}{U_a} = \frac{v_s^3 f_s}{v_a^3 f_a} \quad . \tag{29}$$

As mentioned by Search [1] , for smooth tubes, it is found in general that the overall heat transfer coefficient can be

correlated by:

$$U_s = C\sqrt{v_s} = F_1F_2F_3C'\sqrt{v_s} \qquad (30)$$

where

C' = empirically determined coefficient

F_1 = cleanliness correction factor

F_2 = material correction factor

F_3 = inlet water correction factor.

Therefore, C is a coefficient which varies with tube size, material and water inlet temperature. Also, from equation (14), it is known that

$$f_s = \frac{.046}{Re_s^{0.2}} \quad . \qquad (14)$$

When equations (14) and (30) are substituted into equation (29), together with the use of equation (27a), the smooth tube velocity can be found:

$$v_s = \left[\frac{f_a v_a^3 C}{(U_a)(.046)} \left(\frac{\rho D_i}{\mu}\right)^{1/5}\right]^{\frac{1}{2.3}} \quad . \qquad (31)$$

To find the area ratio, the procedure begins by choosing a value of v_a. The related values of U_a and f_a are found from experimental data. Equation (31) is then solved for v_s and this value is used in equation (30) to find U_s. Equation (29) is then solved for the area ratio.

In selecting the values of the constants to substitute into equation (31), the following procedures were utilized:

(1) U_a was corrected to 21.1°C coolant inlet temperature using the procedure defined in reference [22],

(2) C' was determined by using the values of U_n and v_s for the smooth copper-nickel tube in Run 7, and solving for C' in equation (30) with application of correction factors defined in reference [22]. The value for C' was not a constant over the range of flows observed; therefore, an average volue of C' = 2883 was computed and used. As mentioned above, C varies for a given tube size, material and water inlet temperature. The related correction factors obtained from reference [23] were applied to the above value of C' as shown in Appendix B, the sample calculations.

(3) The dynamic viscosities used were obtained in the data reduction program at each flow point.

The area ratio equations were added to the data reduction program. The values obtained above using both equations (24) and (29) appear in the table of results for each tube.

6. Data Reduction Computer Program

An existing computer program of Reilly [11] for reduction of data was modified to include the area ratio equations (24) and (29), and to convert the results to SI units. Details of the program may be found in Reilly [11].

IV. RESULTS AND DISCUSSION

A. INTRODUCTION

Table III lists the various runs made and the corresponding tubes used during these tests. Table IV lists special characteristics of the TURBOTEC and KORODENSE tubes. Tables V through XVII contain all the raw data used to evaluate the performance of the enhanced and smooth tubes.

In Table III it can be seen that all runs for tubes K-1 through K-5 were data runs. Run 10 for tube K-3 was not a full data run as the thermocouple measuring tube wall temperature detached about halfway through the run. Therefore, the thermocouple was reattached and the tube was retested during run 13.

Tube T-1 was initially run solely for practice of system operation and not for data. Run 4 was the data run for tube T-1, while runs 18 and 19 were performed to take movies of the alternate flooding and draining phenomena of the condensate. Similar movies were taken to compare this tube to tubes T-3a and T-3b.

Tube T-2 was observed to vibrate visually and audibly at its maximum cooling water flow rates. Tube T-3a was also observed to vibrate during data run 6. The onset of vibration of tube T-3a occurred at much lower cooling water flow rates than for tube T-2. Run 16 was conducted to take movies of this phenomena. Movies were made with varying cooling water

flow rates through the tube to observe the initiation of tube vibration. This was done both with and without steam condensing on the tube. Vibration was observed to begin visually at a cooling water velocity of about 1 m/sec when steam was not supplied to the condenser. With steam supplied however, vibration was not visually detectable until velocities of about 3 m/sec. This was felt to be due to the damping effect of the added mass of the condensate flooding the tube grooves. Audible evidence of the vibration was heard both with and without steam supplied to the condenser at cooling water velocities of about 1.8 m/sec and above.

It was decided to run the Low Pitch TURBOTEC (T-3b) with additional supports to see if the vibration could be controlled, and to observe the effect on tube performance. For run 17 the 1 meter active length of the tube was supported by two circular braces equally spaced such that the active length was reduced to three equal lengths of 1/3 meter each. Again, during this run, movies were made of the condensation process. No vibration was observed either visually or audibly. Copies of the 16 mm movie film showing the vibration phenomena, both with and without condensation taking place, are available on request.

Figures 18 and 19 also illustrate the phenomena mentioned above. As a note of clarification, the reader may wish to refer to Figure 5 while studying Figures 18 and 19. The pictures are views upward between the smooth dummy half-tube and the smooth dummy whole tube below it, such that the

bottom of the enhanced tube can be seen just below the smooth dummy half-tube. Figure 18 shows condensation on tube T-3a. The cooling water velocity is 3 m/sec. A drop of condensate can be seen falling off the tube on the left side of the photograph. On the right side, the condensate can be seen to be building up to form a drop. Notice that all grooves are flooded with condensate. It was also observed that the condensate on the tightly pitched tube T-3 dropped off of the tube between the flute tips. In contrast to this, condensate on the longer pitched tube T-1 was observed to begin drop growth in the groove space between flute tips, but as the drop grew in size it would slide over and drop off of the flute tip. This phenomena is easily observed in the 16 mm movie film, mentioned earlier, and the reader is urged to request a copy of this film if further study is desired. Figure 19 shows a view of condensate on tube T-3a with a higher cooling water velocity of 4 m/sec. The light reflections off the surface of the condensate in the figure are due to surface ripples on the condensate from the vibration.

Tubes S-1 and S-2 were smooth tubes run to ensure that earlier experimental results for smooth tubes could be duplicated. Run 2 for tube S-1a was conducted without properly cleaning the outside of the tube, leaving it with a stained appearance. This tube is designated as "fouled" in Table III. For run 7, the tube was properly prepared in accordance with the procedure outlined by Pence [10], and this tube, S-1b, is designated as "clean" in Table III. Tube S-2

was an additional smooth tube picked at random from a lot of tubes manufactured by Alaskan Copper Works. This tube was observed to have a surface that appeared to have roller marks from the manufacturing process, giving it a "rippled" look, and is designated as such in Table III. The ripples were measured to be about a maximum of 0.03 mm in depth. It should be noted that this tube is not an enhanced tube, and was tested to see if the roller marks would have an effect on the tube's performance when compared to the other smooth tubes mentioned above.

Tube GA-2 was a tube manufactured by General Atomic Company and was one of the tubes tested by Reilly [11]. This tube was re-run here as run 3 which was performed for further practice in system operation and to gain a few data points to confirm the reproducibility of his results.

The computer results of all data runs are provided in Tables XVIII through XXX.

B. SMOOTH TUBE RESULTS

Comparative plots of smooth tube parameters are provided in Figures 20 through 25. Figure 20 shows that the corrected overall heat transfer coefficient versus cooling water mass flow rate of all the smooth tubes matches the results of Reilly [11] within an uncertainty of ±7 percent. The variation of the corrected overall heat transfer coefficient for tube S-1a "fouled" is related to the variance of the outside heat transfer coefficient seen by comparing the results

shown in Tables XVIII and XIX. The reason for this variance in the "fouled" tube is not clear. It could be that improper preparation of tube S-1a renders this set of data unreliable as evidenced by the variations in the outside heat transfer coefficient.

Comparison of the corrected pressure drop versus cooling water mass flow rate, shown by Figure 21, reveals that the effect of the "ripples" on tube S-2 is carried through to the tube's inside surface. The slight increase of the corrected pressure drop compared to that for tube S-1b "clean" is evident at flow rates above about 0.4 kg/sec and reaches a value of about 6.6 percent at a flow rate of 1.06 kg/sec. This is still seen to be within the uncertainly band, and indicates that this tube does not suffer a severe degradation in performance due to the "rippling."

As seen in Tables XVIII, XIX and XX, the Sieder-Tate coefficient for all of the smooth tubes was about 0.025, which is the same as that reported by Reilly [11], and is within ±8 percent of the values of .023 or .027, which are most often found in the literature. Figure 22 shows that the linear regression subroutine used to obtain the slope for the Wilson plot fit the S-1b tube (run 7, "clean") data very well. Variations reflect minor changes in the bulk properties of the cooling water. The constancy of the Sieder-Tate coefficient used in the Nusselt relation over the range of flows is further shown in Figure 23.

The effect of the increased corrected pressure drop for tube S-2 "rippled" is also seen in Figure 24, which shows the fanning friction factor versus Reynolds number. At higher Reynolds numbers, tube S-2 is seen to have slightly higher values of friction factor than either tubes S-1a or S-1b.

Figure 25 reflects the use of the Colburn Analogy by the use of a tube performance factor, 2j/f, versus Reynolds number. In 1883, Reynolds [24] mathematically expressed, for smooth tubes, the analogy between heat transfer and momentum transfer as:

$$St = f/2 \quad . \tag{32}$$

In 1933, Colburn [25] extended this analogy to include Prandtl number effects:

$$StPr^{2/3} = j = f/2 \quad . \tag{33}$$

It can be seen that all of the smooth tubes average about 10 percent higher than the Colburn Analogy, reflecting the uncertainty in the measured Sieder-Tate coefficients.

C. ENHANCED TUBE RESULTS

1. Heat Transfer Coefficients

The corrected overall heat transfer coefficient versus cooling water mass flow rate comparisons are shown in Figures 26 and 27. Figure 26, for the TURBOTEC tubes, shows an

increase of about 100 percent in the corrected overall heat transfer coefficient over the smooth tube value at 0.6 kg/sec for tube T-3a (Run 17), and Figure 27, for the KORODENSE tubes, shows an increase of 46 percent for tube K-5 (Run 14) at the same cooling water mass flow rate. For comparison purposes, Reilly [11] reported an increase of 53 percent in corrected overall heat transfer coefficient for his 45 degree helix angle General Atomic tube at the same cooling water mass flow rate.

Of interest in Figure 26 is the effect of vibration on the TURBOTEC tube performance, as indicated by the solid data points. It can be seen that by comparing tubes T-3a (Run 6) and T-3b (Run 17), there is a significant improvement in the corrected overall heat transfer coefficient when the vibrations do not occur. As indicated earlier in the photographs, these tube vibrations cause the condensate to have surface waves which may hold up the condensate drainage off the exterior of the tube. By additng the additional tube supports, and preventing vibration, the drainage was not affected, leading to higher outside heat transfer coefficients.

Cunningham and Milne [26] reported experimental results of "roped" tubes manufactured by Yorkshire Imperial Metals, Ltd. These are similar in shape to KORODENSE tubes, but are manufactured with differing numbers of indentation (groove) starts. It was found that in geometry, the KORODENSE tube K-5 most closely resembled the "roped" tubes. Figure 28 shows how tube K-5, a 1-start tube, compares to the "roped" tubes of

Cunningham and Milne [26]. The performance of tube K-5 agrees fairly well to the "roped" tubes if the following differences are noted:

(1) differences in wall resistance - tube K-5 was made from Titanium and most likely has a higher wall resistance than that of the "YORCALBRO" alloy used in their tube [26];

(2) differences in steam conditions - steam velocities used with the "roped" tubes are not given by Cunningham and Milne [26] and no comparison can be made with the steam conditions used in these tests; and

(3) the "roped" tube experiments were conducted at atmospheric pressure (101 kPa), while the pressure used throughout these tests was maintained at about 21 kPa.

2. Pressure Drop

Figures 29 and 30 are comparisons of the corrected pressure drop versus cooling water mass flow rate for the enhanced tubes tested. It can be seen that the corrected pressure drops for the enhanced tubes increase at a faster rate than the corrected drops for the smooth tubes. For a cooling water mass flow rate of 0.6 kg/sec, tube T-3a (Run 17), Figure 29, shows a factor of 11 increase in pressure drop over that for a smooth tube while tube K-5 (Run 14), Figure 30, shows a factor of 4 increase. A cause for these increases can be seen by referring to Table IV and Figures 11 and 14. Tube K-5 has the largest helix angle and tightest pitch of the KORODENSE tubes, and tube T-3 has the largest helix angle and

tightest pitch of all the TURBOTEC tubes. These geometries increase the restrictions to internal flow, therefore increasing the pressure drops.

3. Sieder-Tate Parameters

The Wilson plots for the TURBOTEC and KORODENSE tubes are shown by Figures 31 and 32. These are provided to show how well the linear regression subroutine fits the data. Of particular interest are the solid data points shown in Figure 31. These points reflect data affected by vibration of tubes T-2 (Run 5) and T-3a (Run 6). Use of this data would have greatly affected the values obtained for the Sieder-Tate coefficient in an erroneous way. Consequently, the vibration affected data were not used in obtaining a linear regression fit. Figure 33 shows that tube T-3b (Run 17), with an average C_i of .128 ± .01, reflects a factor of about 5 increase over that for a smooth tube, and that it is slightly improved over that for tube T-3a (Run 6). This indicates that the effect of tube vibration may cause deterioration of inside heat transfer as well as the deterioration of outside heat transfer mentioned earlier. From Figure 34, tube K-5 (Run 14), with a C_i of about .065 ± .008, shows a factor of about 2.6 increase over the smooth tube value. These increases presumably are due to increased surface area, turbulence and swirl effects.

4. Friction Factor

The corrected pressure drop results are further reflected by Figures 35 and 36. Here, as expected, the friction

factors for the enhanced tubes are greater than for smooth tubes. Again, tube T-3b (Run 17) shows the largest friction factor overall and tube K-5 (Run 14) shows the largest friction factor for the KORODENSE tubes. Both of these tubes have large helix angles, verifying the effect of helix angle on pressure drop shown with the General Atomic tubes tested by Reilly [11]. The other KORODENSE tubes appear to have friction factors nearer to the smooth tube. For Runs 9 and 13 this is because the low pressure drop (LPD) tubes were used. Tubes for Runs 11 and 12 on the other hand, which are manufactured for maximum heat transfer (MHT), and therefore have deeper indentations, have slightly higher friction factors than LPD tubes. Tube K-5 (Run 14) however, not only has deep indentations but has a significantly smaller pitch (therefore tighter twist) than the other MHT tubes, perhaps causing its higher pressure drop performance.

5. Tube Performance Criteria

a. Colburn Analogy

As shown in section B of this chapter, the Colburn Analogy can be used to define a performance factor that directly relates heat transfer to pressure drop. Comparisons of this tube performance factor (2j/f) versus Reynolds number are shown in Figures 37 and 38. The effect of friction factor is seen to dominate heat transfer (i.e., it requires more of a pressure drop increase to get an increase in heat transfer) for all the TURBOTEC tubes which have high friction factors.

This is also true of the KORODENSE tube, K-5 (Run 14). On the other hand, tubes K-1 (Run 9) through K-4 (Run 11) have friction factors near the smooth tube results (Figure 36), and these lower friction factors give higher results in Figure 38 than tube K-5 (Run 14) agreeing closely with the Colburn Analogy. The analogy therefore appears to break down for the deeply grooved TURBOTEC tubes and for the tightly pitched, yet shallower grooved, KORODENSE K-5 tube. The reader should be cautioned that all of the above-mentioned results in Figures 37 and 38 have been obtained using a smooth inside diameter, D_i. If an appropriately defined hydraulic diameter, D_h were used to reduce the data, it is expected that all the tube performance factors would increase, but the relative magnitudes of the performance factors would remain approximately the same.

b. Surface Area Ratios at Constant Heat Loads

Use of surface area ratios as defined by equation (24) provides an additional performance parameter more useful perhaps for the design engineer than the Colburn Analogy. As explained in Chapter III, with this area ratio method, it is essential that the additional frictional resistance of the enhanced tubes be taken into account by evaluating the area ratio for a constant pumping power. Assuming that the external thermal resistance is zero ($R_{ext} = 0$), Figure 39 shows that this area ratio makes all of the enhanced tubes appear very good for condenser use, with tube T-3b showing

the greatest reduction in required surface area. It is also seen that tube GA-2, the 45 degree helix angle General Atomic tube [11], appears to perform very much like tube T-3b. The results of this figure however, are for an external resistance equal to zero and therefore neglect the effect of wall resistance and outside resistance.

Area ratios for a nonzero external resistance can also be found, and are shown in Figure 40. Again, tube T-3b is seen to have the best overall performance. However, tube GA-2 is now seen to fall between the TURBOTEC and KORODENSE tubes, reflecting the effect of external resistance on this tube. It should be noted that the Reynolds numbers used in the surface area ratio figures are Reynolds numbers for existing smooth tube condensers (Re_s). For example, using a cooling water velocity of 2.74 m/sec (the maximum scoop injection velocity as specified in Reference [22]), the related smooth tube Reynolds number is calculated to be about 40,000. Entering Figure 40 with this Reynolds number, it is seen that tube T-3b would allow for approximately a 53 percent reduction in the required surface area.

c. Internal and External Performance

Table XXXI gives ratios of the average Sieder-Tate coefficients for the augmented tube data ($\overline{C}i_a$) to that of smooth tube data ($\overline{C}i_s$), and average outside heat transfer coefficients for the augmented tube data ($\overline{h}o_a$) to that of smooth tube data ($\overline{h}o_s$) for each of the tube types. Since

increases in corrected overall heat transfer coefficient are related to enhancement of both the inside and outside heat transfer coefficients together, it is clear again that tube T-3b gives the best overall performance. This condfirms the low area ratios observed for this tube in Figures 39 and 40.

Further study of Tables IV and XXXI indicate that the inside and outside heat transfer coefficients are related to change in pitch (for approximately constant groove depth). This is reflected in Figure 41. In this figure, values of the ratios of $\overline{C}i_a/\overline{C}i_s$ and $\overline{h}o_a/\overline{h}o_s$ (from Table XXXI) are plotted versus varying pitch (for constant groove depth). The trends of the data in the $\overline{C}i_a/\overline{C}i_s$ curve reveal that there is perhaps an optimum pitch (at a constant groove depth) to increase the inside heat transfer coefficient. This could be due to the fact that as pitch changes from being very large to very small, the nature of the internal flow changes from predominately swirling motion to turbulent mixing. The optimum pitch could therefore be the one that produces a combination of both these mechanisms. That outside heat transfer improves with decreased pitch is seen in the $\overline{h}o_a/\overline{h}o_s$ curve. With reduced pitch, condensate drainage improves and more channels are provided presenting more tube surface area to the steam flow. The variations in $\overline{h}o_a/\overline{h}o_s$, as noted in Table XXXI, may be caused partially by the uncertainly in the wall resistance used in the Wilson plot technique. Calculation of the actual wall resistance for an enhanced tube with severe corrugations requires a complicated analysis.

It should also be noted that the relative positions of the data for the KORODENSE, General Atomic and TURBOTEC tubes in Figure 41 are related to their respective average groove depths.

The results discussed above show correlation with the work of Catchpole and Drew [5]. Comparison with their data for a groove depth of 0.6 mm with data shown in Figure 41 shows that there is good general agreement. In their results for the 0.6 mm groove depth, decreasing pitch from about 12.8 mm to 6.4 mm increased the $\overline{Ci}_a/\overline{Ci}_s$ ratio from 2.1 to 2.6, and this same decrease in pitch followed the same trend of Figure 41 for increasing the outside heat transfer coefficient, with a maximum $\overline{ho}_a/\overline{ho}_s$ ratio of about 1.7 for their 0.6 mm groove depth tube.

V. CONCLUSIONS

As a result of the above-mentioned tests, the following conclusions are reached.

1. All of the enhanced tubes herein tested would allow for a savings of condenser surface area. Again, related to an earlier example, for a naval condenser with a scoop injection velocity of 2.74 m/sec (9ft/sec) the corresponding smooth tube Reynolds number , is calculated to be about 40,000. Entering Figure 40 with this Reynolds number, it is seen that enhanced tubes would allow for condenser surface areas varying from 83 percent to 47 percent of the smooth tube condenser surface area.

2. The maximum corrected overall heat transfer coefficient was obtained with tube T-3b, and was about 2 times that of the corresponding smooth tube. This is a result of this tube's highest combined improvement in the inside heat transfer coefficient ($\overline{Ci}_a/\overline{Ci}_s$) = 5.0) and the outside heat transfer coefficient ($\overline{ho}_a/\overline{ho}_s$ = 1.3).

3. The largest pressure drops measured for all the enhanced tubes were for tube T-3b. This is due to this tube's severe geometric deformation, presenting the highest degree of restriction to cooling water flow.

4. The best surface area ratios were for tubes T-3b, T-4 and T-2. Again, this is due to these tubes' combined

improvement in the inside and outside heat transfer coefficents for their respective pressure drops. As a result of its lower outside heat transfer coefficient, tube GA-2 was seen to have a higher surface area ratio when external resistance was taken into account. An improvement on this tube could be made however, if its outside heat transfer coefficient was increased.

5. The effect of pitch, which relates to helix angle, (with constant groove depth) on improved heat transfer performance was displayed. The data shows that $\overline{C}i_a/\overline{C}i_s$ could possibly achieve an optimum value for a properly chosen pitch. This could be due to the fact that the choice of pitch could provide the best combination of internal flow swirl and turbulence. The fact that decreasing pitch improves the outside heat transfer coefficient by improving condensate drainage and presenting more tube surface to the steam flow was also determined.

6. Based upon D_i (and not D_h) the Colburn Analogy was found to be valid for tubes K-1, K-2, K-3, and K-4; and invalid for deep grooved, and/or tightly pitched tubes.

7. Tube vibration was seen to cause a decrease in the corrected overall heat transfer coefficient for several of the TURBOTEC tubes. This decrease could be caused by the hold up of condensate in the grooves, affecting condensate drainage, as well as by a deterioriation in the inside heat transfer coefficient.

VI. RECOMMENDATIONS

From the results of this experiment, several unanswered questions can be posed. In an effort to offer ideas for continued use of the test facility, the following recommendations are made.

1. Further investigate the parameters (pitch, groove depth and helix angle) in an attempt to find the desired combination of these parameters that will produce the optimum tube. Along with this effort, newly conceived enhanced tubes should be tested and ranked with those previously tested.

2. Tests of the General Atomic 45 degree helix tube, the KORODENSE Titanium-MHT tube, and the TURBOTEC Low Pitch tube should be expanded to include tests of horizontally mounted tubes in vertical banks. This is needed to determine the effect of condensate drainage from tubes at the top of the bank on the heat transfer coefficient of the tubes near the bottom of the bank.

3. The fouling characteristics of any tube under test should be determined. This includes the cooling water side as well as the steam side. Fouling could prove to be especially critical in the use of tubes with geometries that have possible cooling water flow stagnation areas such as tightly spiralled tubes.

4. In addition to geometric enhancement, tests should be conducted to determine the effectiveness of dropwise condensation promoters. These could be applied to tubes such as those manufactured by General Atomic Company to improve the outside heat transfer coefficient and therefore the tubes' overall performance.

5. Tests should be performed using TURBOTEC tubes of copper-nickel. This would provide stronger tubes than those tested in this experiment, and should decrease the tendency toward vibration with decreased pitch as found with copper 122.

6. Testing of enhanced tubes should be done in a vertical orientation. This would determine the effect of condensate drainage vertically rather than horizontally off the tube's surface which has been shown to be very effective using refrigerants [7,8].

VII. TABLES

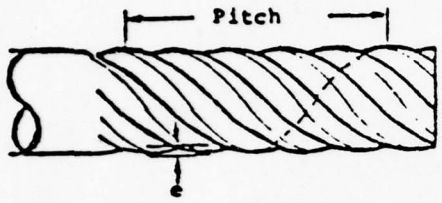
Table I. Location of Stainless Steel Sheathed Copper Constantan Thermocouples.

Channel Number	Location	Channel Number	Location
40	Tc_i	47	T_v
41	Tc_o	48	T_v
42	Tc_o	49	T_v
43	Tc_o	50	T_v
44	Tc_o	51	T_w
45	T_v	52	Hotwell
46	T_v		

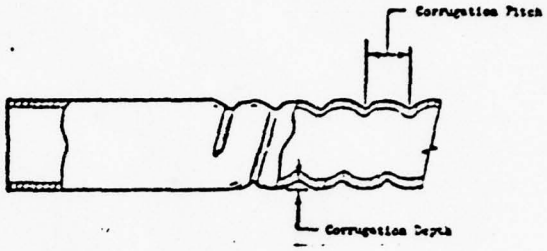
Table II. Location of Teflon Coated Copper Constantan Thermocouples

Channel Number	Location	Channel Number	Location
1	Hot Well	6	Condensate Header
2	Feedwater Tank	7	T_c into Cooling Tower
3	Condenser Window	8	T_c out of Cooling Tower
4	Tc_i	9	Cooling Tower Ambient
5	Tc_o		

Table III. Summary of Test Tubes



TURBOTEC Schematic



KORODENSE Schematic

Tube No.	Tube Type	Helix (a) Angle (Deg)	No. of Groove Starts n	Groove Depth (mm) e	Pitch (mm) p	p/D_o	e/D_o
	TURBOTEC						
T-1	High Pitch	30	3	2.67	50.48	3.18	0.168
T-2	Medium Pitch	45	3	3.25	36.78	2.32	0.205
T-3 a&b	Low Pitch	60	3	3.35	22.58	1.42	0.211
T-4	Variable Pitch	40/60	3	3.23	37.31/ 23.97	2.35/ 1.51	0.203/ 0.214
	KORODENSE						
K-1	CuNi-LPD	65	1	0.36	9.81	0.62	0.022
K-2	CuNi-MHT	70	1	0.51	9.64	0.61	0.032
K-3	Aℓ-LPD	64	1	0.41	9.67	0.61	0.026
K-4	Aℓ-MHT	74	1	0.58	9.58	0.60	0.037
K-5	Ti-MHT	75	1	0.61	5.97	0.38	0.038

(a) Helix Angle = angle measured from tube horizontal axis to flute axis

Twist Direction: TURBOTEC - left-handed spiral
KORODENSE - right-handed spiral

Table IV. Enhanced Tubing Characteristics

Tube No.	Tube Type	Material	Run No.	Date	Type Run	A_h ($\times 10^4$ m^2)	A_c* ($\times 10^4$ m^2)	D_i (mm)	D_o (mm)	T_w (mm)	K_w (W/m°C)	R_w ($\times 10^6$) (m^2 °C/W)	$\varepsilon_c + \varepsilon_e$
	KORODENSE												
K-1	CuNi-LPD	90-10 CuNi	9	13 JUL 78	Data	456.04	1.354	13.39	15.88	1.24	44.65	33.315	0.015
K-2	CuNi-MHT	90-10 CuNi	12	17 JUL 78	Data	456.04	1.316	13.39	15.88	1.24	44.65	30.315	0.030
K-3	Al-LPD	Al (3003)	10	15 JUL 78	Data	456.04	1.343	13.39	15.88	1.24	172.75	7.836	0.015
			13	18 JUL 78	Data								
K-4	Al-MHT	Al (3003)	11	16 JUL 78	Data	456.04	1.305	13.39	15.88	1.24	172.75	7.836	0.030
K-5	Ti-MHT	Titanium	14	19 JUL 78	Data	456.04	1.409	14.48	15.88	0.70	17.00	43.007	0.075
	TURBOTEC												
T-1	High Pitch	Cu (122)	1	27 APR 78	Practice	456.04	1.296	14.45	15.88	0.71	339.22	2.196	0.145
			4	12 JUN 78	Data								
			18	21 AUG 78	Movie								
			19	24 AUG 78	Movie								
T-2	Medium Pitch	Cu (122)	5	13 JUN 78	Data	456.04	1.110	14.45	15.88	0.71	339.22	2.196	0.255
T-3a	Low Pitch (u)	Cu (122)	6	14 JUN 78	Data	456.04	0.842	14.45	15.88	0.71	339.22	2.196	0.475
			16	3 AUG 78	Movie								
T-3b	Low Pitch (s)	Cu (122)	17	6 AUG 78	Movie/Data	456.04	0.842	14.45	15.88	0.71	339.22	2.196	0.475
T-4	Variable Pitch	Cu (122)	15	28 JUL	Data	456.04	0.963	14.45	15.88	0.71		2.196	0.360
	SMOOTH												
S-1a	"fouled"	90-10 CuNi	2	11 MAY 78	Data	456.04	1.375	13.23	15.88	1.32	44.65	32.351	0.0
S-1b	"clean"		7	11 MAY 78	Data								
S-2	"rippled"	90-10 CuNi	8	12 JUL 78	Data	456.04	1.398	13.34	15.88	1.27	44.65	30.991	0.0
GA-2	45° General Atomic	Al (6061)	3	22 MAY 78	Practice	456.04	0.984	13.31	16.00	3.66	237.11	7.706	0.330

*A_c was determined by measuring the liquid volume contained within the enhanced section of each tube end dividing by the enhanced section length.

Table V. Raw Data for Smooth "fouled" CuNi, Run 2, 11 MAY 78.

% Flow	T_v(°C)	T_w(°K)	Tc_i(°C)	Tc_o(°C)	ΔP (Pa)
10	61.7	316.0	19.0	28.1	1.098
20	63.9	309.5	18.0	25.3	3.609
30	63.3	304.5	18.0	23.3	7.373
40	63.3	301.9	17.0	22.2	12.708
50	64.2	300.5	17.0	21.6	18.827
60	64.7	298.8	17.0	20.9	26.200
67	65.0	299.9	17.0	20.6	32.005

Table VI. Raw Data for Smooth "clean" CuNi, Run 7, 11 JUN 78.

% Flow	T_v(°C)	T_w(°K)	Tc_i(°C)	Tc_o(°C)	ΔP (Pa)
10	67.2	325.7	19.2	29.3	1.004
15	66.9	322.7	19.0	27.6	2.040
20	66.8	320.3	19.0	26.6	3.514
30	67.0	317.0	19.0	25.0	7.531
40	67.1	317.1	19.3	24.3	12.551
50	67.2	317.0	19.5	23.8	18.764
60	67.0	317.3	19.4	23.2	25 793
70	66.8	317.8	19.2	22.6	34.171
80	66.6	317.4	19.0	22.2	43.427
90	66.7	318.6	18.9	21.8	53.625

Table VII. Raw Data for Smooth "rippled" CuNi, Run 8, 12 JUL 78.

% Flow	T_v(°C)	T_w(°K)	Tc_i(°C)	Tc_o(°C)	ΔP (kPa)
10	67.5	316.9	17.4	27.8	0.941
15	67.3	310.8	17.1	25.9	2.165
20	67.5	307.9	17.0	24.8	3.577
30	67.4	304.3	17.0	23.3	7.562
40	67.4	303.0	17.3	22.5	13.085
50	67.4	300.4	17.7	22.1	19.423
60	67.6	298.9	17.8	21.7	26.860
70	67.5	298.2	17.9	21.5	35.457
80	67.7	297.8	18.0	21.2	44.776
90	67.7	297.4	18.1	21.0	55.790

Table VIII. Raw Data for TURBOTEC Hi Pitch, Run 4, 12 JUN 78

% Flow	T_v(°C)	T_w(°K)	Tc_i(°C)	Tc_o(°C)	ΔP (kPa)
10	67.5	323.8	21.9	37.0	1.977
15	67.4	320.7	21.2	33.8	4.079
20	67.7	318.2	20.9	31.6	6.997
25	67.9	316.4	20.8	30.3	10.512
30	66.5	314.6	20.7	29.2	14.779
40	64.6	311.9	20.6	27.7	25.950
50	63.4	309.1	20.5	26.6	41.544
60	63.7	307.3	20.5	25.9	59.556
70	63.8	306.1	20.4	25.2	81.488
80	63.8	304.9	20.3	24.7	106.999
83.5	63.5	304.5	20.1	24.4	116.412

Table IX. Raw Data for TURBOTEC Medium Pitch, Run 5, 12 JUN 78.

% Flow	T_v(°C)	T_w(°K)	Tc_i(°C)	Tc_o(°C)	ΔP (kPa)
10	66.4	325.4	19.2	38.5	2.573
15	66.1	321.8	18.8	35.0	6.589
20	65.8	319.8	18.5	32.4	11.673
25	66.0	318.6	18.5	30.6	18.199
30	66.6	317.1	18.4	29.2	26.514
40	67.1	313.6	18.4	27.3	44.996
50	66.6	311.7	18.6	26.1	69.596
60	66.2	309.7	18.6	25.2	100.159
70	64.7	306.4	18.6	23.9	136.871
75	64.0	306.0	18.5	23.6	157.831

Table X. Raw Data for TURBOTEC Low Pitch, Run 6, 14 JUN 78.

% Flow	T_v(°C)	T_w(°K)	Tc_i(°C)	Tc_o(°C)	ΔP (kPa)
10	66.2	324.0	19.6	44.3	8.880
15	67.0	320.0	19.5	40.5	18.513
20	67.1	317.4	19.5	37.5	31.472
25	67.1	314.8	19.6	35.0	48.825
30	67.2	312.6	19.6	33.1	66.867
35	67.0	310.8	19.6	31.2	91.154
40	67.1	309.7	19.7	30.2	115.189
45	67.4	308.9	19.6	29.2	146.567
50	67.4	309.1	19.6	28.1	182.338
60	67.5	307.9	19.4	26.6	258.869

Table XI. Raw Data for TURBOTEC Variable Pitch, Run 15, 28 JUL 78.

% Flow	T_v(°C)	T_w(°K)	Tc_i(°C)	Tc_o(°C)	ΔP (kPa)
10	66.6	321.6	19.0	41.3	5.648
15	66.5	318.3	19.0	37.4	11.986
20	66.8	316.0	19.3	35.0	20.427
25	66.9	314.4	19.7	33.4	29.025
30	66.6	312.9	20.0	31.9	43.239
35	66.8	311.7	20.1	31.0	57.547
40	66.8	310.2	20.5	30.1	74.523
50	66.9	308.2	20.8	28.7	113.745
60	66.9	306.7	21.2	28.0	164.578
68&5	66.9	306.0	21.6	27.6	214.155

Table XII. Raw Data for TURBOTEC "supported" Low Pitch, Run 17, 6 AUG 78.

% Flow	T_v(°C)	T_w(°K)	Tc_i(°C)	Tc_o(°C)	ΔP (kPa)
10	66.5	321.9	20.9	45.2	7.939
15	66.6	318.0	20.9	41.4	14.748
20	66.8	316.1	21.5	38.9	30.499
25	66.7	314.7	22.3	37.3	46.188
30	67.0	313.6	23.1	36.2	65.329
35	66.9	312.5	23.6	35.1	88.580
40	66.9	311.7	24.1	34.4	112.428
45	66.9	311.4	24.6	33.9	141.093
50	67.1	311.1	25.0	33.5	173.050
57	67.2	310.8	25.7	33.1	220.274

Table XIII. Raw Data for KORODENSE CuNi-LPD, Run 9, 13 JUL 78

% Flow	T_v(°C)	T_w(°K)	Tc_i(°C)	Tc_o(°C)	ΔP (kPa)
10	66.8	313.7	19.1	32.1	1.600
15	66.9	310.5	19.2	29.9	3.263
20	66.8	308.5	19.8	28.8	5.585
25	67.1	306.5	19.9	27.8	8.252
30	66.6	305.6	19.9	26.9	11.455
40	66.3	303.8	19.9	25.5	18.952
50	66.6	302.7	19.8	24.7	27.456
60	66.7	302.2	20.2	24.5	37.685
70	66.9	302.4	20.7	24.5	48.510
80	67.0	302.6	21.3	24.7	60.528
88.9	67.0	302.4	21.9	24.9	71.573

Table XIV. Raw Data for KORODENSE Aℓ-LPD, Run 13, 18 JUL 78

% Flow	T_v(°C)	T_w(°K)	Tc_i(°C)	Tc_o(°C)	ΔP (kPa)
10	65.5	321.1	23.5	36.6	1.506
15	65.8	317.1	23.6	34.7	3.232
20	66.3	314.6	23.8	33.3	5.460
25	66.3	312.5	24.0	32.2	8.284
30	66.7	311.4	24.1	31.5	11.735
40	66.7	309.7	24.3	30.4	19.423
50	66.6	307.6	24.5	29.6	28.993
60	66.6	307.1	24.6	29.1	30.630
70	65.1	305.7	23.7	27.3	52.088
80	65.8	305.1	23.0	26.3	66.208

Table XV. Raw Data for KORODENSE Aℓ-MHT, Run 11, 16 JUL 78

% Flow	T_v(°C)	T_w(°K)	Tc_i(°C)	Tc_o(°C)	ΔP (kPa)
10	66.8	315.1	16.7	34.3	2.385
15	66.9	311.6	16.5	30.8	5.052
20	67.3	309.6	16.6	28.6	8.692
25	67.3	308.3	16.7	27.3	12.771
30	67.1	307.4	16.9	26.0	17.885
40	67.1	306.1	17.2	24.5	29.244
50	67.3	305.4	17.5	23.8	42.235
60	67.1	304.6	17.9	23.3	57.202
70	67.1	303.9	18.2	22.9	72.766
80	67.2	303.7	18.5	22.6	91.467

Table XVI. Raw Data for KORODENSE CuNi-MHT, Run 12, 17 JUL 78

% Flow	T_v(°C)	T_w(°K)	Tc_i(°C)	Tc_o(°C)	ΔP (kPa)
10	67.5	323.8	24.0	37.6	1.914
15	67.6	321.6	23.6	34.8	4.393
20	67.6	318.8	23.3	32.8	7.374
25	67.5	316.7	23.1	31.2	11.139
30	67.4	315.6	23.0	30.2	15.312
40	67.6	314.6	22.9	28.8	24.883
50	67.6	314.0	22.9	27.8	36.148
60	67.6	313.4	22.9	27.3	48.856
70	67.6	313.5	23.0	26.8	62.944
80	67.6	312.7	23.1	26.5	77.472

Table XVII. Raw Data for KORODENSE Ti-MHT, Run 14, 19 JUL 78

% Flow	T_v(°C)	T_w(°K)	Tc_i(°C)	Tc_o(°C)	ΔP (kPa)
10	68.3	328.2	20.7	35.8	2.353
15	67.9	327.5	20.9	33.0	5.554
20	69.0	326.8	20.5	30.8	9.947
25	67.0	326.7	21.4	30.2	15.595
30	67.2	326.6	22.3	29.7	22.341
40	67.2	326.4	22.8	28.8	38.438
50	67.2	326.1	23.0	28.1	58.834
60	67.0	326.0	23.4	27.7	82.713
70	67.1	326.0	23.6	27.4	110.043
80	67.4	325.8	23.8	27.3	139.067

Table XVIII. Smooth "fouled" Copper-Nickel Results (Tube No. S-1a), Run 2

VELOCITY M/SEC	UA W/(C*M**2)	UC W/(C*M**2)	HI W/(C*M**2)	HO W/(C*M**2)
0.86	2578.181	2812.784	4276.855	13328.125
1.72	3760.523	4281.375	7238.723	14738.506
2.55	4035.515	4642.000	9814.387	10730.309
3.45	5207.305	6262.242	12185.671	16328.133
4.31	5504.438	6696.988	14477.785	15046.238
5.17	5601.059	6840.559	16635.094	13500.141
5.78	5635.047	6891.320	18209.602	12621.191

REYNOLDS NO	PLAIN END REYN NO	FLOW RATE PER AREA KG/(SEC*M**2)	FRICTION FACTOR	SIEDER TATE CONSTANT
12641.18	12641.17	858.15	0.00761073	0.02443808
24278.25	24278.24	1717.43	0.00615840	0.02455489
35620.24	35620.21	2576.95	0.00562853	0.02461505
46432.61	46432.56	3437.03	0.00550472	0.02466484
57604.84	57604.82	4296.73	0.00519661	0.02470686
68647.38	68647.38	5156.56	0.00502331	0.02472716
76351.88	76351.81	5758.47	0.00492223	0.02473880

Table XVIII. Page 2

NUSSELT NO	NU/PR1/3(U/LW)0.14	STANTON NO	J FACTOR	PERFORM FACTOR
89.26293	46.71525	0.00115060	0.0038995	1.0247335
151.76073	79.12450	0.00100660	0.0034001	1.1042223
206.21593	107.80220	0.00090957	0.0031239	1.1100168
256.72876	133.62505	0.00084658	0.0029579	1.0746927
305.28638	158.92203	0.00080451	0.0028271	1.0880566
351.06445	183.00517	0.00077020	0.0027209	1.0833006
384.47363	199.35751	0.00075495	0.0026751	1.0869360

XIA	PRESSURE DROP (KPA)	PRANDTL NO	L/UW	DOTMS(KG/SEC)
0.21556930-03	0.77832	5.92566	1.05511	0.1180370
0.16285160-03	2.52072	6.20621	1.04328	0.2362167
0.12012340-03	5.18527	6.36467	1.03220	0.3544374
0.96754550-04	9.01836	6.53106	1.02784	0.4727324
0.81440080-04	13.30386	6.58747	1.02475	0.5909770
0.70880560-04	18.52040	6.63986	1.02061	0.7092397
0.64752760-04	22.63042	6.67006	1.02453	0.7920263

Table XIX. Smooth "clean" Copper-Nickel Results (Tube No. S-1b), Run 7

VELOCITY M/SEC	UA W/(C*M**2)	UC W/(C*M**2)	HI W/(C*M**2)	HO W/(C*M**2)
0.86	2551.070	2780.545	4480.840	10876.596
1.29	3216.989	3590.677	6119.797	12124.633
1.72	3751.287	4269.406	7635.596	12966.082
2.59	4381.453	5105.063	10426.012	12372.559
3.45	4814.906	5703.281	13111.527	11526.855
4.31	5057.223	6046.449	15652.320	11268.266
5.17	5376.238	6508.176	18086.816	11451.156
6.04	5563.680	6814.652	20436.492	11358.102
6.90	5948.414	7365.871	22674.238	12069.320
7.76	6061.363	7539.852	24953.184	11826.770

REYNOLDS NO	PLAIN END REYN NO	FLOW RATE PER AREA KG/(SEC*M**2)	FRICTION FACTOR	SIEDER TATE CONSTANT
12783.24	12783.23	858.00	0.00670025	0.02490020
18794.32	18794.32	1287.35	0.00602937	0.02495878
24790.90	24790.88	1716.75	0.00594483	0.02499033
36557.66	36557.66	2575.64	0.00581531	0.02504044
48531.84	48531.81	3434.67	0.00543385	0.02505326
60417.05	60417.00	4293.60	0.00519792	0.02506532
71967.81	71967.81	5152.86	0.00493744	0.02506707
83229.00	83229.00	6012.43	0.00469504	0.02511301
94466.19	94466.19	6872.02	0.00467473	0.02513338
105719.50	105719.50	7731.59	0.00455644	0.02514869

Table XIX. Page 2

[illegible] NO	NU/PR1/3(U/UW)C.14	STANTON NO	J FACTOR	PERFORM FACTOR
[illegible]	48.03020	0.00124804	0.0040508	1.2091541
[illegible]	65.53058	0.00113583	0.0037432	1.2416630
[illegible]	81.88513	0.00106266	0.0035309	1.1878777
[illegible]	111.95006	0.00096691	0.0032546	1.1193342
[illegible]	140.50266	0.00091188	0.0030796	1.1334839
[illegible]	167.45440	0.00087079	0.0029500	1.1350613
[illegible]	192.82350	0.00083839	0.0028562	1.1569414
[illegible]	216.82935	0.00081181	0.0027841	1.1578789
[illegible]	240.14354	0.00078759	0.0027166	1.1622629
[illegible]	262.93091	0.00077075	0.0026678	1.1709919

XIA	PRESSURE DROP (KPA)	PRANDTL NO	L/LA	DOTMS(KG/SEC)
0.26648240-03	0.68505	5.84756	1.07813	0.1180096
0.19659470-03	1.38747	5.98276	1.07357	0.1770688
0.15756530-03	2.43241	6.05663	1.06958	0.2361299
0.11540620-03	5.35503	6.17554	1.06282	0.3542839
0.91771560-04	8.89615	6.20627	1.06274	0.4724084
0.76675510-04	13.25750	6.23521	1.06405	0.5905461
0.66530270-04	18.19075	6.28796	1.06601	0.7087305
0.58882930-04	24.11877	6.35115	1.06868	0.8269585
0.53073100-04	30.62531	6.40126	1.06865	0.9451854
0.46226500-04	37.78212	6.43960	1.07266	1.0634117

Table XX. Smooth "rippled" Copper-Nickel Results (Tube No. S-2), Run 8

VELOCITY M/SEC	LA W/(C*M**2)	UC W/(C*M**2)	HI W/(C*M**2)	HO W/(C*M**2)
0.85	2507.875	2719.217	4312.445	10905.477
1.27	3145.711	3485.510	5833.457	12073.676
1.70	3652.149	4118.270	7259.043	12686.930
2.55	4329.695	5000.695	9852.945	12557.121
3.40	4706.750	5510.563	12366.640	11714.883
4.25	5029.652	5956.422	14658.504	11515.875
5.10	5341.840	6401.625	16916.852	11649.852
5.94	5641.773	6837.227	19066.727	11920.914
6.79	5737.844	6976.836	21201.586	11475.785
7.64	5935.281	7273.105	23264.711	11584.539

REYNOLDS NO	PLAIN END REYN NO	FLOW RATE PER AREA KG/(SEC*M**2)	FRICTION FACTOR	SIEDER TATE CONSTANT
12241.36	12241.36	845.43	0.00640622	0.02517331
17942.57	17942.58	1268.57	C.CC695294	0.02524173
23611.58	23611.57	1691.75	0.00640115	0.02528082
34817.05	34817.05	2538.23	0.00614132	0.02533179
46153.02	46152.99	3384.58	C.00604364	0.02534920
57723.41	57723.39	4230.70	C.00572763	C.C2534753
69057.31	69057.25	5077.05	C.C0549C50	C.C2535665
80405.81	80405.75	5923.38	C.00532453	0.02536249
91718.75	91718.69	6769.76	C.00513339	0.02536630
103126.00	103125.94	7616.04	C.00506665	C.02536996

Table XX. Page 2

NUSSELT NO	NU/PR1/3(U/UW)0.14	STANTON NO	J FACTOR	PERFORM FACTOR
50.85431	46.90327	0.00121665	C.CC4C642	1.2688131
333.23285	63.86072	0.00109840	0.0037280	1.CEC1144
153.58606	79.66914	0.00102481	C.CC35132	1.C976677
2C5.73592	1C8.91785	0.00C93C75	C.0C32324	1.0526867
242.78ECS	136.55585	0.00087392	0.0030486	1.008.444
311.81C06	163.31151	0.00082562	0.0C28928	1.0101194
356.55654	188.56353	0.00079564	0.0027807	1.0125251
4C5.1354C	213.02852	0.00076941	0.0026931	1.0115747
45C.13306	236.73218	0.0007478C	C.0C26213	1.0212736
493.56602	260.02366	0.00072935	0.0025578	1.C092764

XIA	PRESSURE DROP (KPA)	PRANCTL NC	L/LA	DCTPS(KG/SEC)
C.27674622C-C3	0.63076	6.05025	1.06071	C.1160734
C.20CC847C-03	1.52976	6.25276	1.04745	C.17717C2
C.16562C3C-C3	2.52236	6.34720	1.C412C	C.2362716
C.1215335C-C3	5.44626	6.47216	1.03325	0.3544927
C.97CC6795-C4	5.52901	6.51530	1.03032	C.4726552
C.81ECC7EC-C4	14.11046	6.51117	1.C2246	C.55C8645
C.71C7483C-C4	19.47865	6.53384	1.01838	0.7C50670
C.62955200-C4	25.71184	6.5484C	1.01653	0.8272675
C.5671181C-04	32.37816	6.56251	1.01555	0.9454739
C.51682C3C-04	4C.46204	6.567C5	1.01444	1.0636654

Table XXI. TURBOTEC High Pitch Results (Tube No. T-1), Run 4

VELOCITY M/SEC	UN W/(C*M**2)	UC W/(C*M**2)	HI W/(C*M**2)	HO W/(C*M**2)
0.72	4345.867	4387.746	6961.398	14261.211
1.08	5173.234	5232.688	9453.379	13348.801
1.45	5605.344	5675.211	11740.141	12100.102
1.81	6083.211	6165.590	13914.676	12011.875
2.17	6661.199	6760.105	15970.797	12634.234
2.89	7628.879	7758.883	19869.020	13586.664
3.61	8229.887	8381.391	23488.238	13784.102
4.34	8597.719	8763.203	26987.008	13621.789
5.06	8839.641	9014.664	30357.059	13378.457
5.78	9253.152	9445.113	33607.902	13662.793
6.04	9327.500	9522.582	34683.043	13634.508

REYNOLDS NO	PLAIN END REYN NO	FLOW RATE PER AREA KG/(SEC*M**2)	FRICTION FACTOR	SIEDER TATE CONSTANT
13091.02	13091.01	718.06	0.02607292	0.04356441
18877.66	18877.66	1077.82	0.02383088	0.04376480
24513.09	24513.07	1437.72	0.02303237	0.04390023
30196.27	30196.25	1797.58	0.02219686	0.04367545
35789.34	35789.31	2157.52	0.02166928	0.04403932
46917.60	46917.60	2877.45	0.02148015	0.04412690
57873.93	57873.90	3597.55	0.02217391	0.04419569
68930.00	68930.00	4317.55	0.02213186	0.04423466
79748.63	79748.63	5037.77	0.02232075	0.04427816
90575.19	90575.25	5757.55	0.02250340	0.04431063
93982.63	93982.63	6010.43	0.02248217	0.04434135

Table XXI. Page 2

NUSSELT NO	NU/PR1/3(U/UW)0.14	STANTON NO	J FACTOR	PERFORM FACTOR
156.30679	85.64661	0.00231856	0.0069142	0.5303742
213.23642	115.31424	0.0020976E	0.0064439	0.5407984
265.63745	142.55551	0.0019520E	0.0061201	0.5314314
315.37891	168.72205	0.00185024	0.0058658	0.5285262
362.50706	193.57210	0.00176919	0.0056620	0.5225787
451.88647	240.86383	0.00165012	0.0053493	0.4982729
535.03198	285.34180	0.00156007	0.0051087	0.4807866
615.27148	328.46411	0.00149346	0.0049185	0.4444761
692.78540	369.45972	0.00143969	0.0047717	0.4275557
767.53540	409.36865	0.00139443	0.0046436	0.4127043
792.63867	421.93506	0.00137853	0.0046113	0.4102182

XIN	PRESSURE DROP (KPA)	PRANDTL NO	U/UW	DOTMS(KG/SEC)
0.28023736-03	1.71268	5.14975	1.05683	0.1177993
0.20639586-03	3.52454	5.38646	1.05490	0.1766167
0.16621036-03	6.05854	5.55143	1.05237	0.2358615
0.14024336-03	9.12524	5.64485	1.04981	0.2948965
0.12219386-03	12.83053	5.72517	1.04683	0.3539453
0.98226306-04	22.61676	5.83685	1.04199	0.4720519
0.83095136-04	36.48749	5.92586	1.03617	0.5901853
0.72324156-04	52.44830	5.97675	1.03218	0.7083027
0.64297226-04	72.00645	6.03403	1.02998	0.8264572
0.58079336-04	94.82741	6.07707	1.02743	0.9446105
0.56280116-04	103.21783	6.11803	1.02713	0.9860229

RES	AR AT	RESR	AR ATR
20021.69	0.8707	18457.55	0.6933
28566.20	0.8593	26752.75	0.7152
37374.35	0.8619	35996.56	0.7758
46109.28	0.8614	45012.48	0.8053
54382.02	0.8631	53589.90	0.8074
73525.19	0.8765	71908.88	0.8236
94029.38	0.9008	93026.50	0.8741
113809.44	0.9116	114744.75	0.9328
134126.44	0.9242	137670.69	0.9966
154640.31	0.9357	160353.56	1.0321
161126.38	0.9372	167826.21	1.0505

Table XXII. TURBOTEC Medium Pitch Results (Tube No. T-2), Run 5

VELOCITY M/SEC	UN W/(C*M**2)	UC W/(C*M**2)	HI W/(C*M**2)	HO W/(C*M**2)
0.72	5669.016	5740.492	11643.020	12521.657
1.08	6784.199	6886.816	15810.492	13204.633
1.45	7545.875	7673.043	19643.055	13439.512
1.81	7967.895	8109.820	23287.336	13133.632
2.17	8206.039	8356.656	26721.203	12729.383
2.89	8753.852	8925.461	33152.770	12673.152
3.61	9217.707	9408.180	39317.199	12762.738
4.34	9677.176	9887.328	45123.391	13021.344

REYNOLDS NO	PLAIN END REYN NO	FLOW RATE PER AREA KG/(SEC*M**2)	FRICTION FACTOR	SIEDER TATE CONSTANT
12927.06	12927.06	718.22	0.03385161	0.07303506
18634.64	18634.65	1078.05	0.03550368	0.07337445
24120.38	24120.37	1438.10	0.03550179	0.07362926
29573.42	29573.41	1798.17	0.03952480	0.07379621
34910.25	34910.23	2158.35	0.04017805	0.07393849
45630.64	45630.64	2878.67	0.03825636	0.07411146
56426.27	56426.24	3598.92	0.03791236	0.07420558
67037.88	67037.88	4319.34	0.03795416	0.07429302

Table XXII. Page 2

NUSSELT NO	NU/PR1/3(U/UW)0.14	STANTON NO	J FACTOR	PERFORM FACTOR
261.80835	142.14476	0.00387665	0.0116715	0.6895911
357.17136	191.33801	0.00350619	0.0108805	0.5508596
445.25257	236.02461	0.00326481	0.0103624	0.5246545
529.10278	278.45435	0.00309502	0.0099689	0.5044367
608.25321	318.59009	0.00295838	0.0096484	0.4882844
756.46548	395.63013	0.00275156	0.0091106	0.4762546
898.26709	469.48389	0.00260990	0.0087128	0.4596278
1032.13403	539.51465	0.00249553	0.0083946	0.4423521

XIA	PRESSURE DROP (KPA)	PRANDTL NO	U/UW	COTMS(KG/SEC)
0.28050500-03	2.22413	5.22429	1.06148	0.1178252
0.20659840-03	5.84379	5.46663	1.05967	0.1768569
0.16630760-03	10.39247	5.65462	1.05898	0.2355229
0.14025210-03	16.25418	5.78063	1.05875	0.2949538
0.12227110-03	23.79889	5.88988	1.05725	0.3540822
0.98558260-04	40.29771	6.02498	1.05075	0.4722518
0.83109010-04	62.40901	6.09958	1.04717	0.5904058
0.72417650-04	89.98145	6.16955	1.04307	0.7085964

RES	ARAT	RESR	ARATR
17376.97	0.4684	18049.66	0.5209
28002.56	0.5097	29015.37	0.5630
37128.51	0.5178	39038.70	0.5955
46420.60	0.5248	49558.77	0.6446
56118.82	0.5338	61697.56	0.7024
73433.25	0.5331	83906.88	0.7743
92278.94	0.5393	108057.31	0.8390
111534.94	0.5461	132811.75	0.8904

Table XXIII. TURBOTEC Low Pitch Results (Tube No. T-3a), Run 6

VELOCITY M/SEC	UA W/(C*M**2)	UC W/(C*M**2)	HI W/(C*M**2)	HO W/(C*M**2)
0.72	8137.406	8285.492	19EC4.E71	1533C.168
1.08	9417.445	9616.352	2EE36.E16	15857.914
1.45	1C239.64E	10475.23E	33282.734	16010.105
1.81	1C620.418	10874.070	39263.E52	15628.297
2.17	1C816.137	11079.344	44918.496	15196.547

REYNOLDS NO	PLAIN END REYN NO	FLOW RATE PER AREA KG/(SEC*M**2)	FRICTION FACTOR	SIEDER TATE CONSTANT
13760.59	13760.59	717.41	0.12511581	0.12150186
19846.45	19846.46	1076.85	C.11536783	0.12205565
25670.59	25670.58	1436.61	C.10999535	0.12248725
31329.66	31329.85	1796.49	0.10927933	C.12282926
36846.22	36846.19	2156.51	0.10350418	0.12311852

Table XXIII. Page 2

NUSSELT NO	NU/PR1/3(U/UW)0.14	STANTON NO	J FACTOR	PERFORM FACTOR
442.12183	248.59477	0.0066C415	0.0189616	0.3030953
6C1.E3276	334.73657	0.0059603E	0.0176313	0.3056543
745.C2588	412.70386	0.00553955	0.0167704	0.3045202
E86.C9741	485.36426	0.00522545	0.0161C85	0.2948141
1016.C9814	553.90674	0.00497930	0.0155866	0.3011777

XIN	PRESSURE DROP (KPA)	PRANDTL NO	U/UW	DOTMS(KG/SEC)
0.2762678D-03	8.21145	4.865C6	1.04955	0.1176929
C.2C39C91C-03	17.C4794	5.08765	1.04536	0.1766658
0.1644366C-03	28.91216	5.26690	1.04313	C.2356795
0.1394CC6C-03	44.89621	5.41282	1.03979	0.2947188
0.1218E69D-C3	61.25697	5.53827	1.03683	C.3537801

RES	ARAT	RESR	ARATR
27744.18	0.3894	29144.75	0.4470
39766.26	0.3857	42934.77	0.4781
51443.33	0.3844	57099.95	0.5148
63748.82	0.3880	73049.50	0.5682
74071.31	0.3834	87839.44	0.6179

Table XXIV. TURBOTEC Variable Pitch Results (Tube No. T-4), Run 15

VELOCITY M/SEC	UN W/(C*M**2)	UC W/(C*M**2)	HI W/(C*M**2)	HO W/(C*M**2)
0.72	6817.508	6921.145	16353.715	12933.523
1.08	7934.602	8075.332	22188.113	13453.684
1.45	8719.398	8889.641	27607.883	13754.398
1.81	9333.645	9528.988	32755.023	14003.926
2.17	9827.422	9835.395	37619.941	13797.707
2.53	10023.648	10249.504	42321.691	13964.215
2.89	10102.074	10331.305	46833.070	13635.202
3.61	10210.152	10444.371	55511.547	13165.145
4.34	10436.324	10681.160	63858.746	13083.391
4.95	10491.711	10739.184	70903.375	12882.418

REYNOLDS NO	PLAIN END REYN NO	FLOW RATE PER AREA KG/(SEC*M**2)	FRICTION FACTOR	SIEDER TATE CONSTANT
13227.14	13227.14	717.08	0.07889372	0.10247058
19066.88	19066.88	1077.57	0.07422346	0.10294491
24878.93	24878.92	1437.28	0.07102144	0.10320425
30713.95	30713.94	1796.97	0.06416225	0.10335416
36398.04	36398.04	2156.80	0.06666815	0.10350531
42099.82	42099.82	2516.62	0.06510544	0.10360962
47861.77	47861.74	2876.38	0.06454861	0.10367334
59178.08	59178.05	3596.09	0.06295001	0.10380576
70754.94	70754.94	4315.55	0.06339252	0.10365013
80730.94	80730.94	4926.97	0.06333047	0.10385728

Table XXIV. Page 2

NUSSELT NO	NU/PR1/3(U/UW)0.14	STANTON NO	J FACTOR	PERFORM FACTOR
366.55546	203.12881	0.00544860	0.0161154	0.4085352
499.66530	273.41846	0.00492363	0.0150097	0.4044467
623.30713	339.12671	0.00455237	0.0142218	0.4007738
740.58838	401.97125	0.00435757	0.0136325	0.4249378
851.82861	461.13110	0.00416943	0.0131687	0.3950507
959.25586	518.58926	0.00401964	0.0127790	0.3925641
1062.16305	574.98623	0.00389163	0.0124216	0.3848765
1260.55668	682.25854	0.00368928	0.0118736	0.3770004
1451.67969	787.42944	0.00353862	0.0114205	0.3603120
1610.92529	875.12158	0.00343924	0.0111048	0.3506937

XIN	PRESSURE DROP (KPA)	PRANDTL NO	U/UW	COTMS(KG/SEC)
0.28103890-03	5.18108	5.08670	1.04935	0.1177655
0.20717050-03	10.97496	5.32270	1.04671	0.1767775
0.16651400-03	18.67610	5.45548	1.04407	0.2357850
0.14035450-03	26.36850	5.53346	1.04164	0.2947968
0.12221020-03	39.46162	5.61303	1.03943	0.3538275
0.10863670-03	52.45993	5.66848	1.03742	0.4128566
0.98173830-04	67.93677	5.70257	1.03557	0.4718754
0.82829060-04	103.60895	5.77396	1.02952	0.5899461
0.71956160-04	150.15885	5.79803	1.02620	0.7079756
0.64849450-04	195.52775	5.80193	1.02443	0.8062795

RES	ARAT	RESR	ARATR
22968.65	0.4097	24782.84	0.5065
33233.57	0.4091	36716.16	0.5456
43507.43	0.4091	49146.00	0.5756
52100.98	0.3987	60256.19	0.5951
63966.06	0.4095	75640.13	0.6548
74151.06	0.4099	89105.81	0.6855
84956.44	0.4123	104707.06	0.7393
105975.25	0.4145	136334.50	0.8353
129374.88	0.4213	171091.44	0.9215
149457.00	0.4256	202682.63	0.9980

Table XXV. TURBOTEC Low Pitch "supported" Results (Tube No. T-3b), Run 17

VELOCITY M/SEC	UA W/(C*M**2)	UC W/(C*M**2)	HI W/(C*M**2)	HJ W/(C*M**2)
0.72	8221.465	8372.652	20625.078	15104.402
1.08	9631.402	9839.591	27973.867	16034.695
1.45	10453.996	10699.666	34862.805	16141.035
1.81	11134.688	11413.824	41422.941	16367.725
2.17	11440.375	11735.250	47755.512	16073.653
2.53	11652.484	11958.543	53777.309	15823.563
2.89	11882.695	12201.133	59683.809	15734.250
3.25	12098.879	12429.168	65527.684	15700.258
3.61	12180.340	12515.152	71249.000	15507.117
4.12	12130.766	12462.820	79125.313	15070.086

REYNOLDS NO	PLAIN END REYN NO	FLOW RATE PER AREA KG/(SEC*M**2)	FRICTION FACTOR	SIEDER TATE CONSTANT
14012.51	14012.51	717.12	0.11084348	0.12630755
20236.98	20236.99	1076.44	0.08994156	0.12686116
26474.89	26474.88	1435.74	0.10638664	0.12714034
32810.00	32809.97	1794.95	0.10298234	0.12726724
39266.18	39266.15	2154.05	0.10106218	0.12730700
45533.38	45533.35	2513.32	0.10069597	0.12729604
51932.75	51932.72	2872.47	0.09764057	0.12742656
58404.72	58404.69	3231.55	0.09673011	0.12743157
64945.20	64945.17	3590.56	0.09614348	0.12741595
74279.50	74279.38	4093.00	0.09403992	0.12737167

Table XXV. Page 2

NUSSELT NO	NU/PR1/3(U/UW)0.14	STANTON NO	J FACTOR	PERFORM FACTOR
459.49780	262.20508	0.00688465	0.0194897	0.3516614
625.64673	353.38257	0.00621637	0.0181120	0.4027514
781.43634	439.08569	0.00580776	0.0171676	0.3227388
929.40576	521.81958	0.00551935	0.0164221	0.3185299
1071.82446	602.65112	0.00530226	0.0158085	0.3126465
1207.82788	678.92358	0.00511714	0.0153270	0.3044223
1340.60151	754.41821	0.00496903	0.0149064	0.3053318
1472.14258	828.77148	0.00484935	0.0145511	0.3006595
1600.53174	902.14014	0.00474557	0.0142312	0.2960400
1776.75179	1004.07617	0.00462332	0.0138302	0.2941351

XIN	PRESSURE DROP (KPA)	PRANDTL NO	C/UW	DCTNS(KG/SEC)
0.27631550-03	7.27152	4.76306	1.04155	0.1176445
0.20385500-03	13.28513	4.97332	1.03721	0.1765918
0.16356460-03	27.94595	5.08218	1.03513	0.2355366
0.13768220-03	42.27470	5.13229	1.03256	0.2944659
0.11942610-03	59.74336	5.14806	1.03001	0.3533757
0.10605580-03	81.03131	5.18380	1.02794	0.4123156
0.95560930-04	102.62909	5.19579	1.02613	0.4712344
0.87038740-04	128.67958	5.19778	1.02544	0.5301418
0.80049200-04	157.89804	5.19312	1.02450	0.5890365
0.72079550-04	200.70287	5.17384	1.02313	0.6714645

RES	ARAT	RESR	ARATR
28128.16	0.3515	28566.82	0.4518
35166.65	0.3313	39656.04	0.4630
51371.16	0.3609	58686.42	0.5235
62962.67	0.3615	74615.00	0.5570
77154.94	0.3642	92505.50	0.6045
90654.44	0.3677	111293.69	0.6525
103150.63	0.3669	129313.38	0.6905
118825.19	0.3685	148547.19	0.7284
130901.54	0.3712	170387.13	0.7728
150956.13	0.3721	200922.50	0.8420

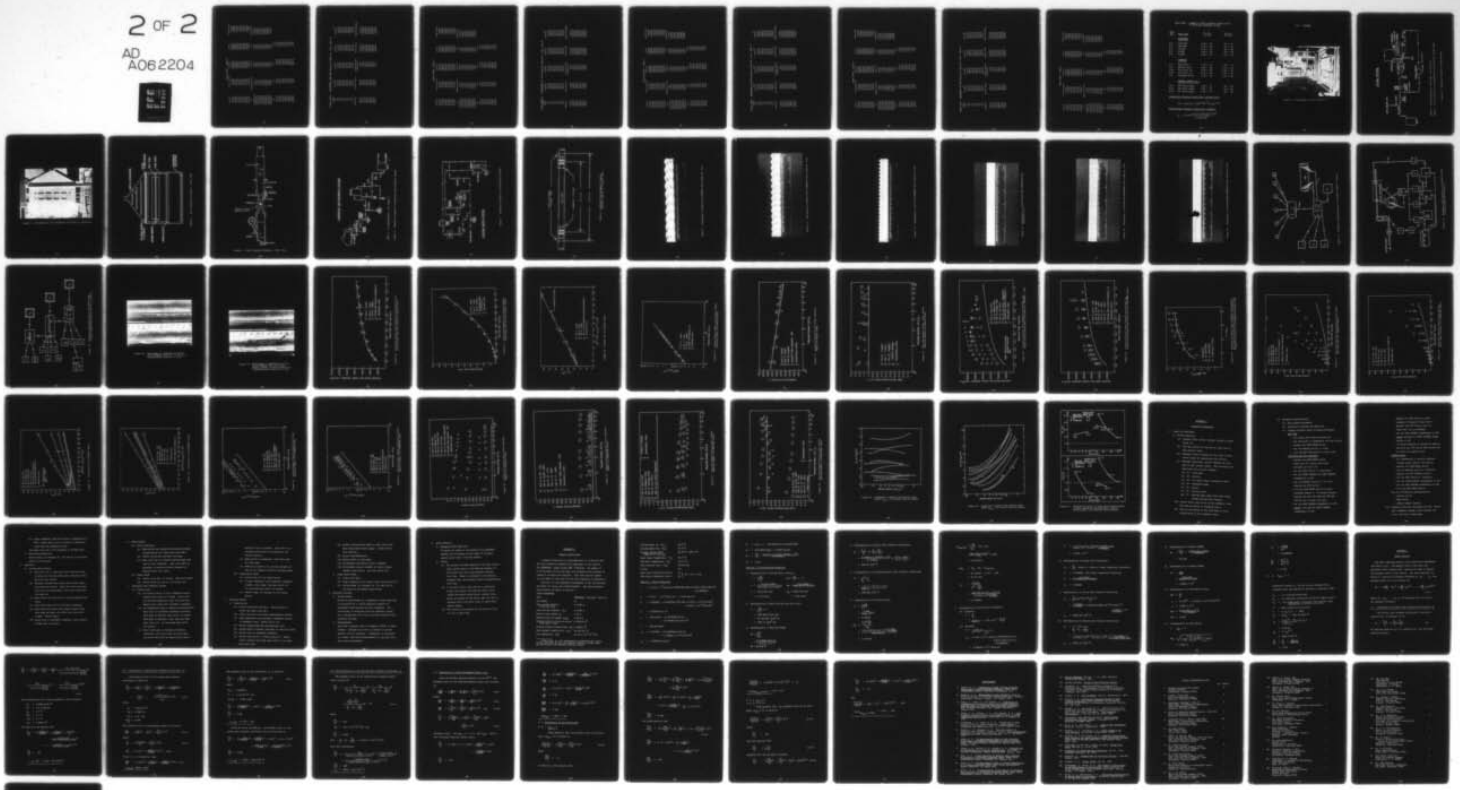
Table XXVI. KORODENSE CuNi-LPD Results (Tube No. K-1), Run 9

VELOCITY M/SEC	UN W/(C*M**2)	LC W/(C*M**2)	HI W/(C*M**2)	HO W/(C*M**2)
0.84	3449.565	3852.432	6970.258	11181.824
1.26	4115.902	4702.680	9495.578	11356.176
1.69	4619.316	5371.523	11877.922	11584.625
2.11	4930.691	5797.516	14088.590	11330.008
2.53	5236.695	6224.914	16207.367	11432.391
3.37	5577.262	6712.129	20216.207	11071.711
4.21	5924.813	7221.973	24022.469	11223.645
5.06	6310.086	7832.680	27775.582	11700.941
5.90	6426.695	7981.762	31481.777	11413.652
6.74	6650.141	8329.348	35138.105	11586.676
7.49	6623.977	8288.344	38304.125	11149.551

REYNOLDS NO	PLAIN END REYN NO	FLOW RATE PER AREA KG/(SEC*M**2)	FRICTION FACTOR	SIEDER TATE CONSTANT
13010.39	13010.39	838.19	0.01341556	0.04026243
19077.74	19077.75	1257.73	0.01214029	0.04036942
25315.76	25315.74	1677.10	0.01177227	0.04039202
31317.43	31317.41	2096.71	0.01117707	0.04044124
37220.58	37220.58	2516.42	0.01076251	0.04048696
48911.50	48911.47	3355.96	0.00997351	0.04055607
60513.92	60513.92	4195.58	0.00917143	0.04066508
72813.94	72813.94	5034.50	0.00871721	0.04059215
85364.31	85364.31	5873.16	0.00819452	0.04056893
98432.06	98432.13	6711.29	0.00779372	0.04052652
110356.00	110356.00	7456.92	0.00742333	0.04048440

AD-A062 204 NAVAL POSTGRADUATE SCHOOL MONTEREY CALIF F/G 13/11
AN EXPERIMENTAL COMPARISON OF ENHANCED HEAT TRANSFER CONDENSER --ETC(U)
SEP 78 J H FENNER
UNCLASSIFIED NPS69-78-015 NL

2 OF 2
AD A062204



END
DATE FILMED
3-79
DDC

Table XXVI. Page 2

NUSSELT NO	NU/PR1/3(U/Uw)0.14	STANTON NO	J FACTOR	PERFORM FACTOR
144.29463	78.76468	0.00196772	0.0063107	0.9408027
199.62661	107.26891	0.00180430	0.0058280	0.9601094
250.10101	134.58833	0.00169254	0.0054869	0.9321786
296.84155	159.75432	0.00160474	0.0052436	0.9382735
342.06372	183.62897	0.00153853	0.0050655	0.9413223
427.40336	228.86746	0.00143921	0.0047899	0.9605172
506.48413	271.68335	0.00136782	0.0045880	1.0004588
587.73901	314.92896	0.00131801	0.0044118	1.0122128
665.78223	357.44849	0.00128061	0.0042708	1.0223546
742.33308	400.17334	0.00125093	0.0041437	1.0333335
808.37451	438.05005	0.00122738	0.0040383	1.0380127

XIA	PRESSURE DROP (KPA)	PRANDTL NO	L/Uh	DOTMS (KG/SEC)
0.27688086E-03	1.29473	5.65694	1.04240	0.1179556
0.20320595E-03	2.63717	5.80522	1.03651	0.1769969
0.16245510-03	4.54651	5.83693	1.03208	0.2360135
0.13704720-03	6.74584	5.90653	1.02792	0.2950642
0.11906800-03	9.35509	5.97178	1.02675	0.3541288
0.95462180-04	15.41536	6.07156	1.02365	0.4722747
0.80339700-04	22.15285	6.14318	1.02192	0.5904332
0.69483240-04	30.31905	6.12421	1.02005	0.7084917
0.61302230-04	38.79030	6.09029	1.01993	0.8265139
0.54921500-04	48.18045	6.02874	1.01923	0.9444621
0.50380200-04	56.66183	5.96813	1.01736	1.0493927

RES	ARAT	RESR	ARATR
14837.93	0.7449	14709.39	0.7270
21476.86	0.7353	21595.28	0.7467
28861.05	0.7423	29340.42	0.7774
35515.42	0.7383	36884.27	0.8208
42117.08	0.7362	44368.55	0.8517
54707.69	0.7281	59828.09	0.9354
66262.50	0.7150	74237.81	0.9866
79196.38	0.7114	90008.44	1.0160
91488.94	0.7035	106845.31	1.0863
104412.69	0.6984	123752.69	1.1250
115620.19	0.6923	140663.81	1.1986

Table XXVII. KORODENSE CuNi-MHT Results (Tube No. K-2), Run 12

VELOCITY M/SEC	UN W/(C*M**2)	UC W/(C*M**2)	HI W/(C*M**2)	HO W/(C*M**2)
0.84	4040.391	4172.492	8857.871	9400.336
1.26	4924.137	5121.762	12120.863	10266.848
1.69	5460.352	5704.430	15111.156	10328.441
2.11	5847.070	6127.832	17921.152	10307.859
2.53	6146.977	6458.047	20638.617	10268.785
3.37	6661.055	7027.883	25795.059	10382.688
4.21	6902.914	7297.656	30609.824	10174.398
5.06	7344.488	7792.988	35316.492	10555.250
5.90	6947.938	7347.996	39493.660	9428.406
6.74	6954.945	7355.832	43657.625	9192.730

REYNOLDS NO	PLAIN END REYN NO	FLOW RATE PER AREA KG/(SEC*M**2)	FRICTION FACTOR	SIEDER TATE CONSTANT
14252.58	14252.58	836.90	0.01253328	0.04865980
20984.25	20984.26	1255.76	0.01208469	0.04876507
27645.67	27645.66	1674.69	0.01152392	0.04883301
34256.02	34255.99	2093.67	0.01129129	0.04888270
40826.96	40826.96	2512.70	0.01114958	0.04892164
53933.54	53933.54	3350.79	0.01023959	0.04857449
66999.88	66999.88	4188.91	0.00986918	0.04900990
80021.13	80021.13	5027.09	0.00923088	0.04903689
90835.69	90835.69	5867.54	0.00898437	0.04919394
101990.31	101990.38	6707.64	0.00873101	0.04929592

Table XXVII. Page 2

NUSSELT NO	NU/PR1/3(U/UW)0.14	STANTON NO	J FACTOR	PERFORM FACTOR
184.78058	102.39630	0.00254251	0.0075337	1.2020350
252.25648	139.83742	0.00230831	0.0069353	1.1477776
314.52773	174.58806	0.00215772	0.0065421	1.1354036
373.87026	207.46458	0.00204674	0.0062471	1.1065273
430.90503	238.92329	0.00196353	0.0060256	1.0898601
535.14600	298.85205	0.00184055	0.0056870	1.1000357
640.24268	355.74780	0.00174702	0.0054235	1.0996782
739.09521	410.28516	0.00167952	0.0052327	1.1215868
829.16089	455.52905	0.00160883	0.0051179	1.1392870
918.48242	500.79175	0.00155551	0.0050153	1.1486514

XIN	PRESSURE DROP (KPA)	PRANDTL NO	U/UW	DOTMS(KG/SEC)
0.26477150-03	1.20772	5.09838	1.04848	0.1177741
0.19438170-03	2.62097	5.20782	1.04072	0.1767192
0.15592320-03	4.44420	5.27946	1.03594	0.2356745
0.13147900-03	6.80492	5.33235	1.03150	0.2946372
0.11417040-03	9.67719	5.37413	1.02964	0.3536053
0.91250870-04	15.95660	5.43125	1.02632	0.4715471
0.76983660-04	23.80032	5.46981	1.02144	0.5894945
0.66725130-04	32.40565	5.49933	1.02057	0.7074487
0.59674000-04	42.48856	5.67378	1.02054	0.8257240
0.53586050-04	53.94536	5.78948	1.02141	0.9439486

RES	ARAT	RESR	ARATR
14422.18	0.5601	18645.04	0.7035
21645.27	0.5677	23498.12	0.7141
28611.13	0.5663	31611.81	0.7514
35834.66	0.5726	40304.36	0.7958
43173.75	0.5771	49382.47	0.8407
50443.43	0.5717	66489.31	0.9044
65980.75	0.5704	85251.19	0.9913
82703.81	0.5653	102200.25	1.0226
93147.56	0.5600	122230.63	1.1984
104154.63	0.5572	140887.31	1.2966

Table XXVIII. KORODENSE Aℓ- LPD Results (Tube No. K-3), Run 13

VELOCITY M/SEC	UN W/(C*M**2)	LC W/(C*M**2)	HI W/(C*M**2)	HO W/(C*M**2)
0.84	4689.770	4868.688	11390.582	9673.945
1.26	5421.699	5662.258	15441.387	10019.629
1.69	5869.582	6142.676	19212.656	9894.375
2.11	6360.875	6694.559	22802.301	10270.676
2.53	6511.008	6861.066	26232.176	9946.297
3.37	6852.707	7286.246	32784.305	9854.102
4.21	7312.711	7757.219	39061.176	10147.074
5.06	7598.727	8079.832	45086.234	10260.543
5.90	7585.160	8064.492	50875.078	9931.555
6.74	7563.785	8062.941	56582.828	9702.660

REYNOLDS NO	PLAIN END REYN NO	FLOW RATE PER AREA KG/(SEC*M**2)	FRICTION FACTOR	SIEDER TATE CONSTANT
12583.05	12583.05	838.21	0.02143038	0.06561226
18720.30	18720.30	1258.10	0.02024282	0.06591642
24403.00	24403.00	1678.03	0.01566798	0.06609136
30101.49	30101.49	2097.95	0.01852071	0.06619453
35700.71	35700.68	2517.97	0.01801943	0.06626585
46992.19	46992.16	3357.91	0.01649238	0.06638640
58450.04	58450.04	4197.69	0.01515549	0.06642514
70101.44	70101.38	5037.25	0.01419308	0.06642544
81626.94	81627.00	5876.97	0.01317564	0.06644458
93314.13	93314.13	6716.50	0.01265517	0.06644237

Table XXVIII. Page 2

NUSSELT NC	NU/PR1/3(U/UW))0.14	STANTON NC	J FACTOR	PERFORM FACTOR
239.12886	128.14040	0.00324812	0.0103287	0.9659339
325.67212	172.52151	0.00293260	0.0096104	0.9455072
406.28687	213.84485	0.00273539	0.0091187	0.9272628
482.94922	253.33315	0.00259638	0.0087431	0.9441419
556.36035	290.77759	0.00248844	0.0084546	0.9383910
626.37915	362.82568	0.00233181	0.0080004	0.9701909
830.19165	432.27441	0.00222236	0.0076536	1.0100107
958.30859	499.56655	0.00213760	0.0073648	1.0378008
1081.59717	564.64082	0.00206729	0.0071334	1.0624833
1202.90308	628.64063	0.00201153	0.0069405	1.0968676

XIN	PRESSURE DROP (KPA)	PRANDTL NC	U/UW	DOTMS(KG/SEC)
0.2759721D-03	2.06831	5.67053	1.04650	0.1179556
0.2036057D-03	4.29852	5.93178	1.04282	0.1770486
0.1636538D-03	7.60010	6.08653	1.04058	0.2361451
0.1376976D-03	11.18467	6.17938	1.03887	0.2952392
0.1198725D-03	15.67265	6.26256	1.03803	0.3543472
0.9592068D-04	25.50603	6.35517	1.03619	0.4725503
0.8050750D-04	36.62520	6.39116	1.03469	0.5907291
0.6974543D-04	49.39148	6.39518	1.03263	0.7088902
0.6181344D-04	62.42877	6.40930	1.03087	0.8270499
0.5557800D-04	76.29451	6.40725	1.03024	0.9451962

RES	ARAT	RESR	ARATR
14656.79	0.4534	16148.76	0.5948
21256.14	0.4534	24045.14	0.6404
28306.76	0.4561	32598.07	0.6976
34210.91	0.4519	40412.26	0.7204
40682.30	0.4522	49507.63	0.7836
52617.65	0.4452	66693.25	0.8646
64103.88	0.4376	83371.31	0.9134
75763.13	0.4325	101019.06	0.9679
88305.31	0.4249	119443.31	1.0554
97964.19	0.4226	139734.19	1.1416

Table XXIX. KORODENSE Aℓ-MIT Results (Tube No. K-4), Run 11

VELOCITY M/SEC	UN W/(C*M**2)	UC W/(C*M**2)	HI W/(C*M**2)	HO W/(C*M**2)
0.84	4046.648	4612.484	9627.851	10681.094
1.26	4759.902	5562.570	13130.684	11179.004
1.69	5224.180	6207.238	16310.172	11313.578
2.11	5444.910	6521.352	19294.754	10884.135
2.53	5702.129	6893.805	22186.188	10916.660
3.37	6106.473	7493.707	27736.938	11026.824
4.21	6262.539	7730.109	33016.395	10791.598
5.06	6646.410	8323.504	38080.664	11236.156
5.90	6717.094	8434.652	43039.434	10988.605
6.74	6788.648	8547.785	47968.168	10838.285

REYNOLDS NO	PLAIN END REYN NO	FLOW RATE PER AREA KG/(SEC*M**2)	FRICTION FACTOR	SIEDER TATE CONSTANT
14468.44	14468.44	836.67	0.01671752	0.05201293
21015.03	21015.04	1255.72	0.01737395	0.05220737
27370.57	27370.56	1674.97	0.01641210	0.05234984
33584.81	33584.81	2094.37	0.01594628	0.05246294
39826.17	39826.17	2513.74	0.01518683	0.05253560
52288.95	52288.95	3352.49	0.01375036	0.05263028
64678.30	64678.27	4191.31	0.01274708	0.05269491
77188.00	77187.94	5030.01	0.01189908	0.05272682
89694.06	89694.13	5868.72	0.01120712	0.05275345
102266.63	102266.69	6707.36	0.01049045	0.05276796

Table XXIX. Page 2

NUSSELT NO	NU/PR1/3(U/UW)0.14	STANTON NO	J FACTOR	PERFORM FACTOR
199.59317	110.77664	0.00275254	0.0080611	0.9643640
273.22607	149.88394	0.00250070	0.0075050	0.8639322
340.31177	185.66997	0.00232837	0.0071134	0.8668520
403.45483	219.16261	0.00220259	0.0068246	0.8558444
464.55737	251.52890	0.00210996	0.0065969	0.8687621
581.83154	313.30176	0.00197767	0.0062562	0.9073264
693.42798	371.85547	0.00188282	0.0060039	0.9419984
800.30493	426.63379	0.00180945	0.0057941	0.9738727
904.94092	483.57178	0.00175276	0.0056256	1.0046473
1008.84912	537.22485	0.00170920	0.0054955	1.0484819

XIA	PRESSURE DROP (KPA)	PRANDTL NO	U/UW	DOTMS(KG/SEC)
0.26195830-03	1.61052	5.01177	1.05288	0.1177423
0.19213020-03	3.76803	5.19912	1.05226	0.1767147
0.15465010-03	6.33041	5.34000	1.04863	0.2357147
0.13077150-03	9.61473	5.45405	1.04582	0.2947252
0.11373370-03	13.18675	5.52837	1.04453	0.3537514
0.90978470-04	21.29282	5.62644	1.04413	0.4717868
0.76433570-04	30.75821	5.69422	1.04428	0.5898323
0.66270250-04	41.34888	5.73007	1.04340	0.7078605
0.58635940-04	53.01096	5.75619	1.04419	0.8258892
0.52611520-04	64.81354	5.77165	1.04650	0.9439084

RES	APAT	RESR	APATR
16379.42	0.5733	17170.55	0.6542
25128.54	0.5967	26661.46	0.7043
32616.65	0.5934	35436.32	0.7485
40224.29	0.5945	45068.73	0.8175
47314.50	0.5899	54149.88	0.8607
60774.35	0.5786	72132.56	0.9348
72783.13	0.5693	91192.25	1.0303
86564.50	0.5612	108744.75	1.0630
99074.94	0.5542	128391.69	1.1452
110719.31	0.5452	147430.88	1.2157

Table XXX. KORODENSE Ti-MHT Results (Tube No. K-5), Run 14

VELOCITY M/SEC	UN W/(C*M**2)	UC W/(C*M**2)	HI W/(C*M**2)	HO W/(C*M**2)
0.72	4120.527	5008.004	8687.680	13611.307
1.08	4801.230	6050.602	11910.293	13659.281
1.44	5142.234	6602.367	14856.074	12877.766
1.80	5767.867	7670.648	17772.121	14562.434
2.16	5888.797	7886.012	20582.086	13599.379
2.88	6224.777	8500.430	25866.285	13288.977
3.60	6605.590	9226.816	30857.152	13727.727
4.32	6705.023	9421.984	35690.219	13260.445
5.04	6882.063	9775.355	40360.090	13310.207
5.76	7302.133	10645.195	44907.672	14383.836

REYNOLDS NO	PLAIN END REYN NO	FLOW RATE PER AREA KG/(SEC*M**2)	FRICTION FACTOR	SIEDER TATE CONSTANT
12691.84	12691.84	715.86	0.03259499	0.05461306
18545.20	18545.20	1074.26	0.03462725	0.05478032
24065.34	24065.33	1432.68	0.03507061	0.05495308
30176.50	30176.48	1791.13	0.03541131	0.05493348
36363.79	36363.79	2149.21	0.03530702	0.05490662
48282.38	48282.35	2865.81	0.03420818	0.05493348
60051.23	60051.17	3582.55	0.03354866	0.05496568
72061.38	72061.31	4299.06	0.03276976	0.05496568
83983.19	83983.19	5015.66	0.03203691	0.05497244
96081.81	96081.81	5732.08	0.03097348	0.05496568

Table XXX. Page 2

REYNOLDS NO	NU/PR1/3(U/UW)0.14	STANTON NO	J FACTOR	PERFORM FACTOR
155.58678	104.74065	0.00290154	0.0088450	0.5427245
265.51025	142.30058	0.00265061	0.0082416	0.4760174
337.23413	175.83665	0.00247806	0.0078656	0.4485561
403.28027	210.65482	0.00237175	0.0075101	0.4241663
466.81494	244.43263	0.00228919	0.0072256	0.4093037
586.55117	306.80811	0.00215747	0.0068316	0.3954141
700.61230	365.51685	0.00205876	0.0065435	0.3801154
810.34790	422.91431	0.00198435	0.0063074	0.3849534
916.49023	478.07715	0.00192337	0.0061185	0.3819651
1019.63037	532.35742	0.00187262	0.0059523	0.3843474

XIN	PRESSURE DROP (KPA)	PRANDTL NO	U/UW	DOTMS(KG/SEC)
0.28021050-03	2.12332	5.32131	1.07179	0.1178511
0.20441350-03	5.07757	5.48274	1.07408	0.1768546
0.16386750-03	9.14638	5.65493	1.07650	0.2359101
0.13700360-03	14.42935	5.63467	1.07584	0.2948729
0.11825750-03	20.71565	5.60782	1.07495	0.3538233
0.94131960-04	35.68410	5.63467	1.07509	0.4717563
0.78500560-04	54.68568	5.66697	1.07511	0.5897930
0.66222910-04	76.91930	5.66697	1.07474	0.7077511
0.60325430-04	102.35619	5.67378	1.07483	0.8257240
0.54219930-04	129.24959	5.66697	1.07429	0.9436683

RES	ARAT	RESR	ARATR
19324.43	0.6920	18157.49	0.5813
30182.27	0.7277	28766.45	0.6362
40392.61	0.7435	39675.64	0.7071
52070.38	0.7604	50881.54	0.7128
63849.09	0.7715	64171.51	0.7824
85825.31	0.7787	89512.13	0.8761
106010.19	0.7856	115088.38	0.9364
130456.25	0.7897	143567.06	1.0326
152638.75	0.7921	171667.50	1.1007
174042.50	0.7961	196455.56	1.1091

Table XXXI. Summary of Heat Transfer Capabilities of Enhanced Condenser Tubing.

Tube No.	Tube Type	$\overline{Ci}_a/\overline{Ci}_s$	$\overline{ho}_a/\overline{ho}_s$
	KORODENSE		
K-1	CuNi-LPD	1.60 ± .18	.97 ± .11
K-2	CuNi-MHT	2.12 ± .21	.93 ± .09
K-3	Aℓ-LPD	2.60 ± .47	.85 ± .09
K-4	Aℓ-MHT	2.60 ± .29	.85 ± .09
K-5	Ti-MHT	2.20 ± .27	1.15 ± .12
	TURBOTEC		
T-1	High Pitch	1.76 ± .24	1.03 ± .13
T-2	Medium Pitch	2.92 ± .33	1.10 ± .10
T-3a	Low Pitch (u)	4.88 ± .82	1.32 ± .12
T-3b	Low Pitch (s)	5.12 ± .90	1.34 ± .13
T-4	Variable Pitch	4.12 ± .72	1.14 ± .09
	GENERAL ATOMIC [11]		
GA-1	30° Helix Angle	3.28 ± .51	.94 ± .06
GA-2	45° Helix Angle	3.24 ± .50	.94 ± .06
GA-3	60° Helix Angle	3.28 ± .51	.99 ± .09

Inside Heat Transfer Coefficient (Sieder-Tate)

$$Nu_i = h_i D_i / k_b = C_i Re^{0.8} Pr^{1/3} (\mu/\mu_w)^{0.14}$$

Outside Heat Transfer Coefficient (Nusselt)

$$h_o = 0.725 \left[\frac{\rho_f(\rho_f-\rho_v)g\, h_{fg} k_f^3}{\mu_f D_o (T_s-T_w)}\right]^{0.25}$$

VIII. FIGURES

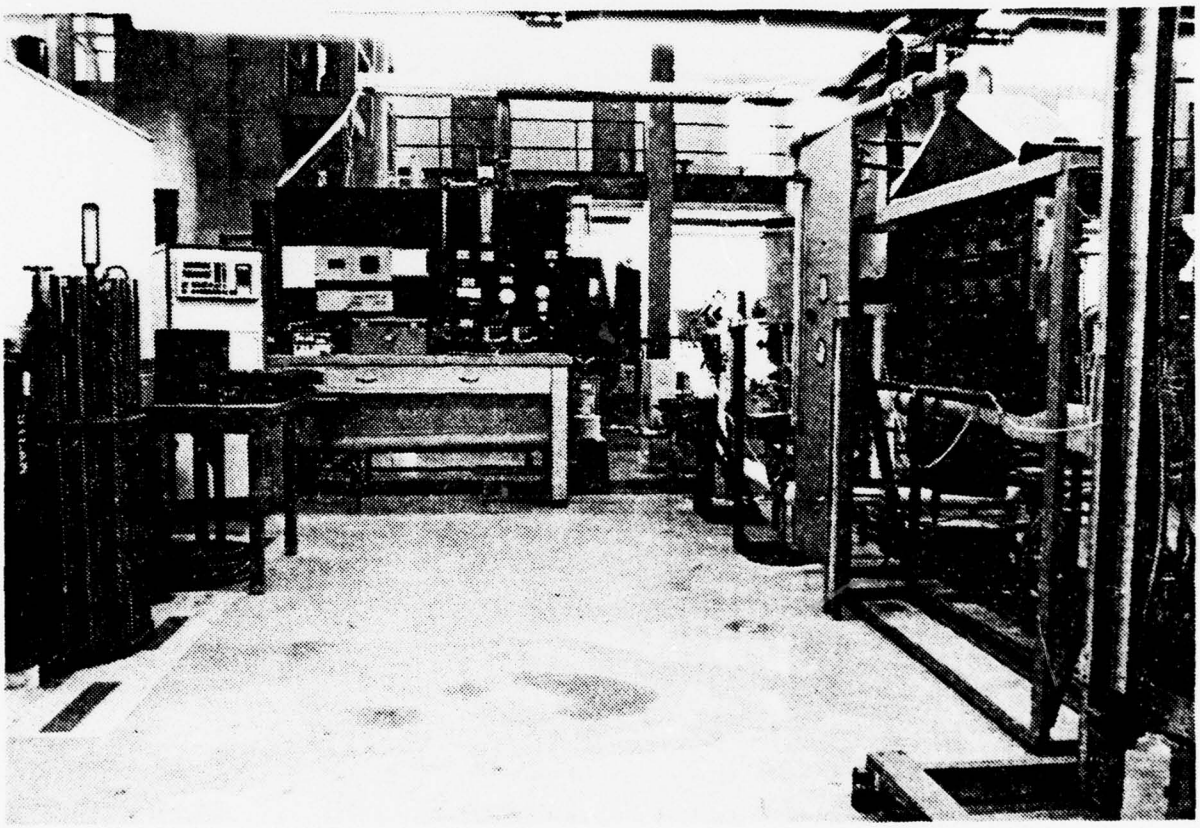
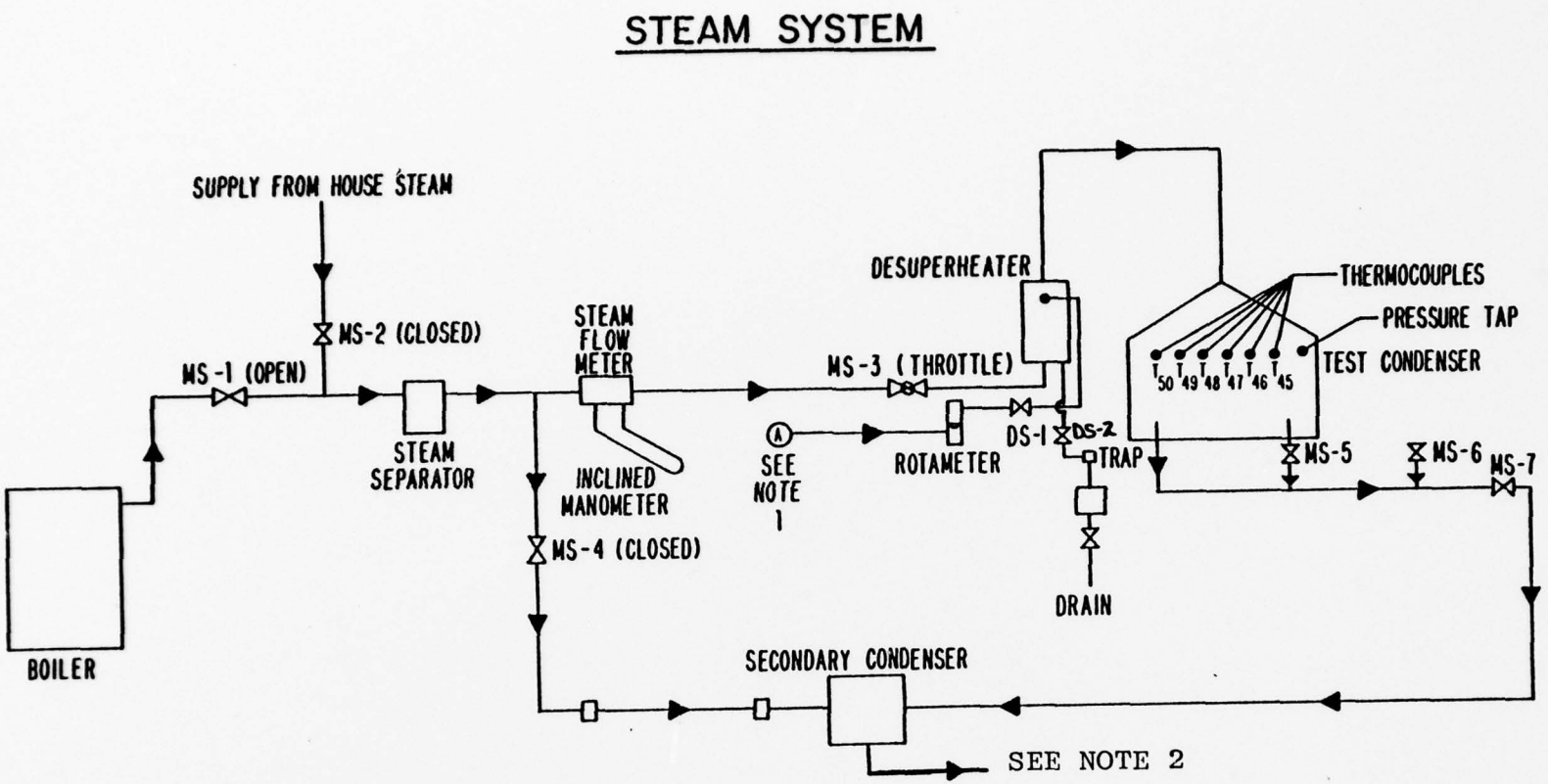


Figure 1. Photograph of Test Facility



NOTE 1: From discharge of feed pump, see Figure 6

NOTE 2: To air ejector via refrigerated cold trap and vacuum pump

Figure 2. Schematic Diagram of Steam System

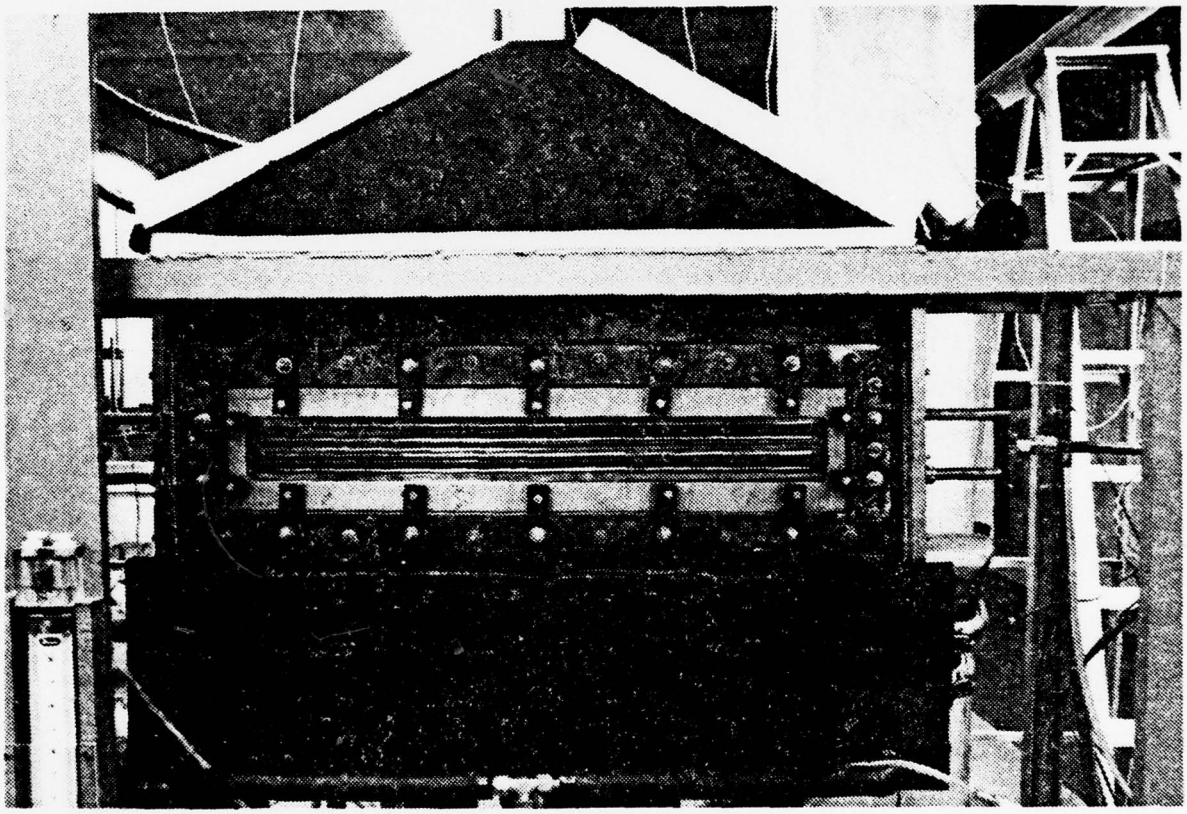


Figure 3. Photograph of Test Condenser with Partial Insulation

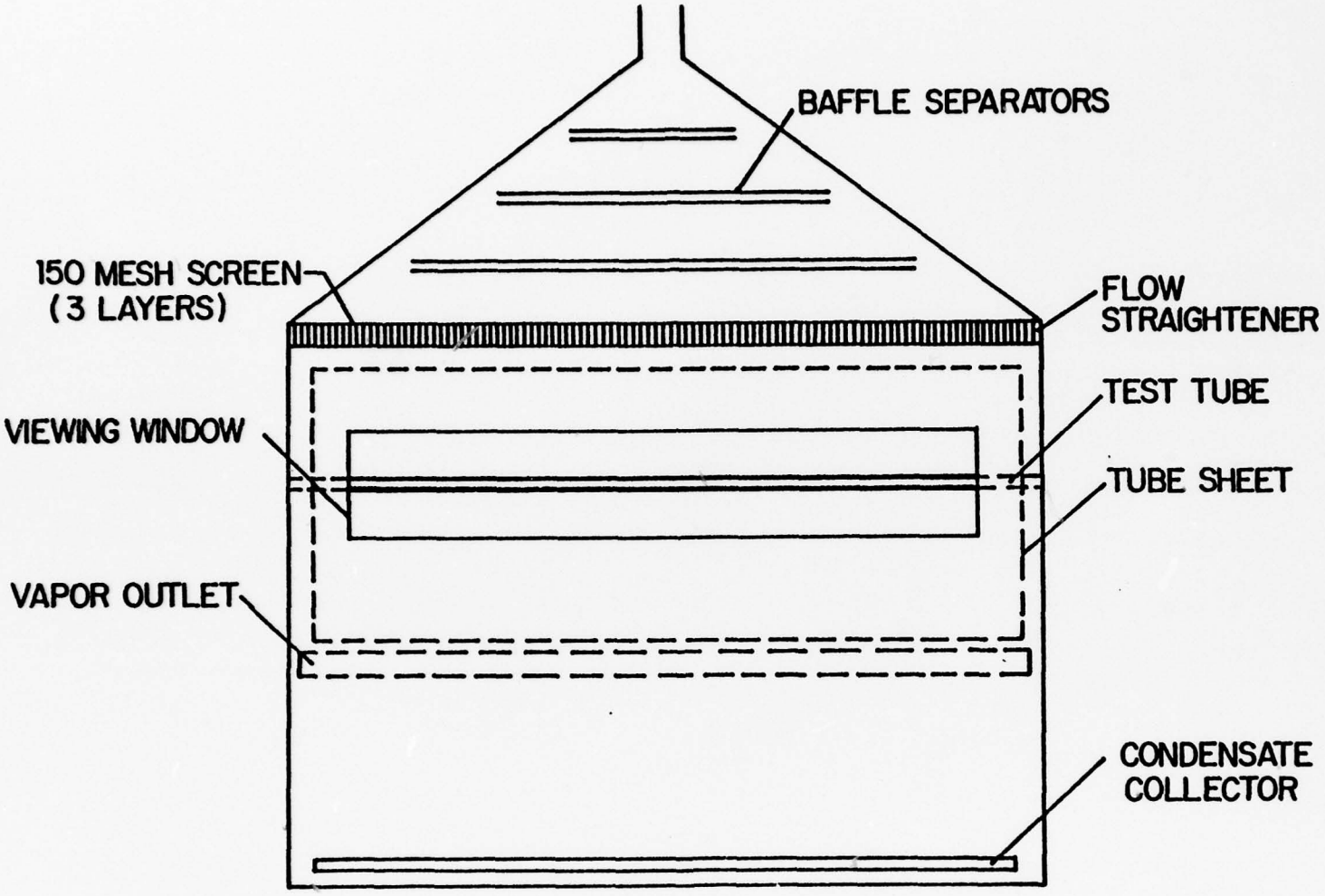


Figure 4. Test Condenser Schematic, Front View

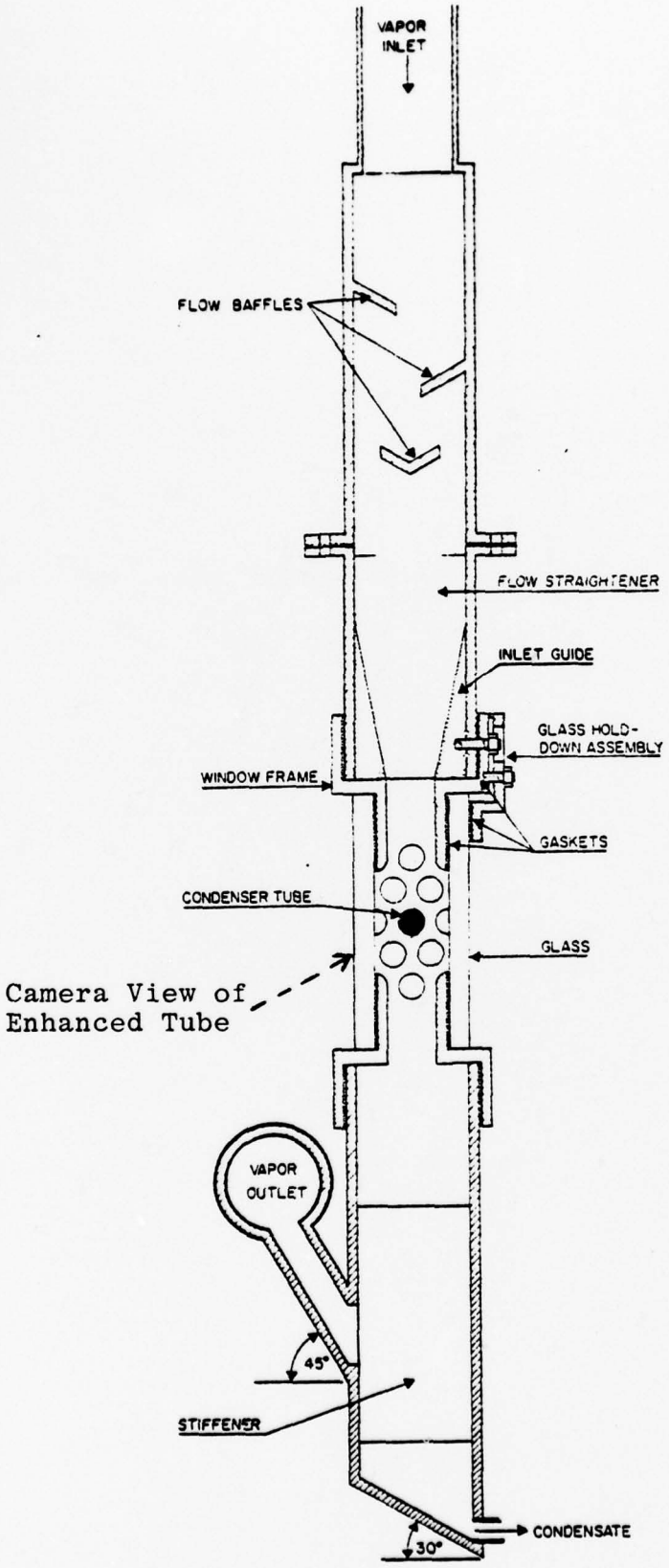
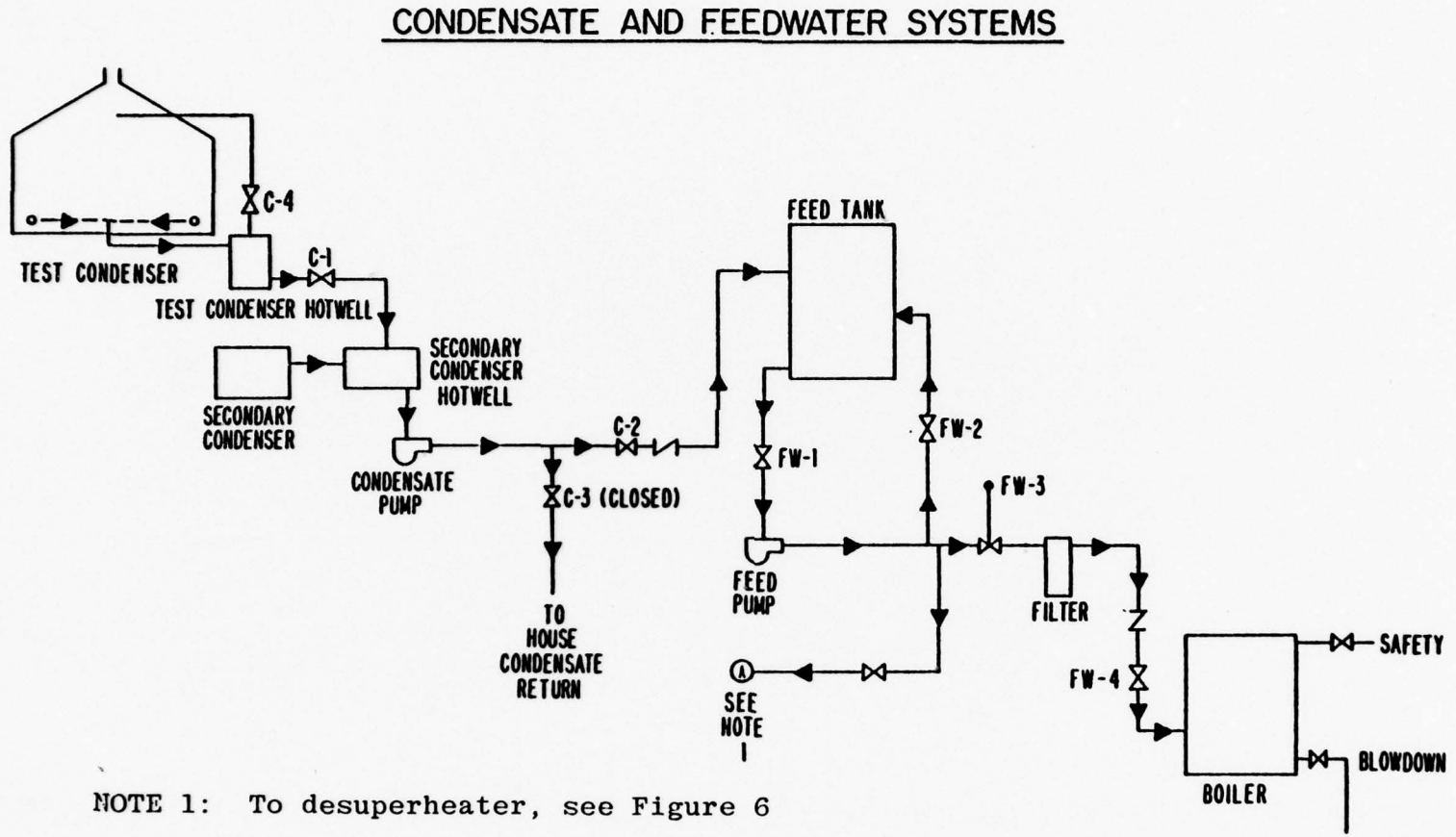
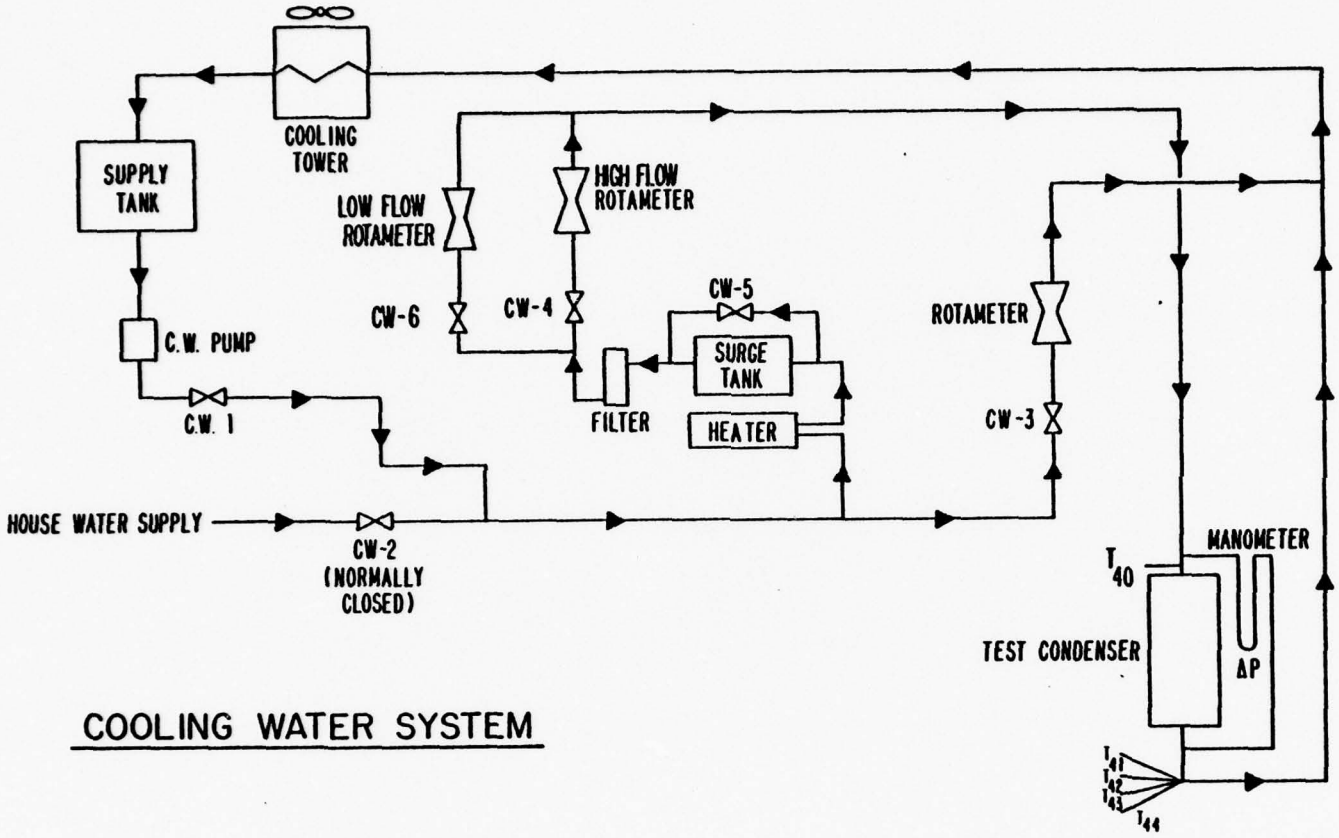


Figure 5. Test Condenser Schematic, Side View



NOTE 1: To desuperheater, see Figure 6

Figure 6. Schematic Diagram of Condensate and Feedwater System



COOLING WATER SYSTEM

Figure 7. Schematic Diagram of Cooling Water System

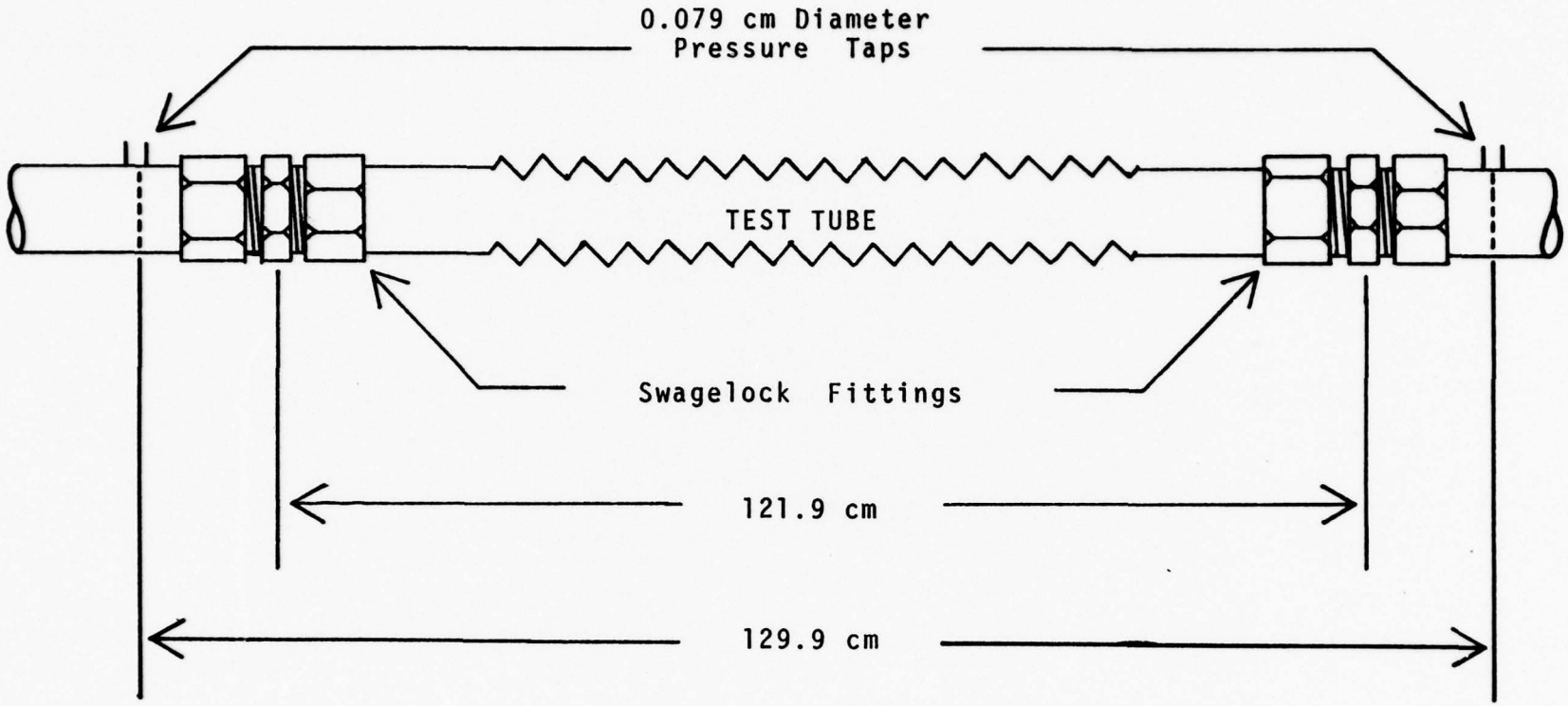


Figure 8. Enhanced Tube Schematic Drawing Showing Location of Pressure Taps.

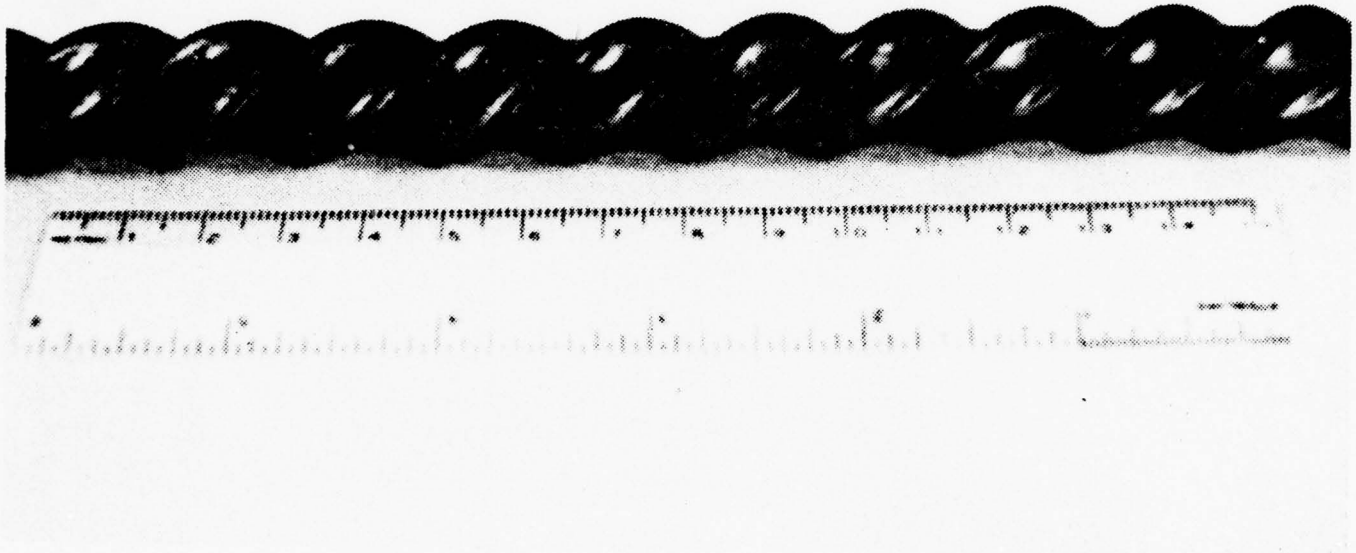


Figure 9. Photograph of High Pitch TURBOTEC Tube (Tube No. T-1)

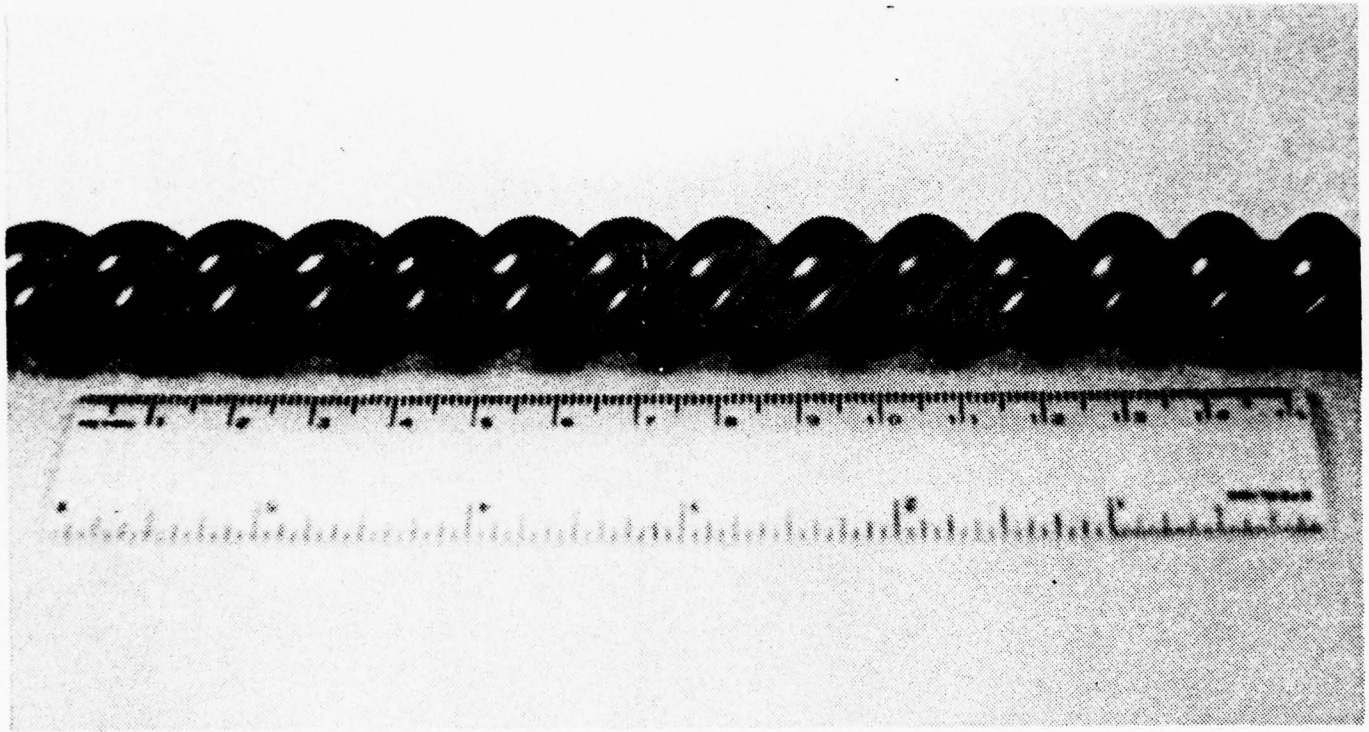


Figure 10. Photograph of Medium Pitch TURBOTEC Tube (Tube No. T-2)

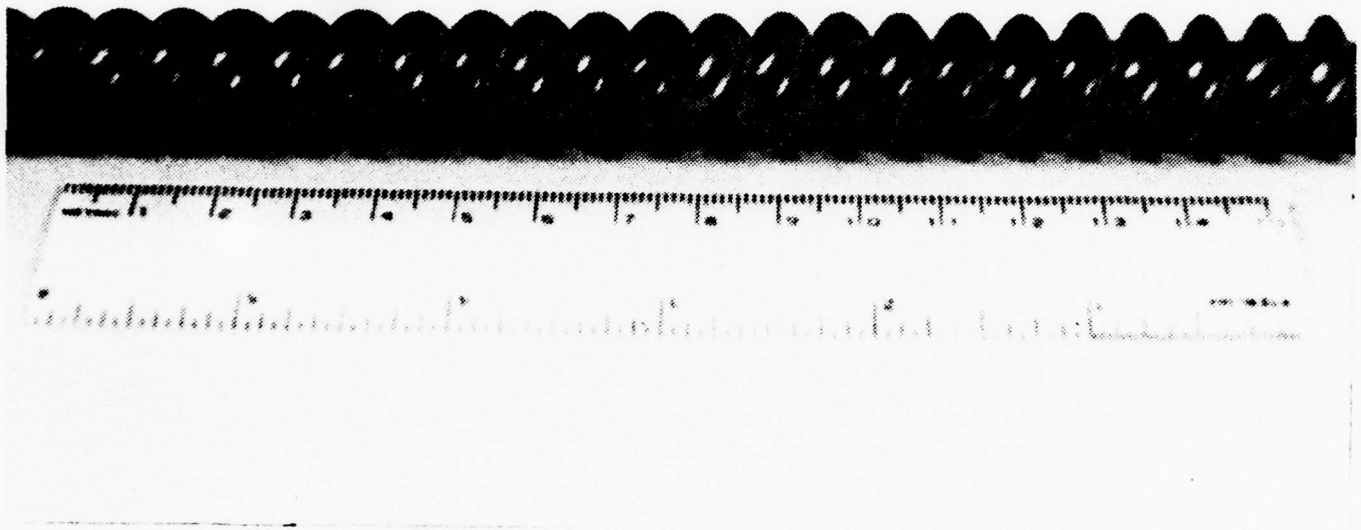


Figure 11. Photograph of Low Pitch TURBOTEC Tube (Tube No. T-3)

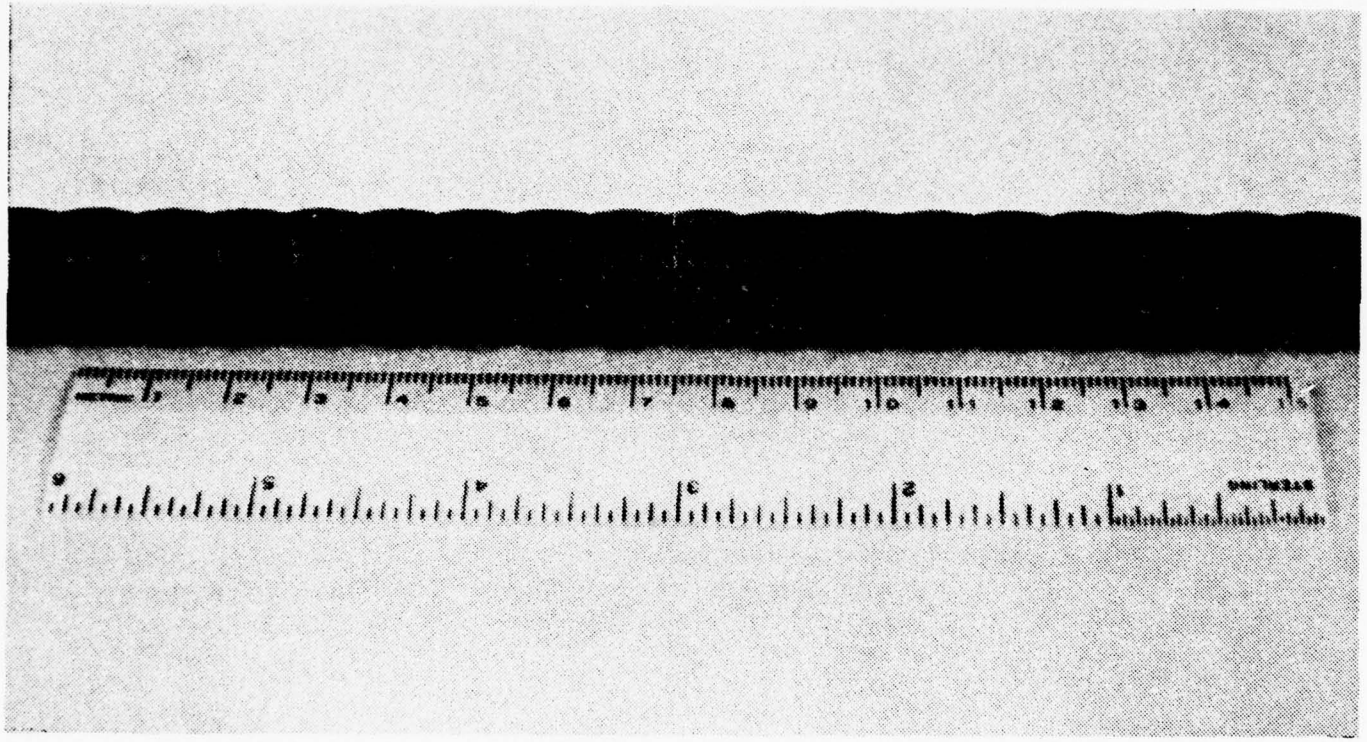


Figure 12. Photograph of Copper-Nickel-MHT KORODENSE Tube (Tube No. K-2)

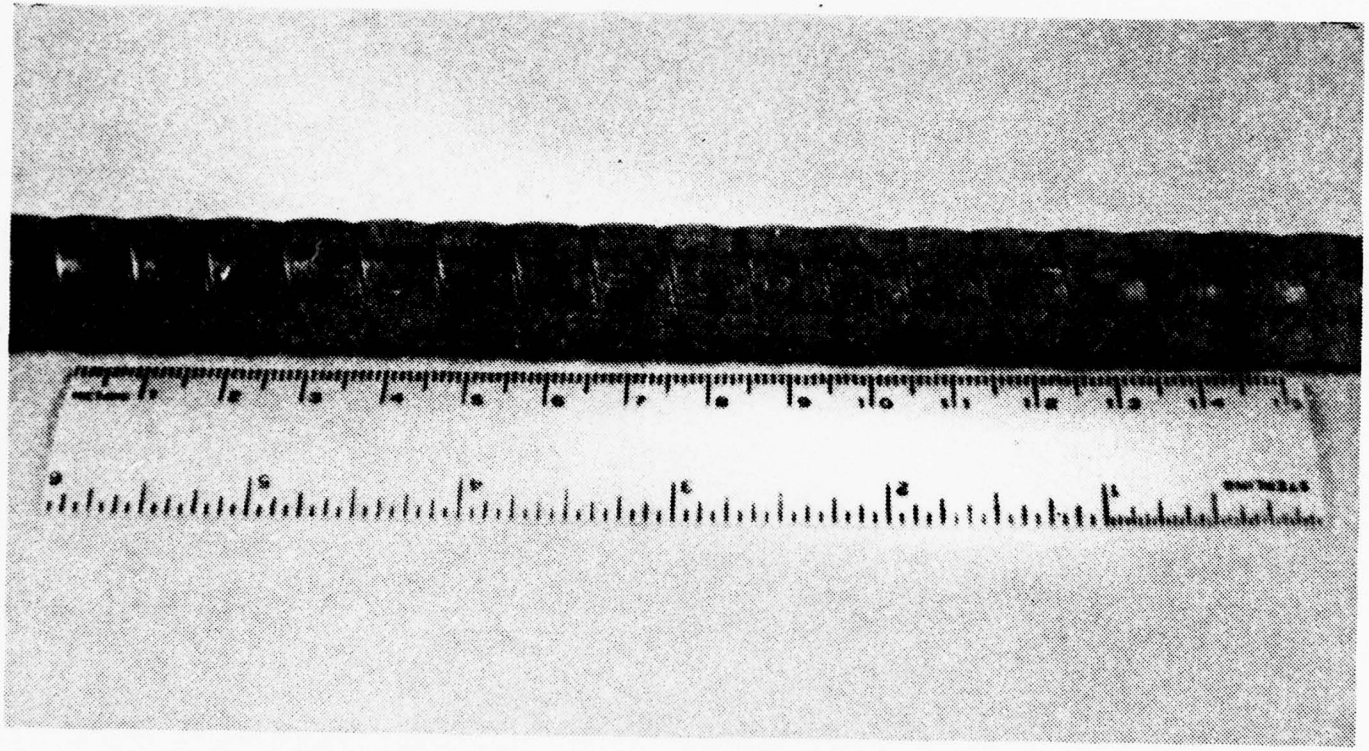


Figure 13. Photograph of Aluminum-MHT KORODENSE Tube (Tube No. K-4)

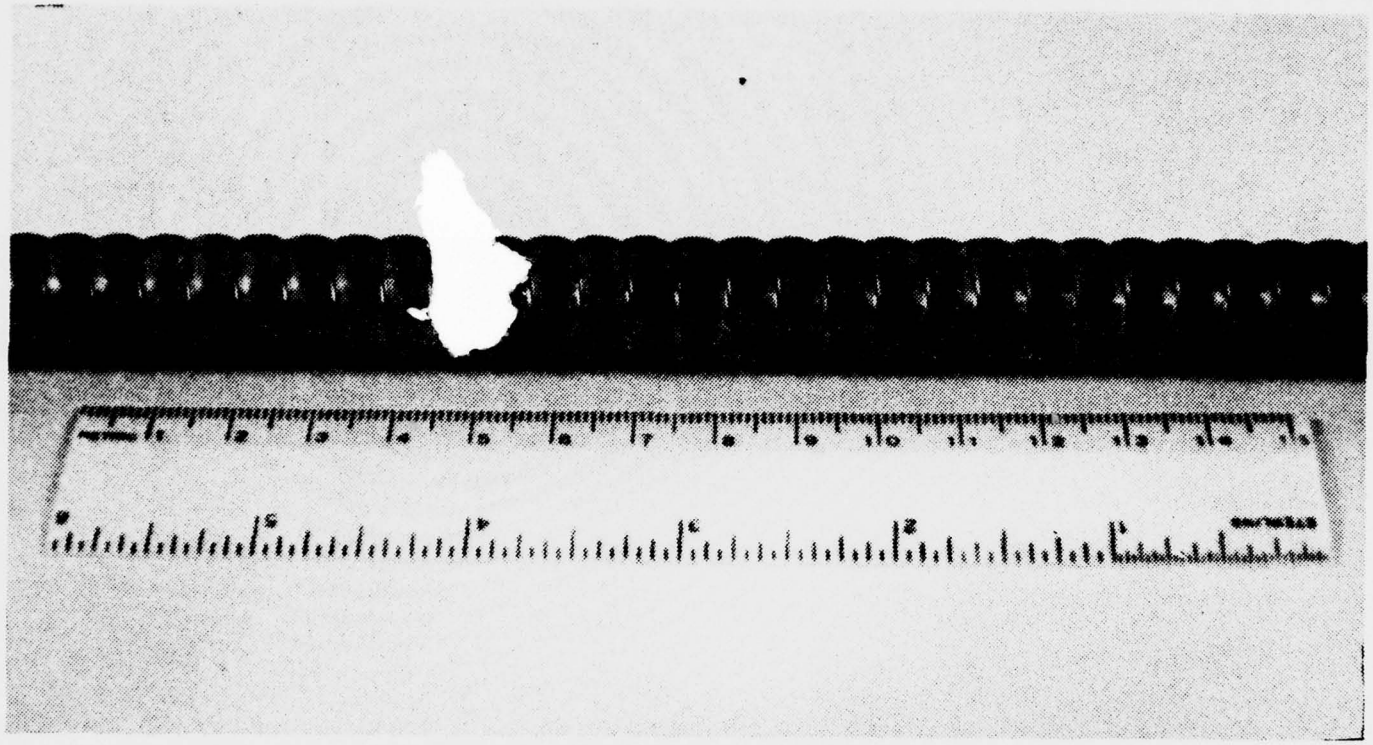


Figure 14. Photograph of Titanium-MHT KORODENSE Tube (Tube No. K-5)

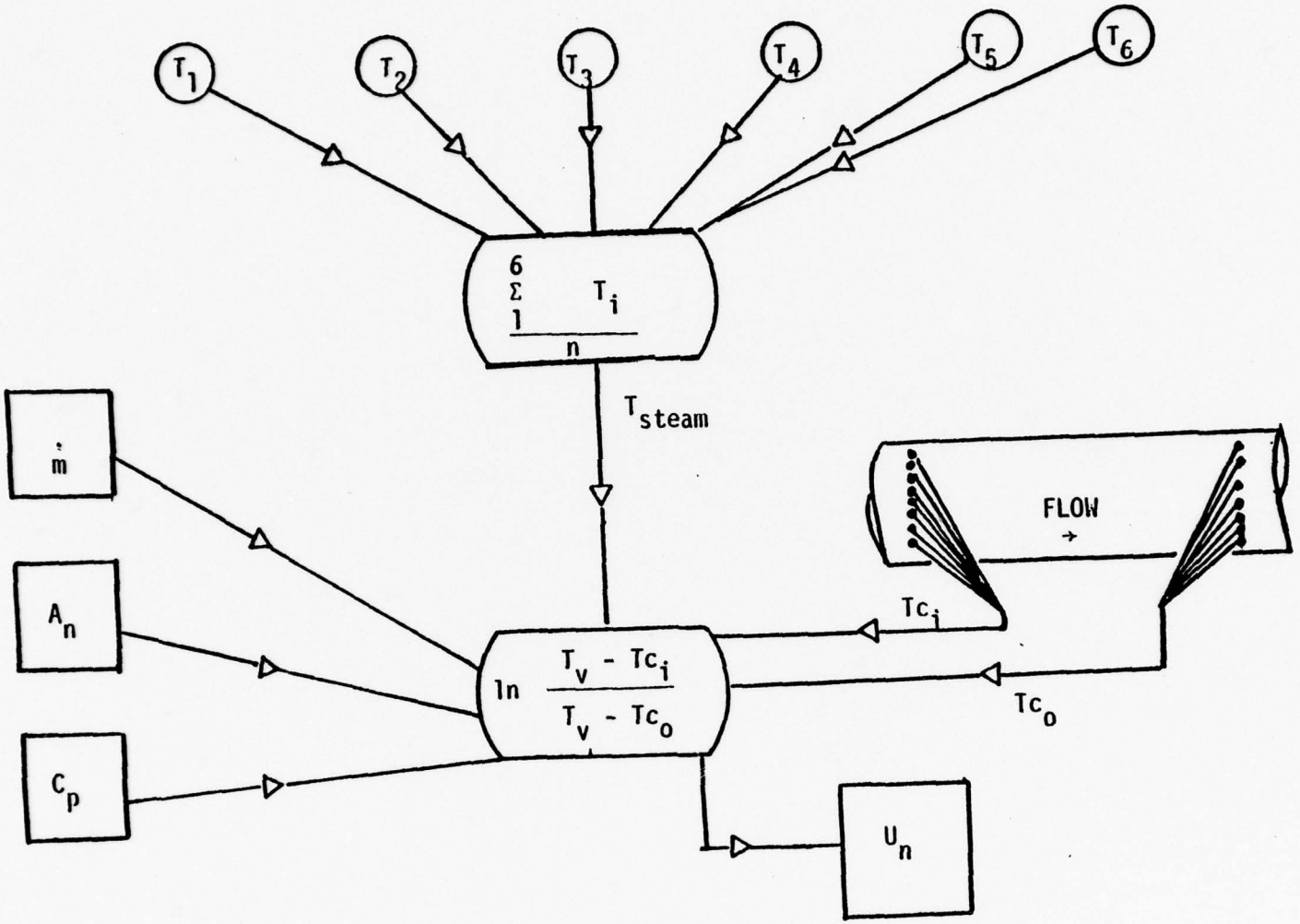


Figure 15. Schematic Representation of Procedure Used to Find U_n

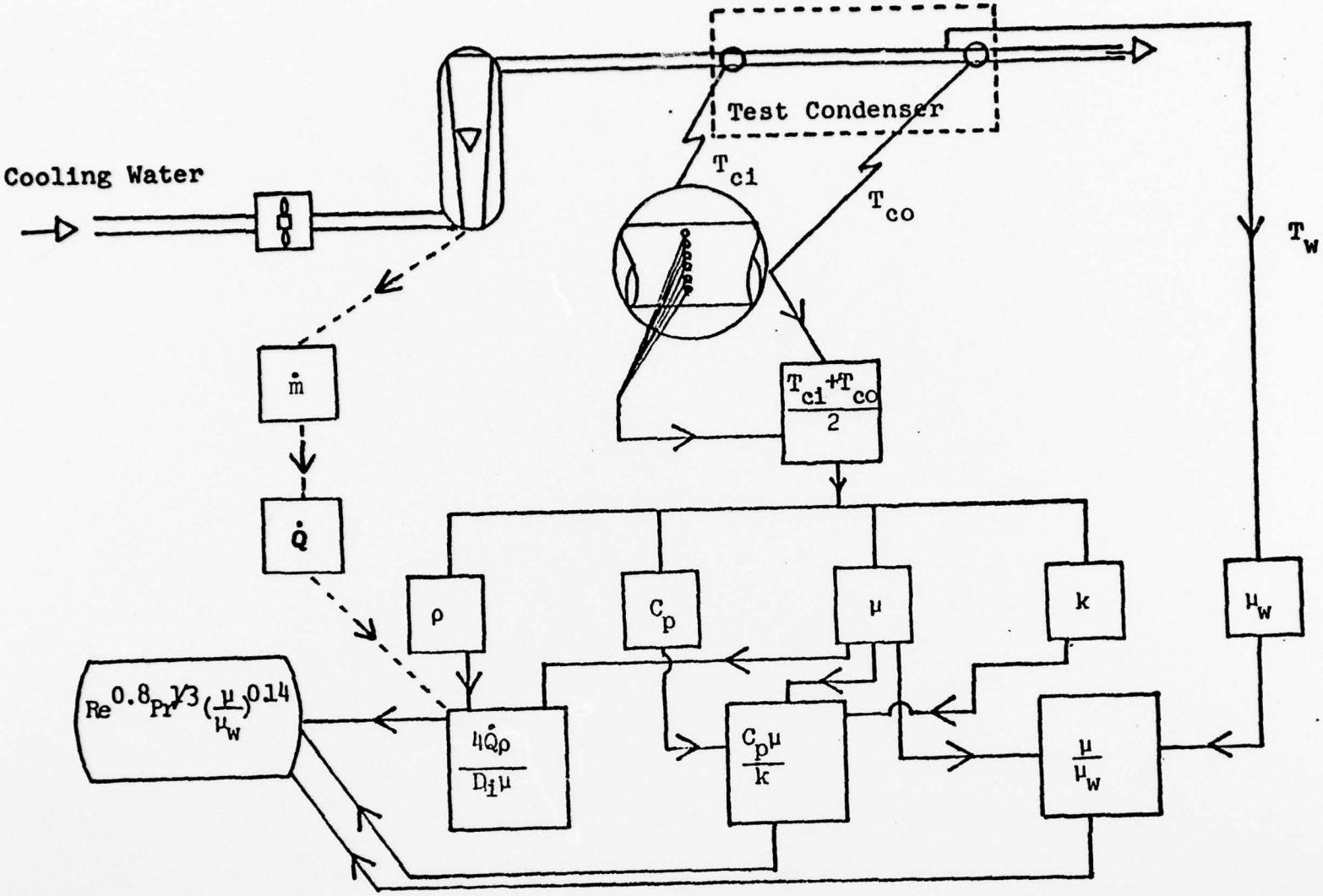


Figure 16. Schematic Representation of Procedure Used to Find Sieder-Tate Parameter

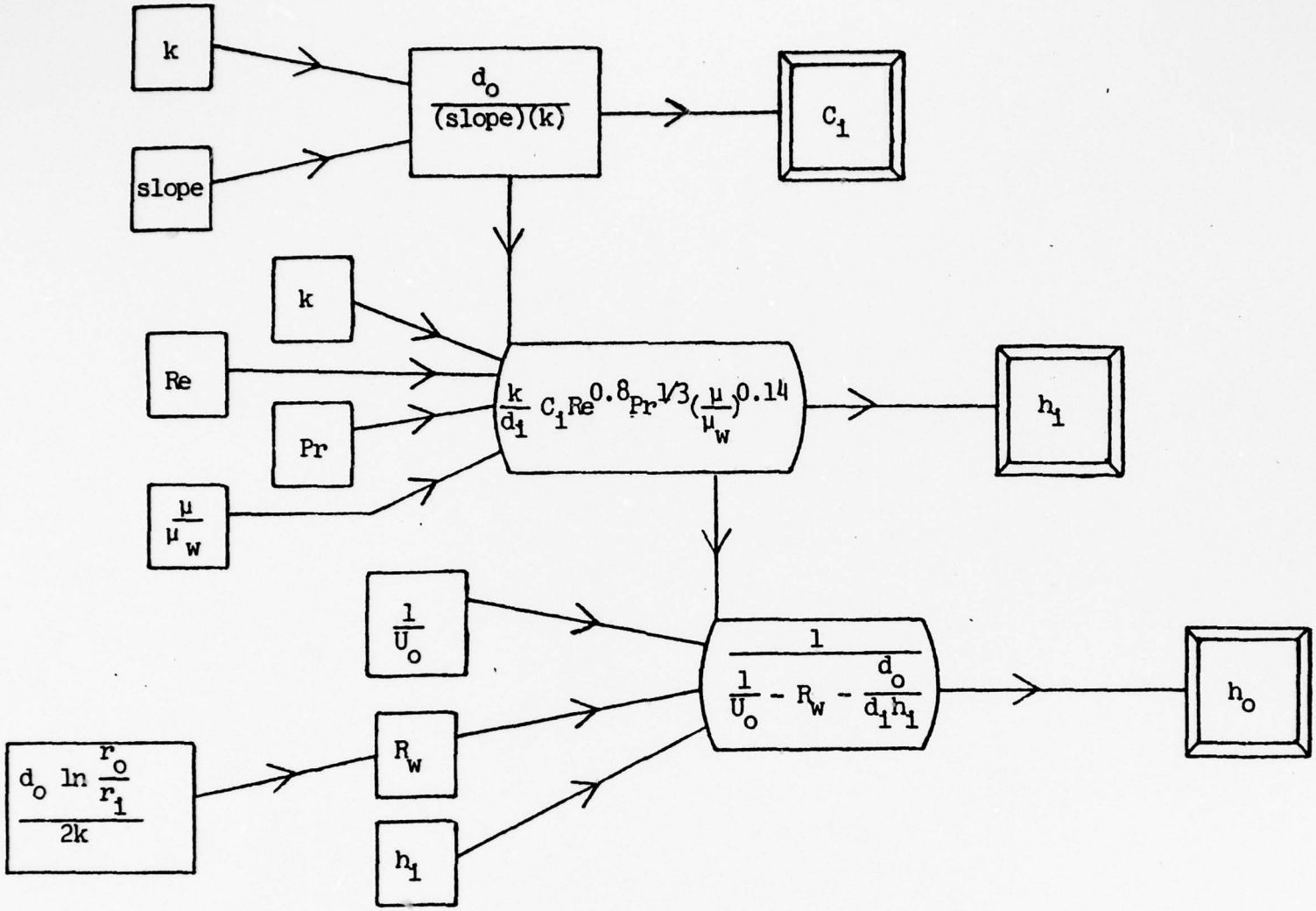


Figure 17. Schematic Representation of Procedure Used to Find Sieder-Tate Coefficient C_i, h_i and h_o

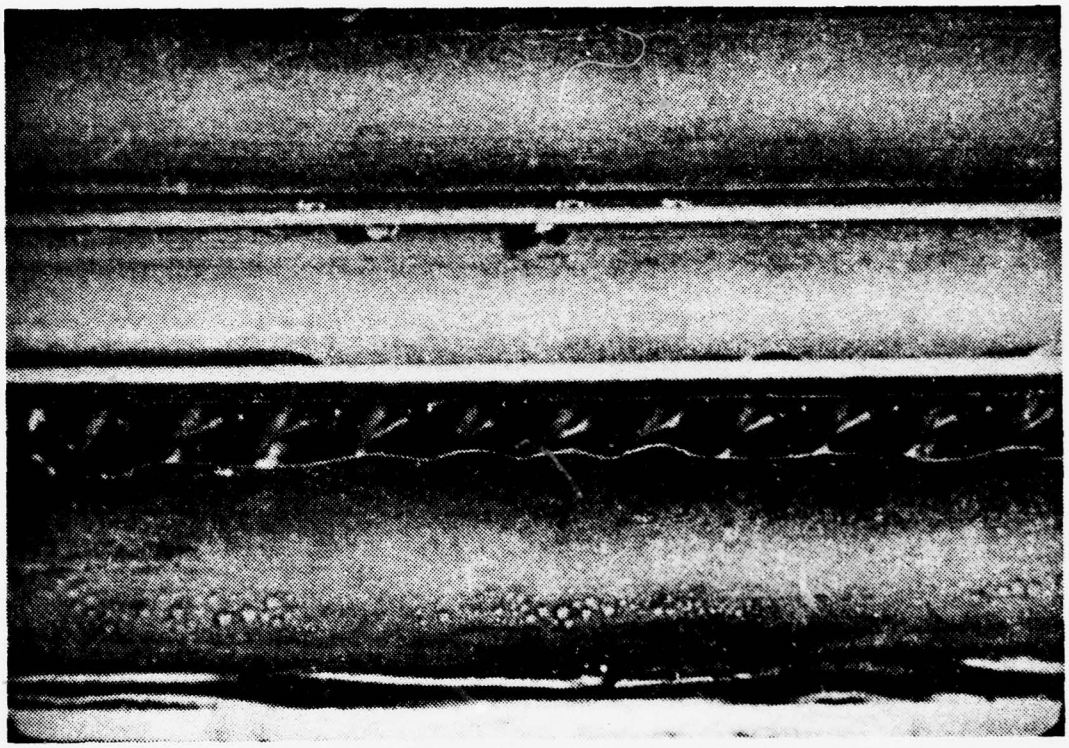


Figure 18. Photograph of Condensation on Low Pitch TURBOTEC Tube (No. T-3a) at a Cooling Water Velocity of 3 m/s

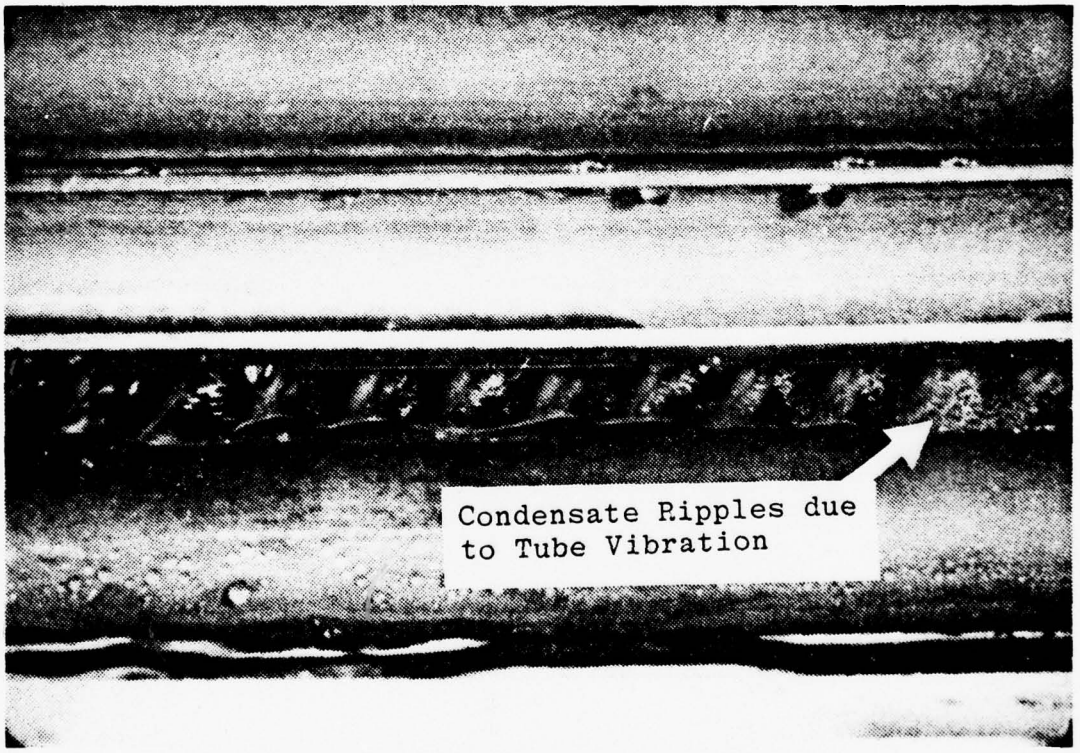


Figure 19. Photograph of Condensation on Low Pitch TURBOTEC Tube (No. T-3a) Showing Effect of Tube Vibration at a Cooling Water Velocity of 4 m/s

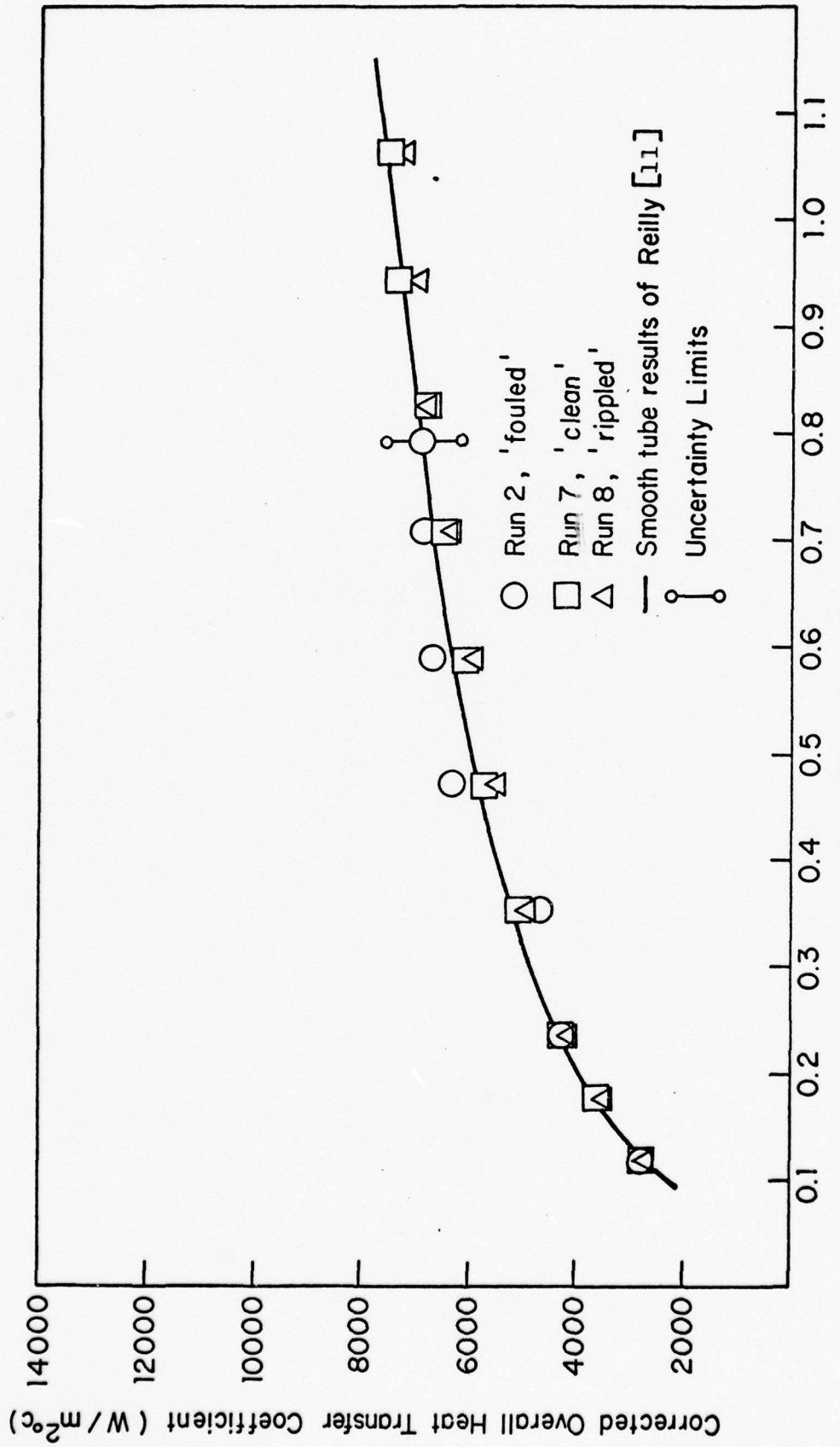


Figure 20. Corrected Overall Heat Transfer Coefficient Versus Cooling Water Mass Flow Rate for Smooth Tubes.

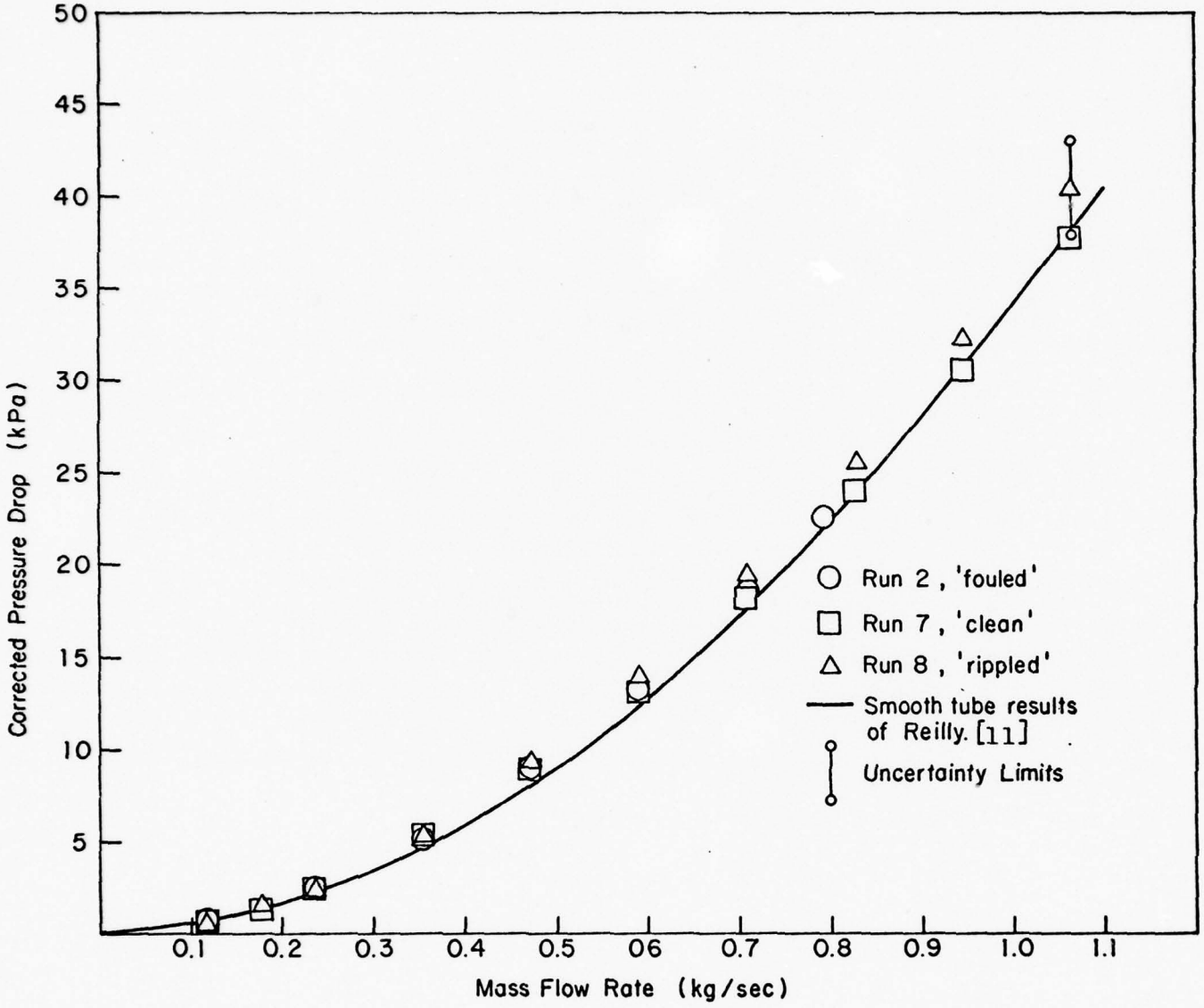


Figure 21. Corrected Pressure Drop Versus Cooling Water Mass Flow Rate for Smooth Tubes.

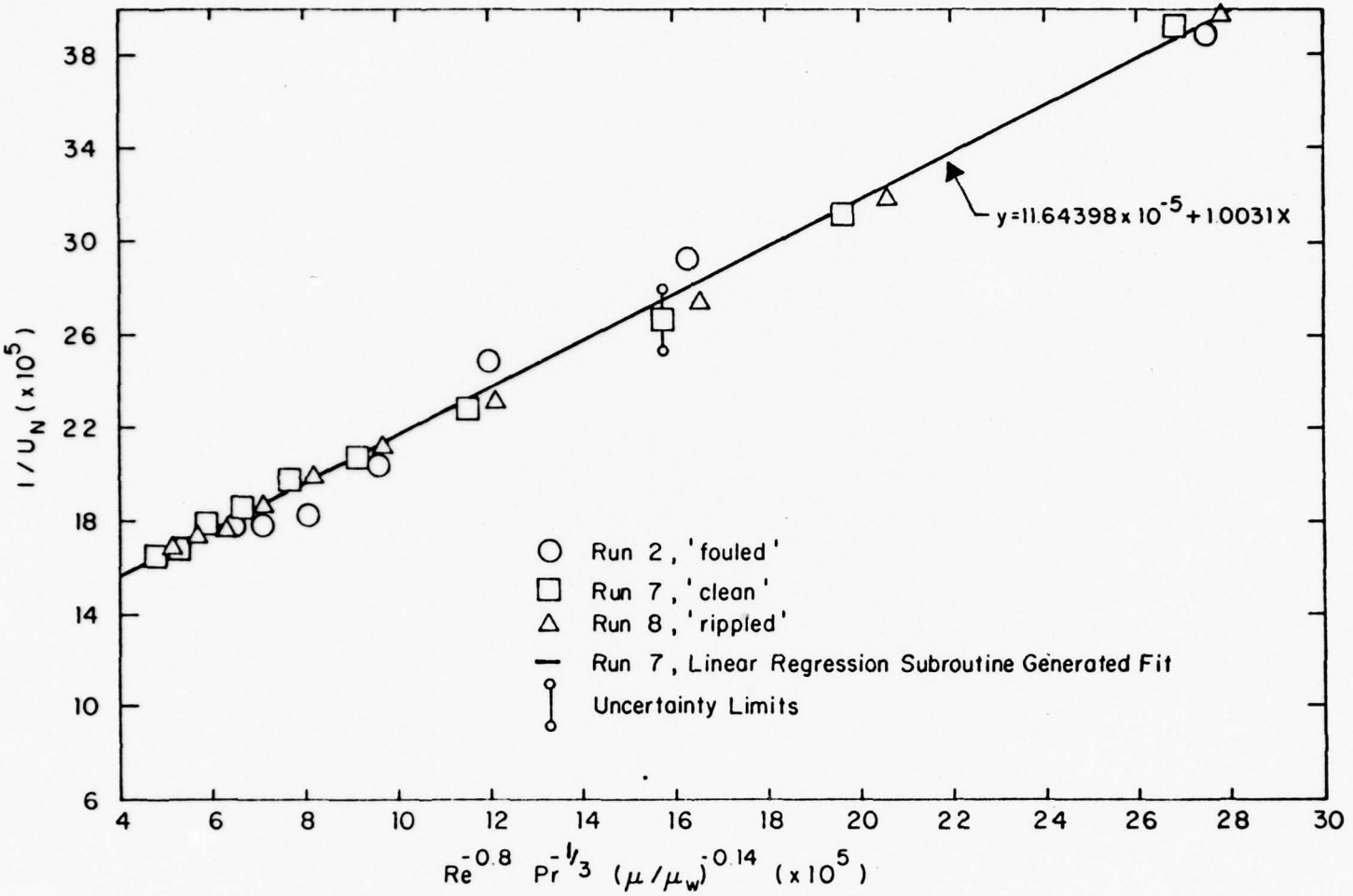


Figure 22. Wilson Plot for Smooth Tubes

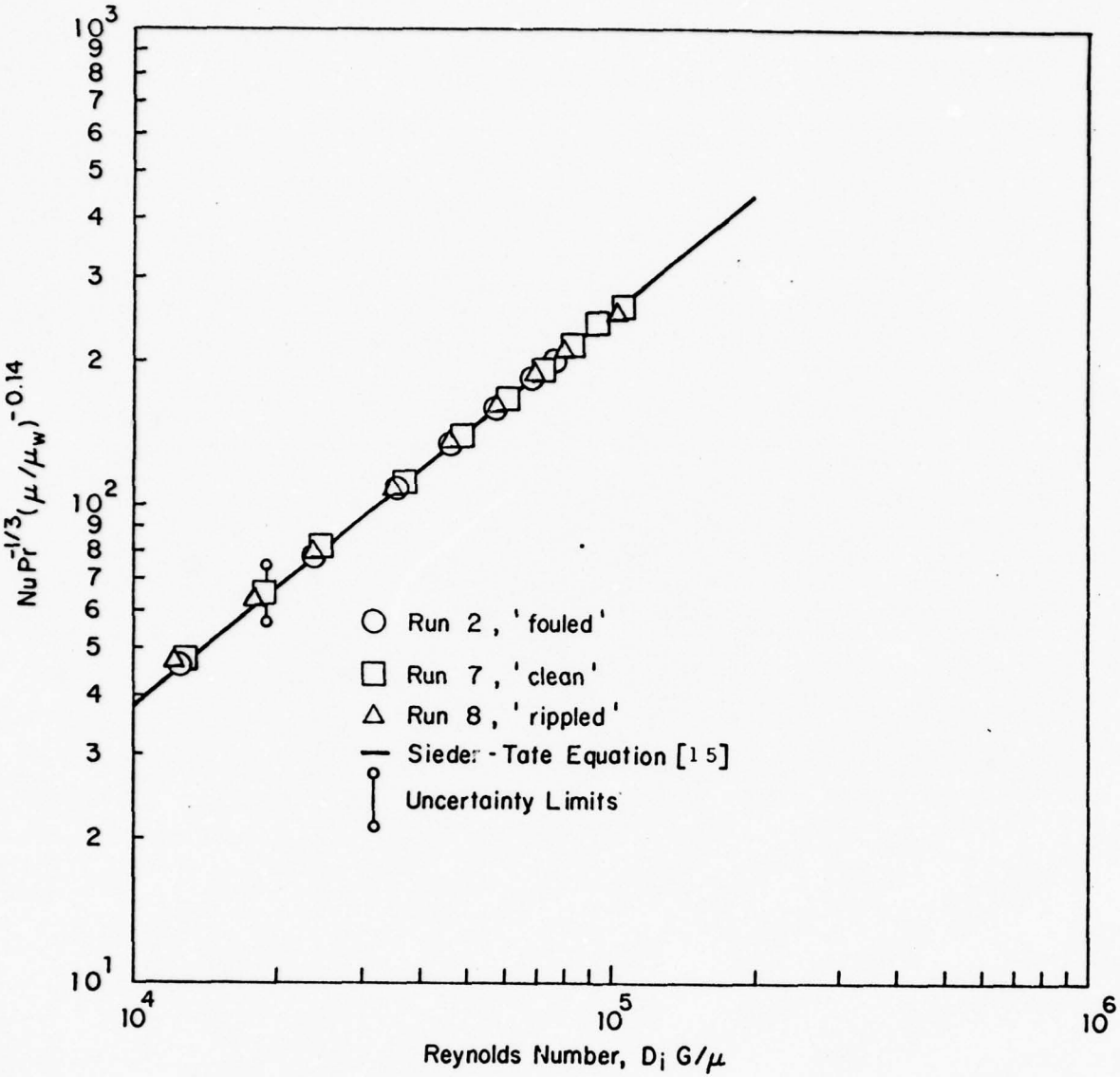


Figure 23. Inside Nusselt Number Correlation Versus Reynolds Number for Smooth Tubes.

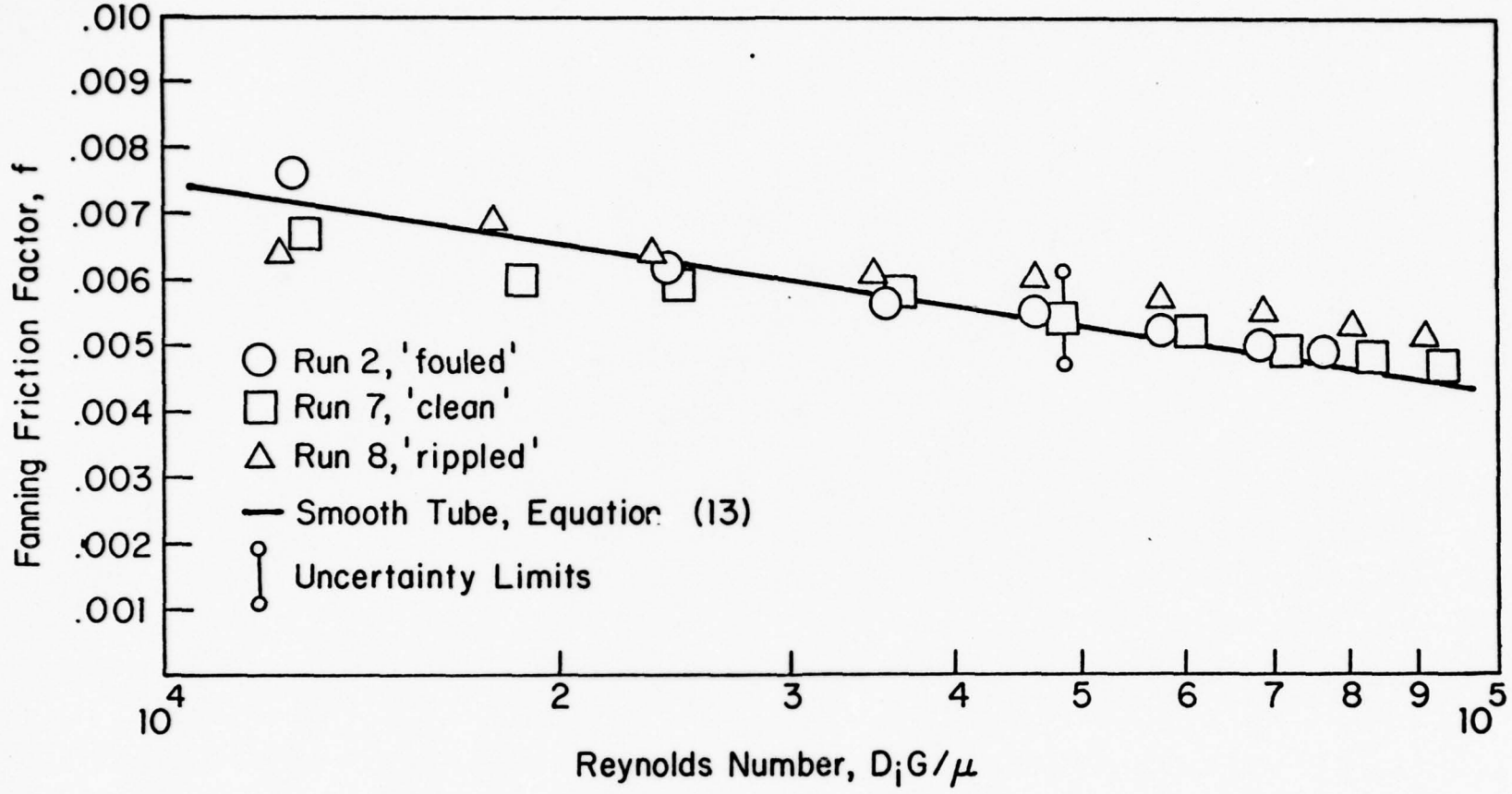


Figure 24. Fanning Friction Factor Versus Reynolds Number for Smooth Tubes.

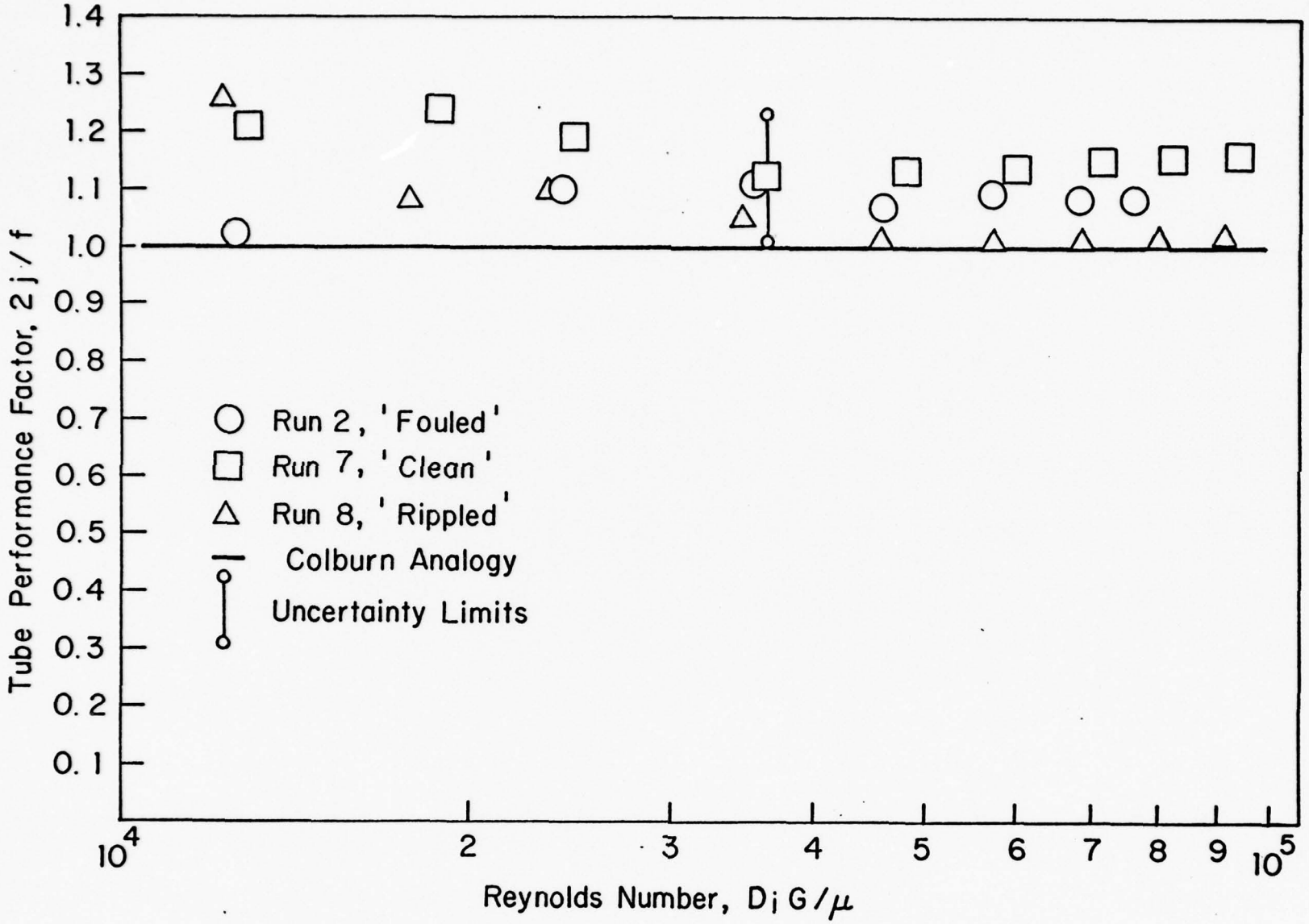


Figure 25. Tube Performance Factor, 2j/f, Versus Reynolds Number for Smooth Tubes.

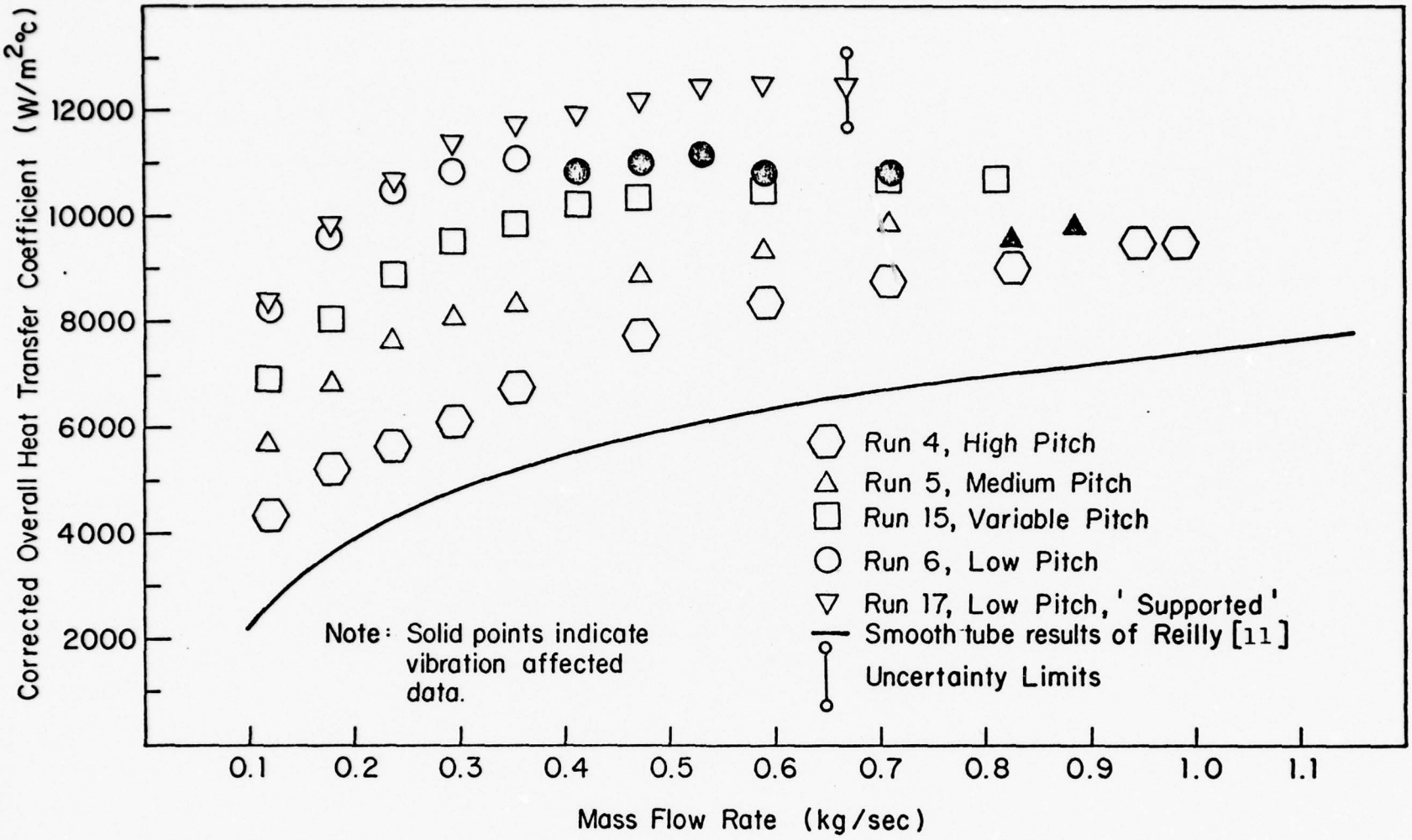


Figure 26. Corrected Overall Heat Transfer Coefficient, U_c, Versus Cooling Water Mass Flow Rate for TURBOTEC Tubes

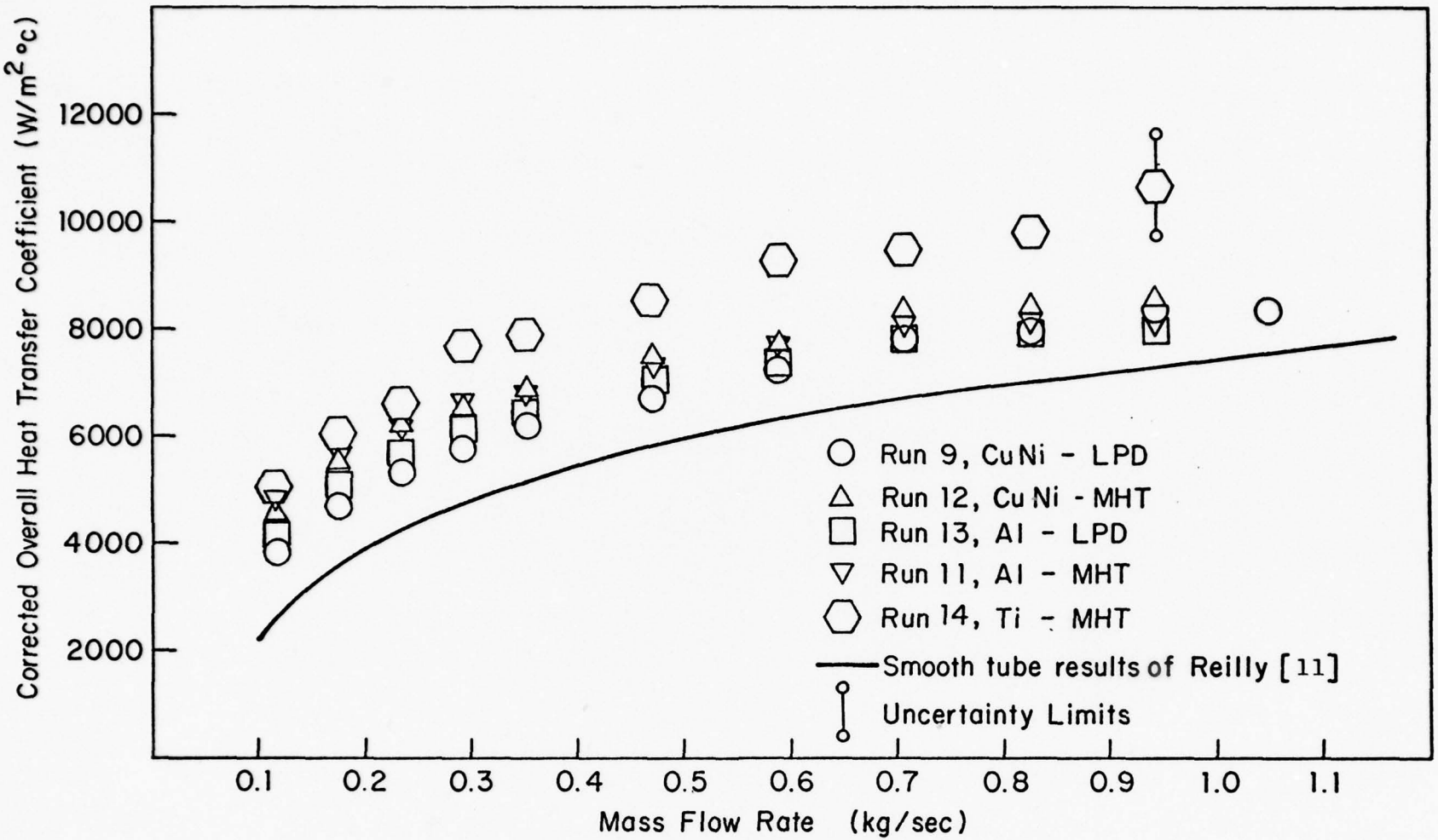


Figure 27. Corrected Overall Heat Transfer Coefficient, U_c, Versus Cooling Water Mass Flow Rate for KORODENSE Tubes.

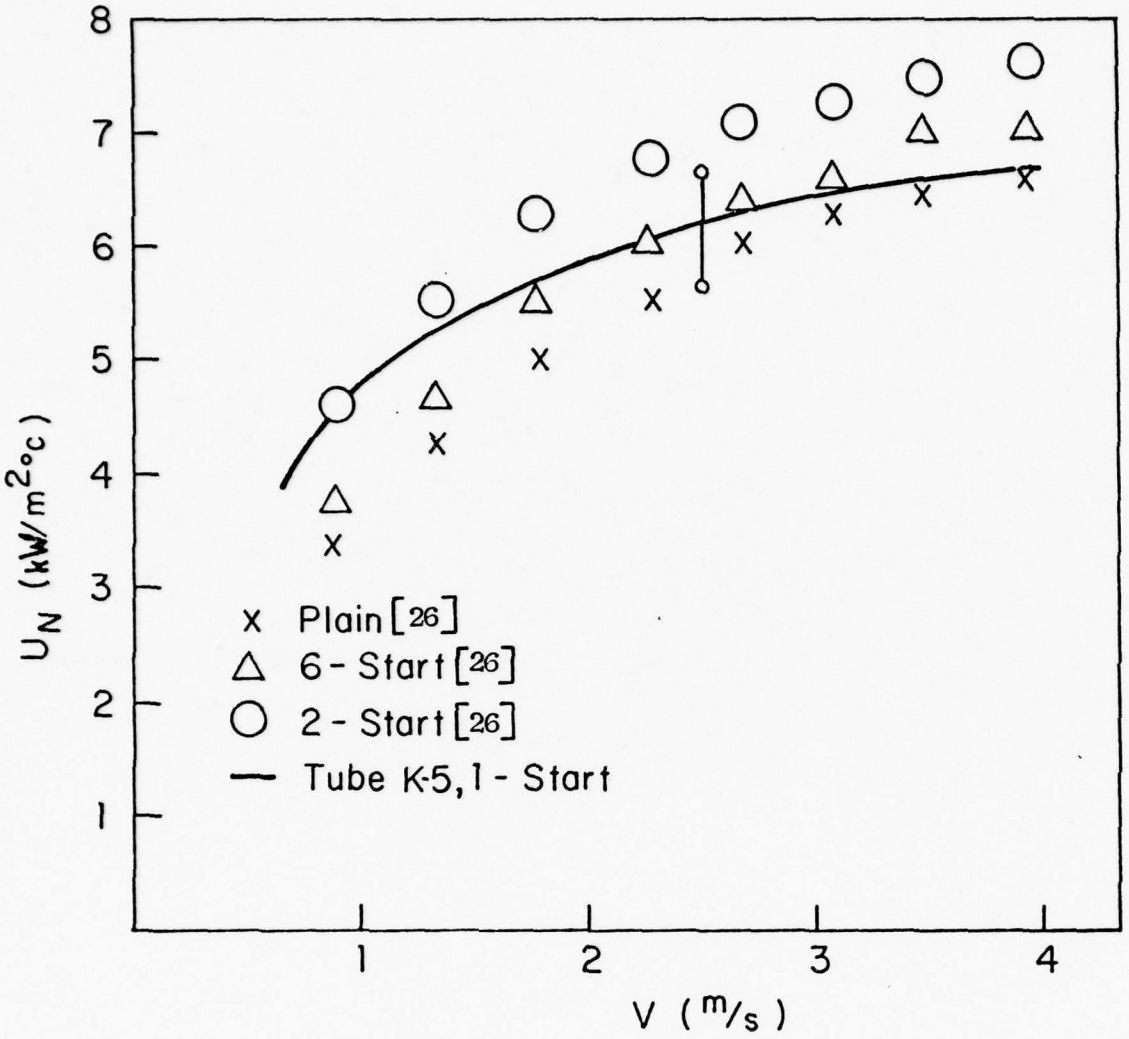


Figure 28. Uncorrected Overall Heat Transfer Coefficient, U_n, Versus Cooling Water Velocity for Tube K-5 Compared with Data of Cunningham and Milne [26]

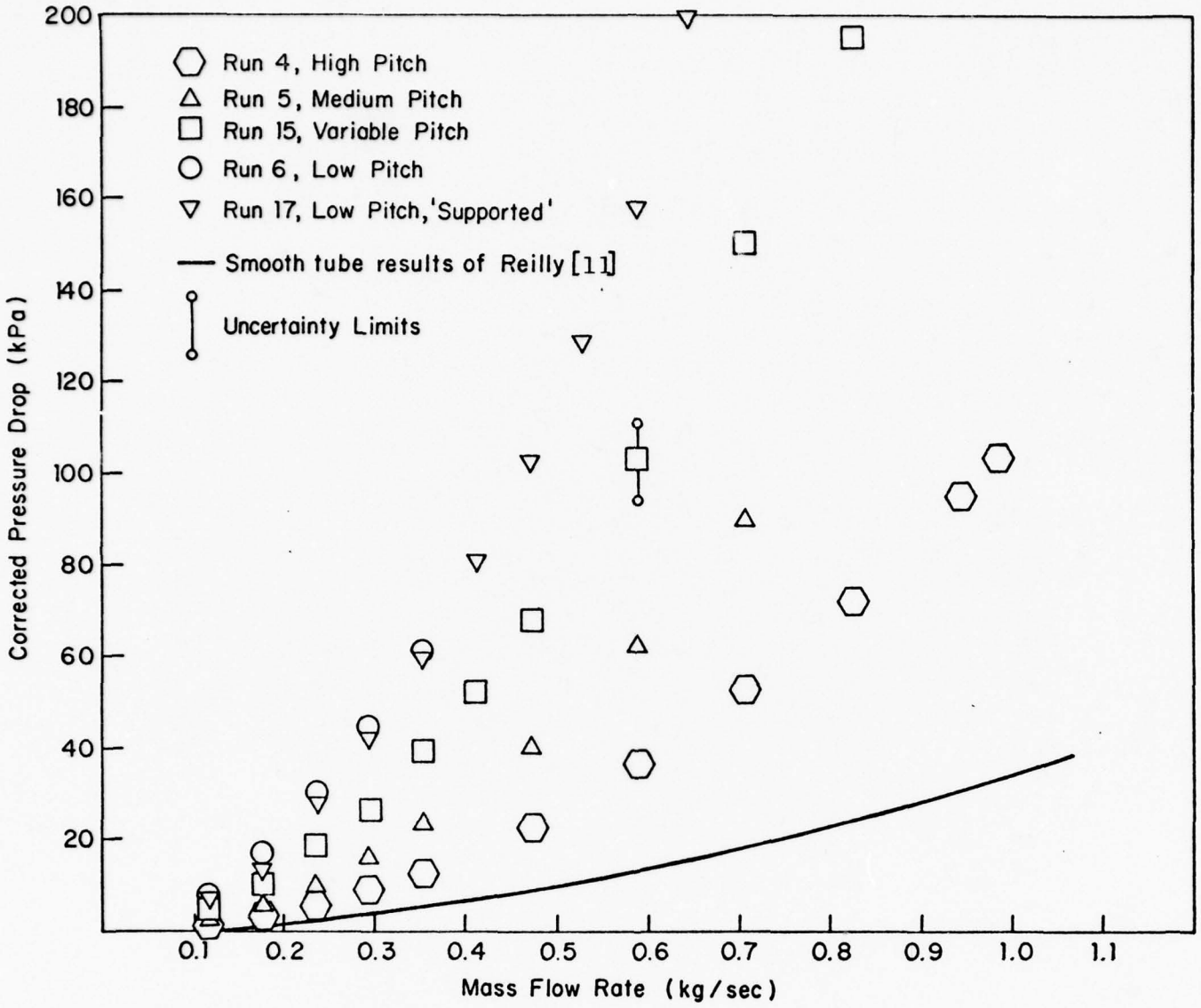


Figure 29. Corrected Pressure Drop Versus Cooling Water Mass Flow Rate for TURBOTEC Tubes.

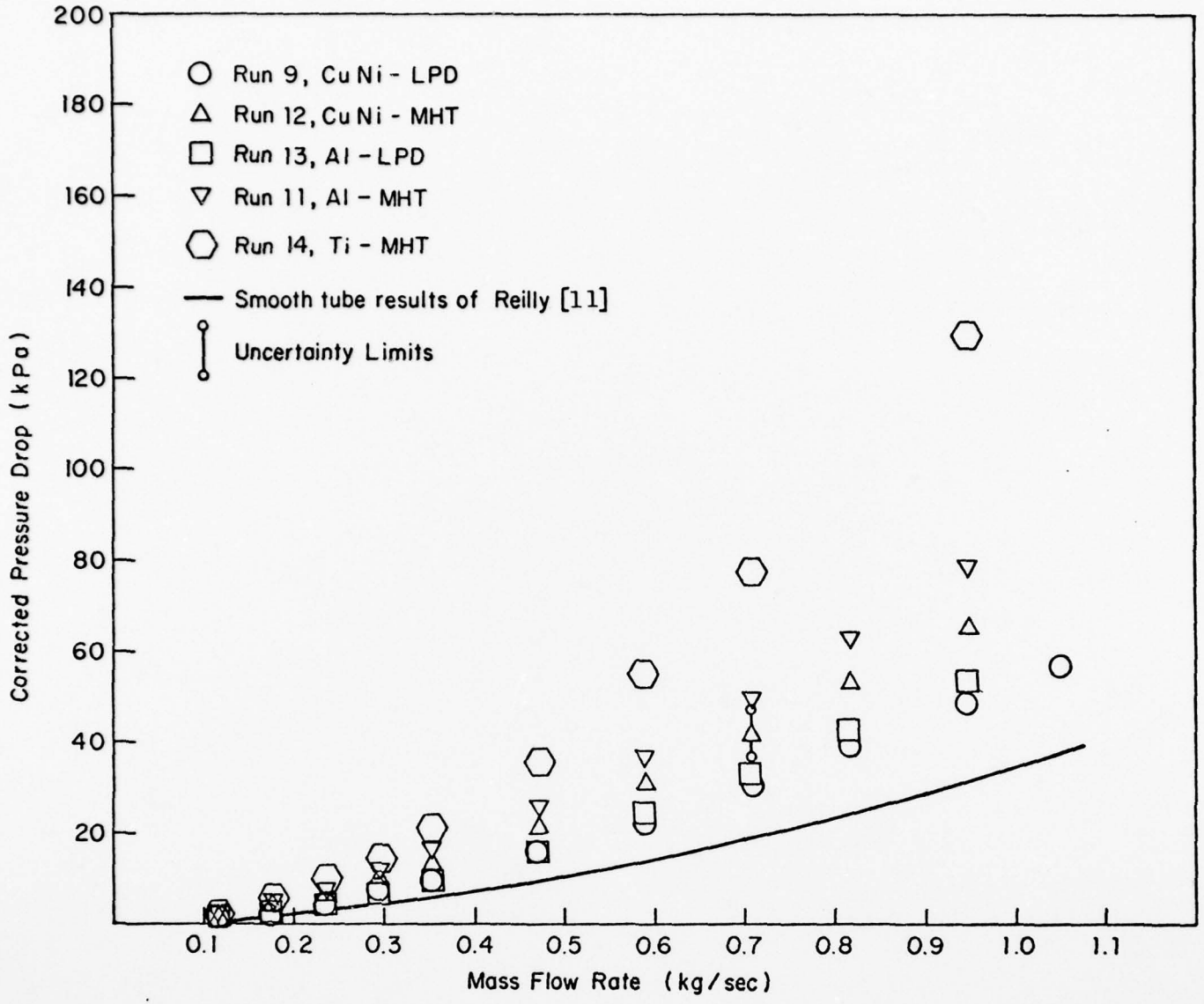


Figure 30. Corrected Pressure Drop Versus Cooling Water Mass Flow Rate for KORODENSE Tubes.

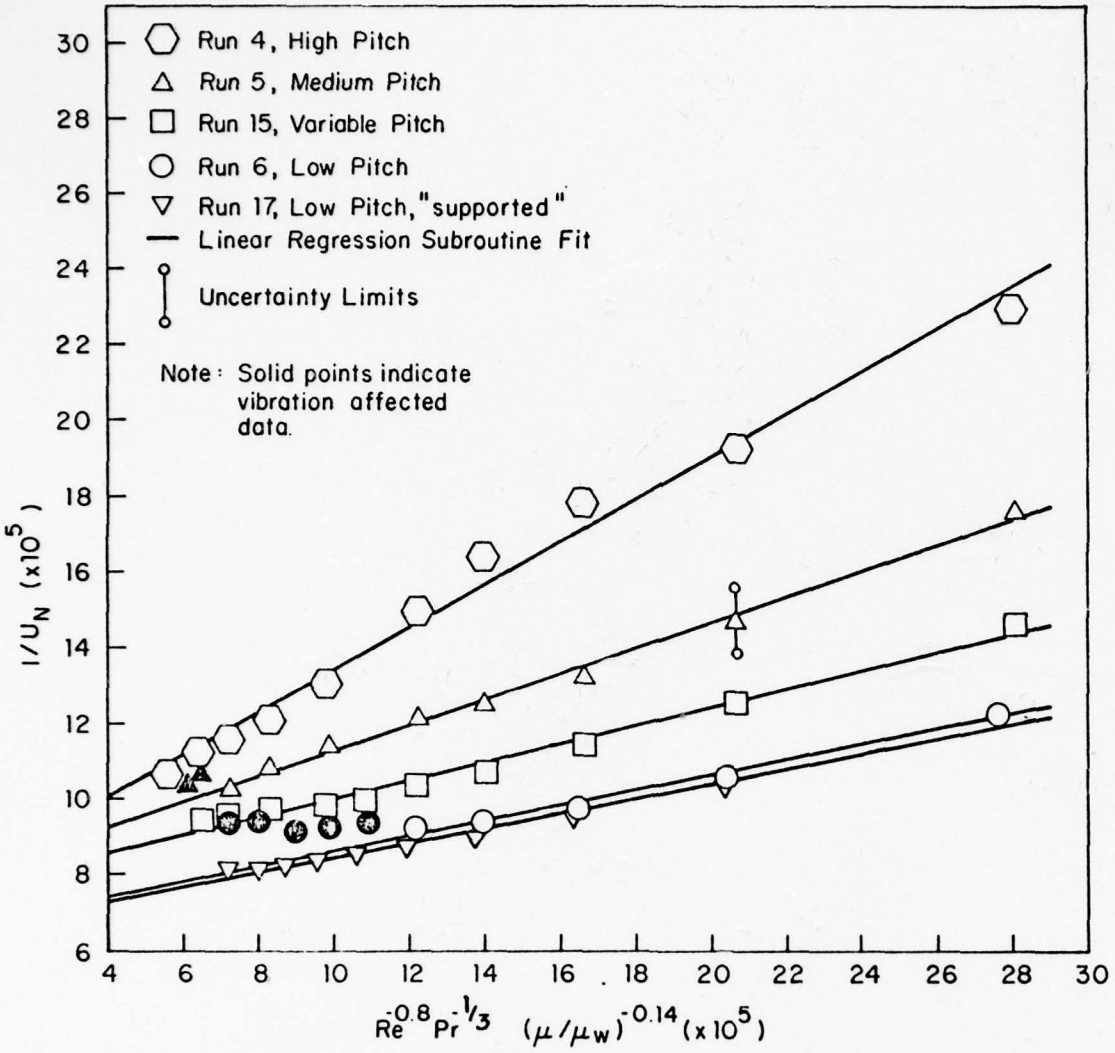


Figure 31. Wilson Plot for TURBOTEC Tubes.

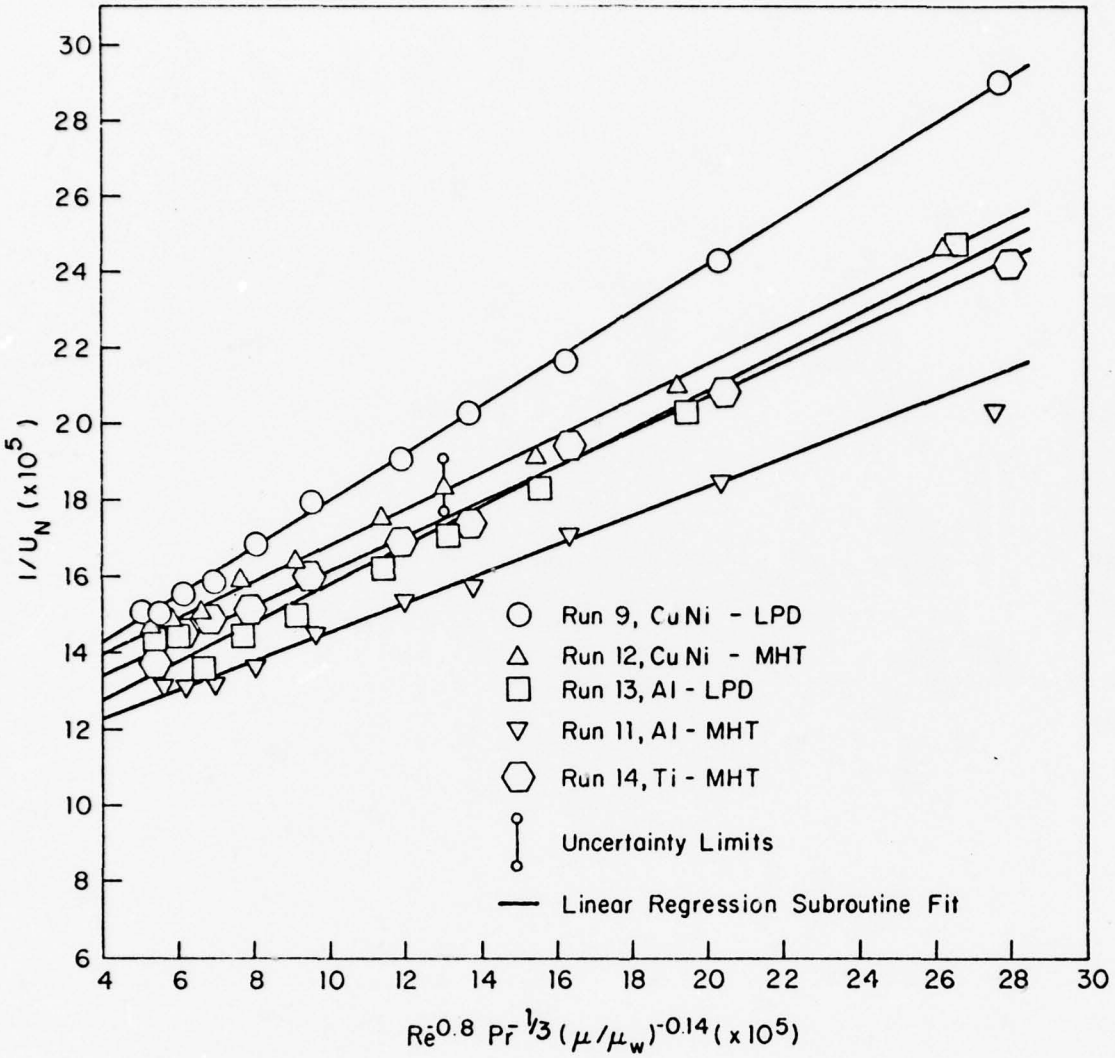


Figure 32. Wilson Plot for KORODENSE Tubes.

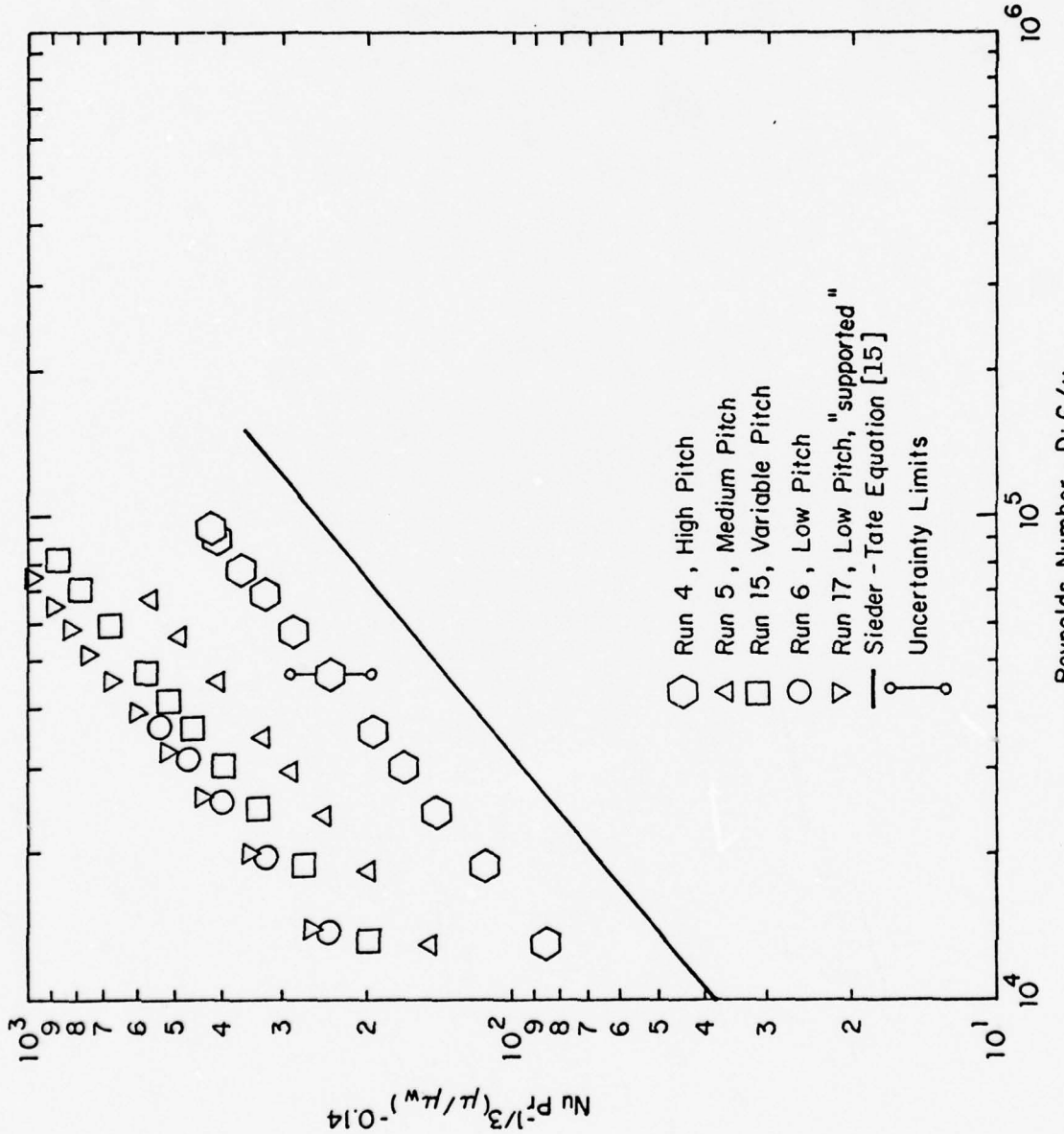


Figure 33. Inside Nusselt Number Correlation Versus Reynolds Number for TURBOTEC Tubes

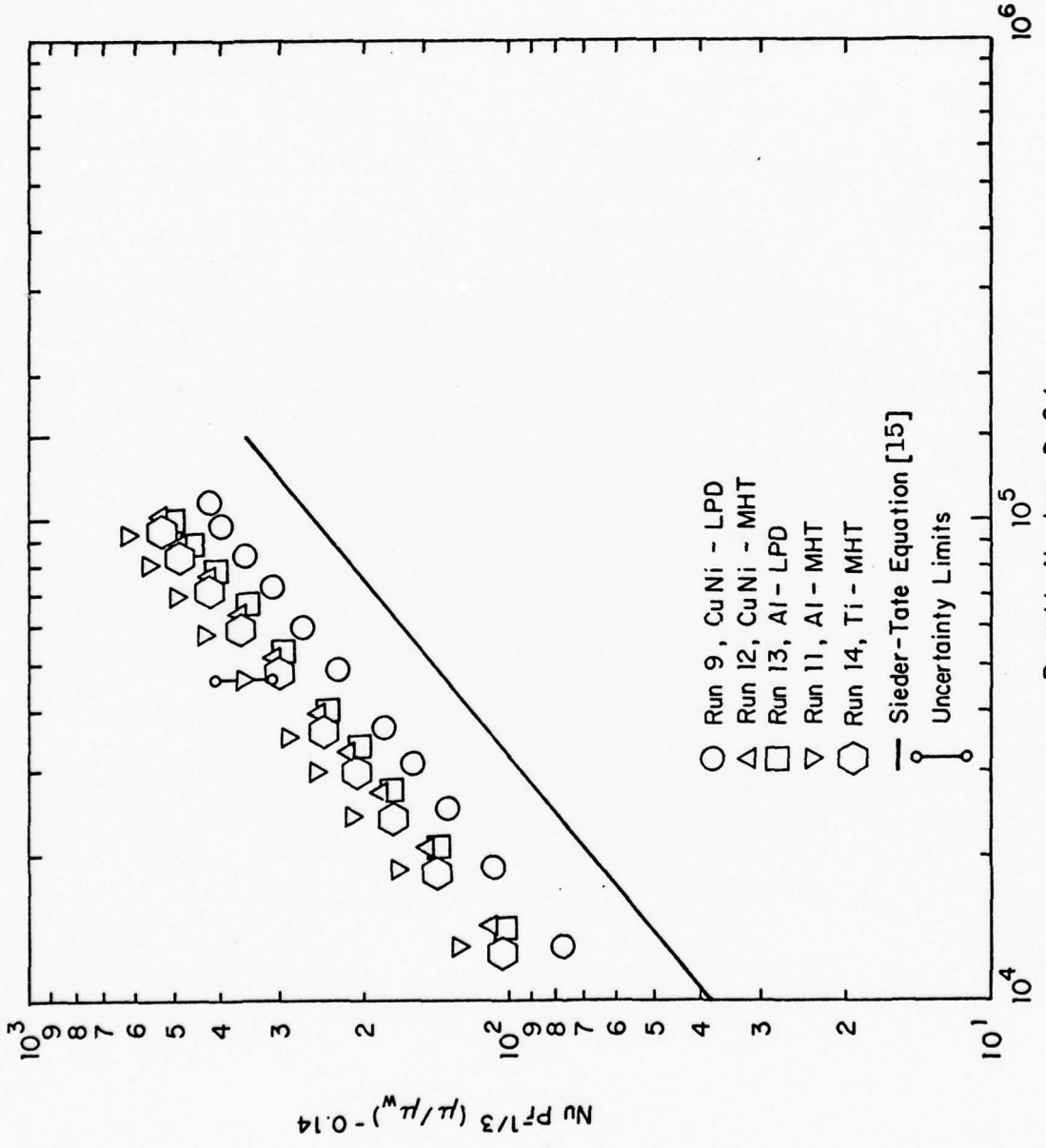


Figure 34. Inside Nusselt Number Correlation Versus Reynolds Number for KORODENSE Tubes

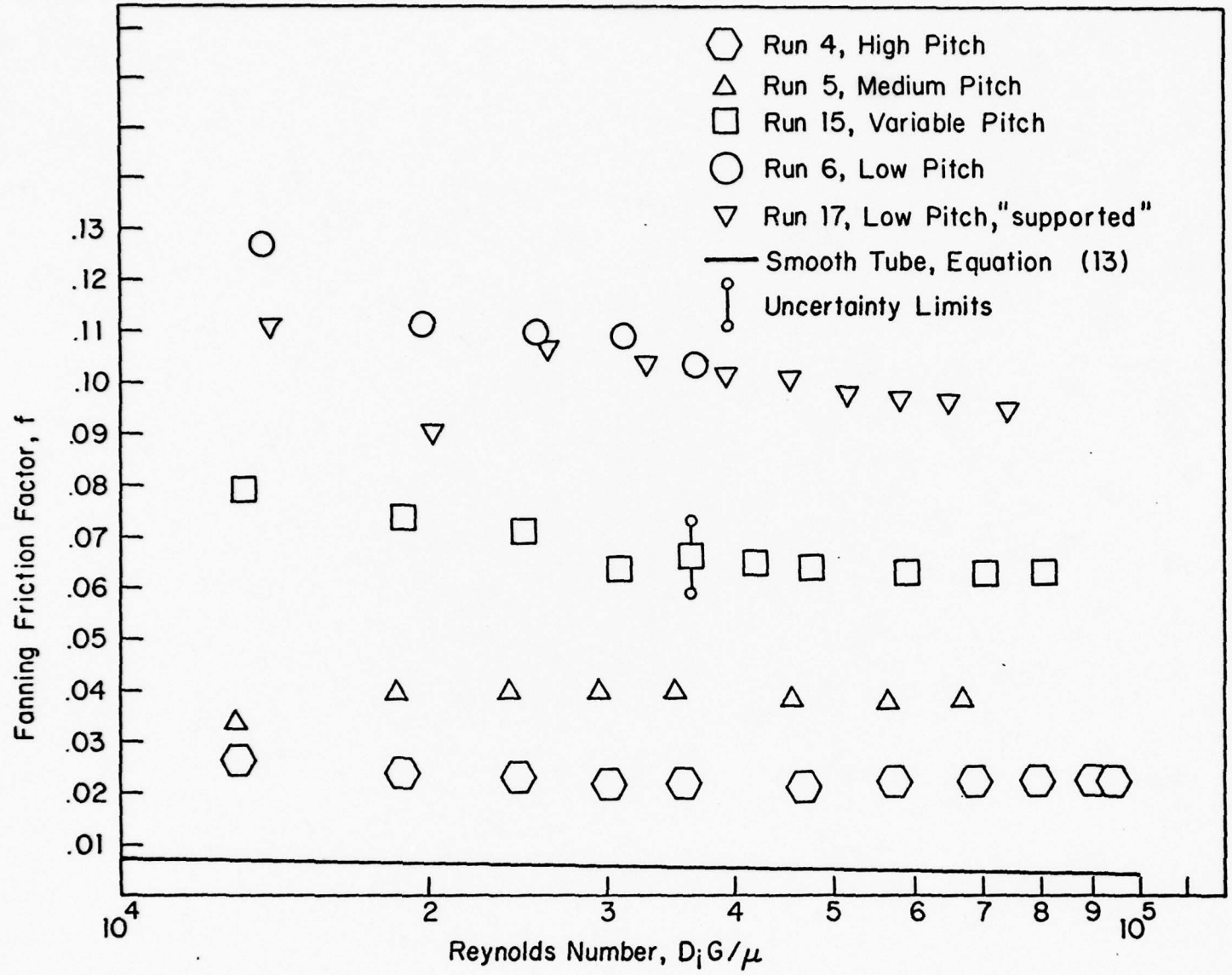


Figure 35. Fanning Friction Factor Versus Reynolds Number for TURBOTEC Tubes.

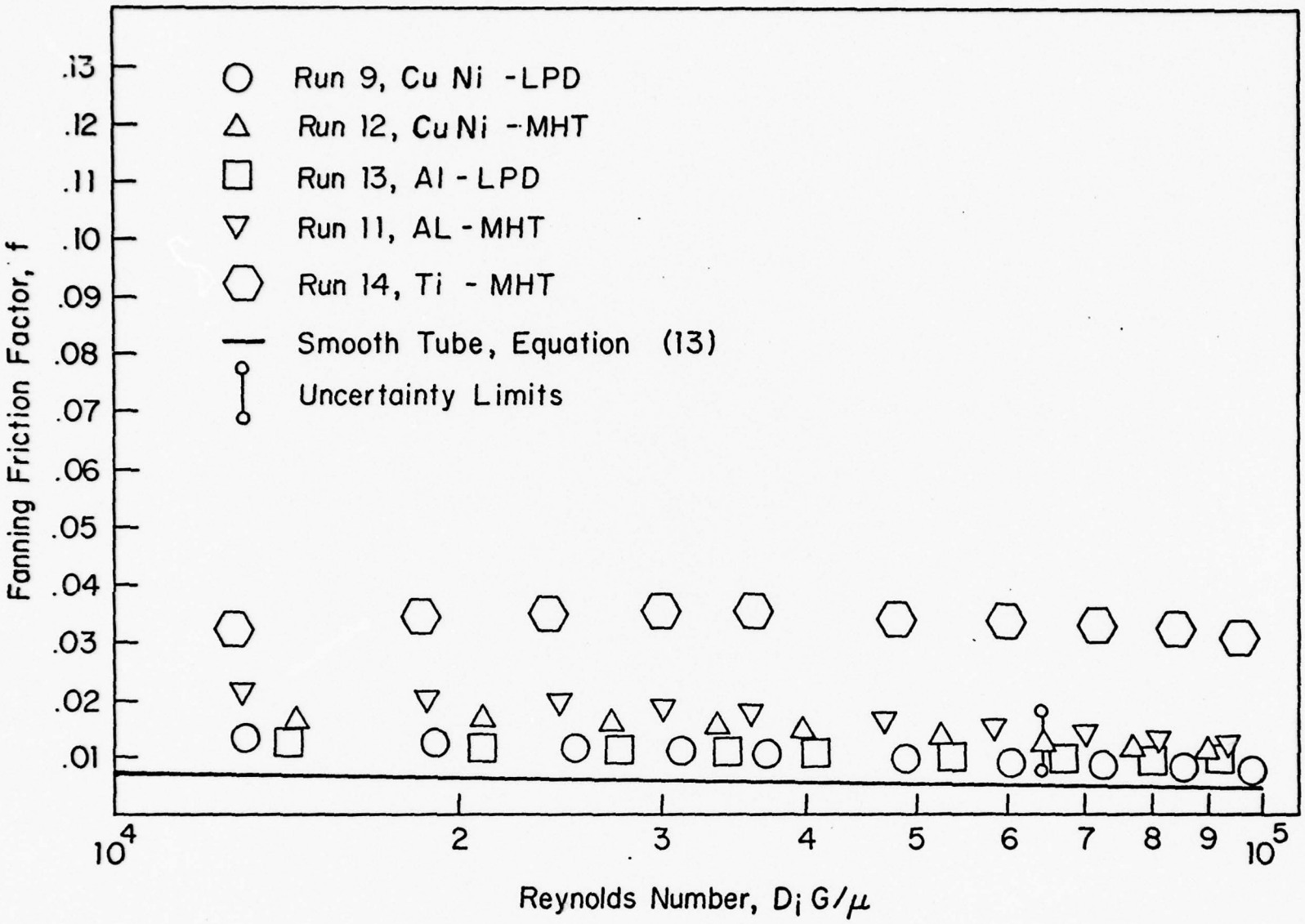


Figure 36. Fanning Friction Factor Versus Reynolds Number for KORODENSE Tubes.

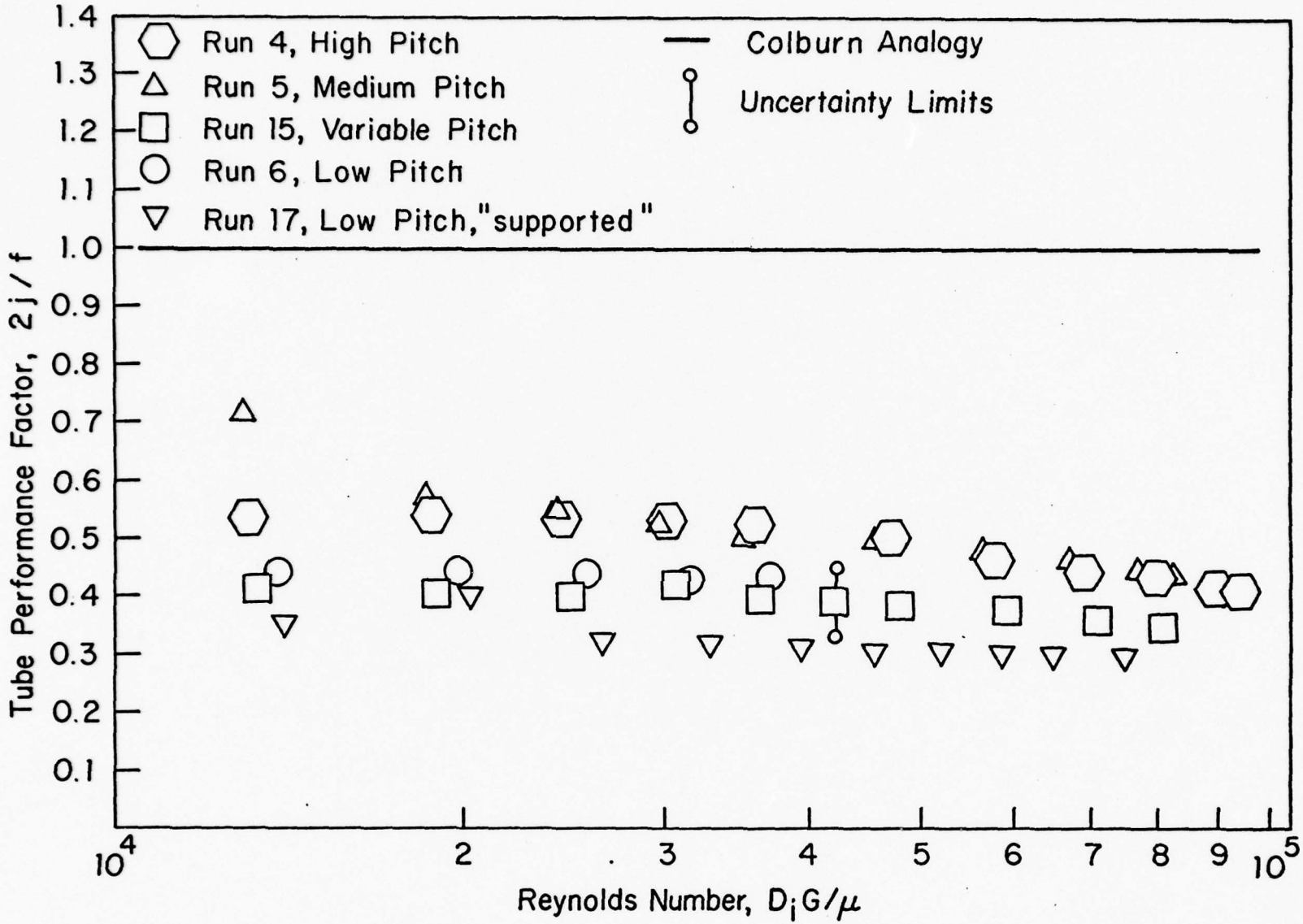


Figure 37. Tube Performance Factor, 2j/f, Versus Reynolds Number for TURBOTEC Tubes.

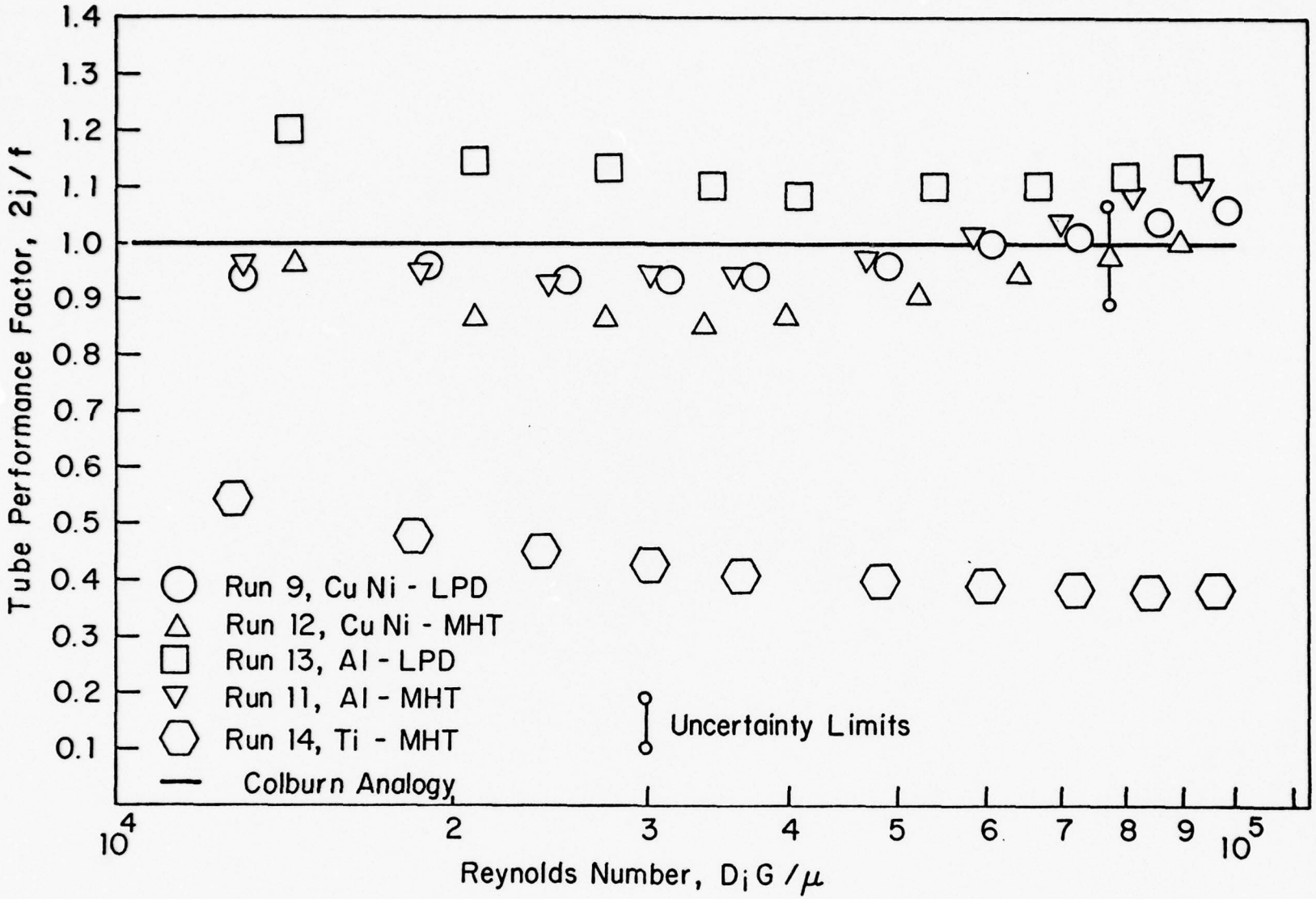


Figure 38. Tube Performance Factor, 2j/f, Versus Reynolds Number for KORODENSE Tubes.

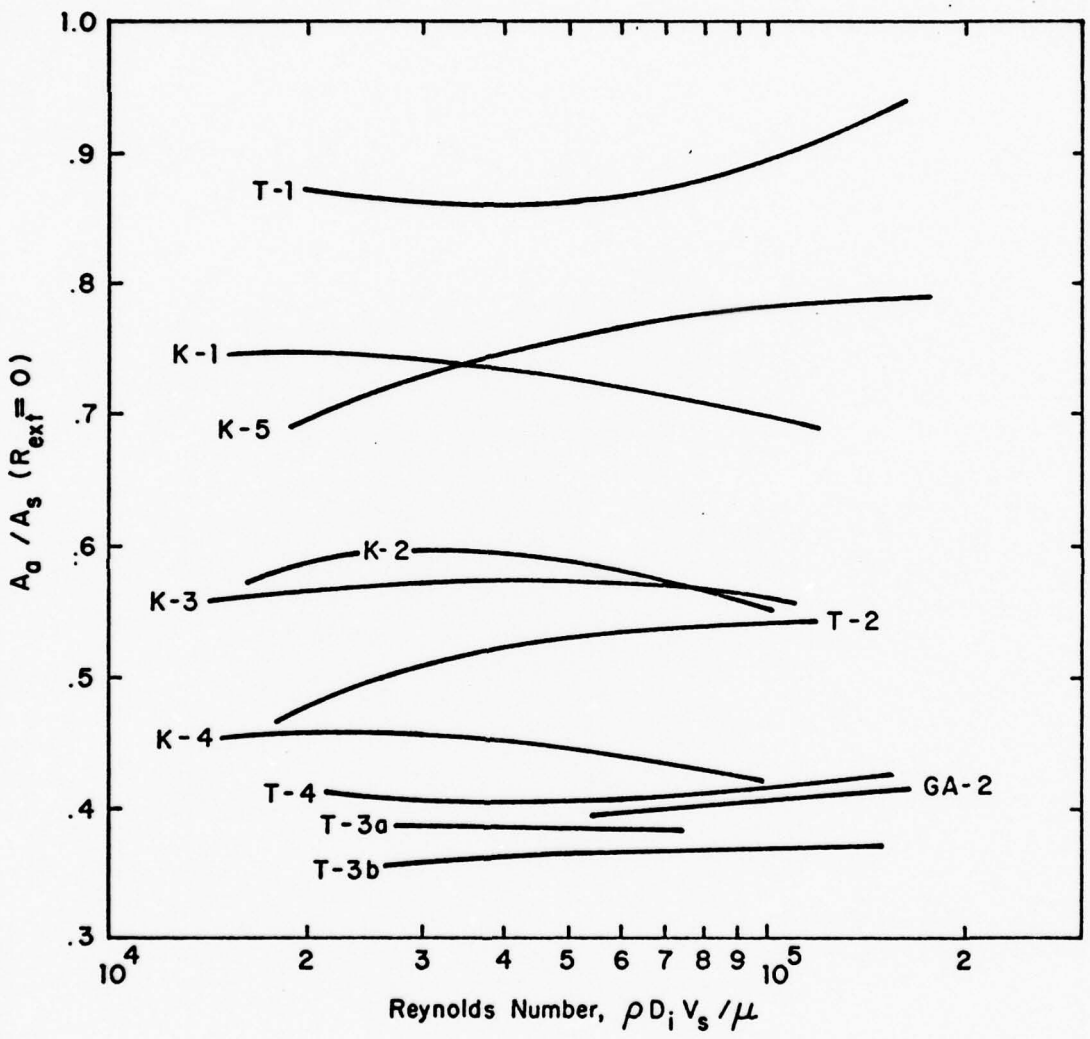


Figure 39. Augmented to Smooth Tube Surface Area Ratio (R_{ext} = 0) Versus Reynolds Number.

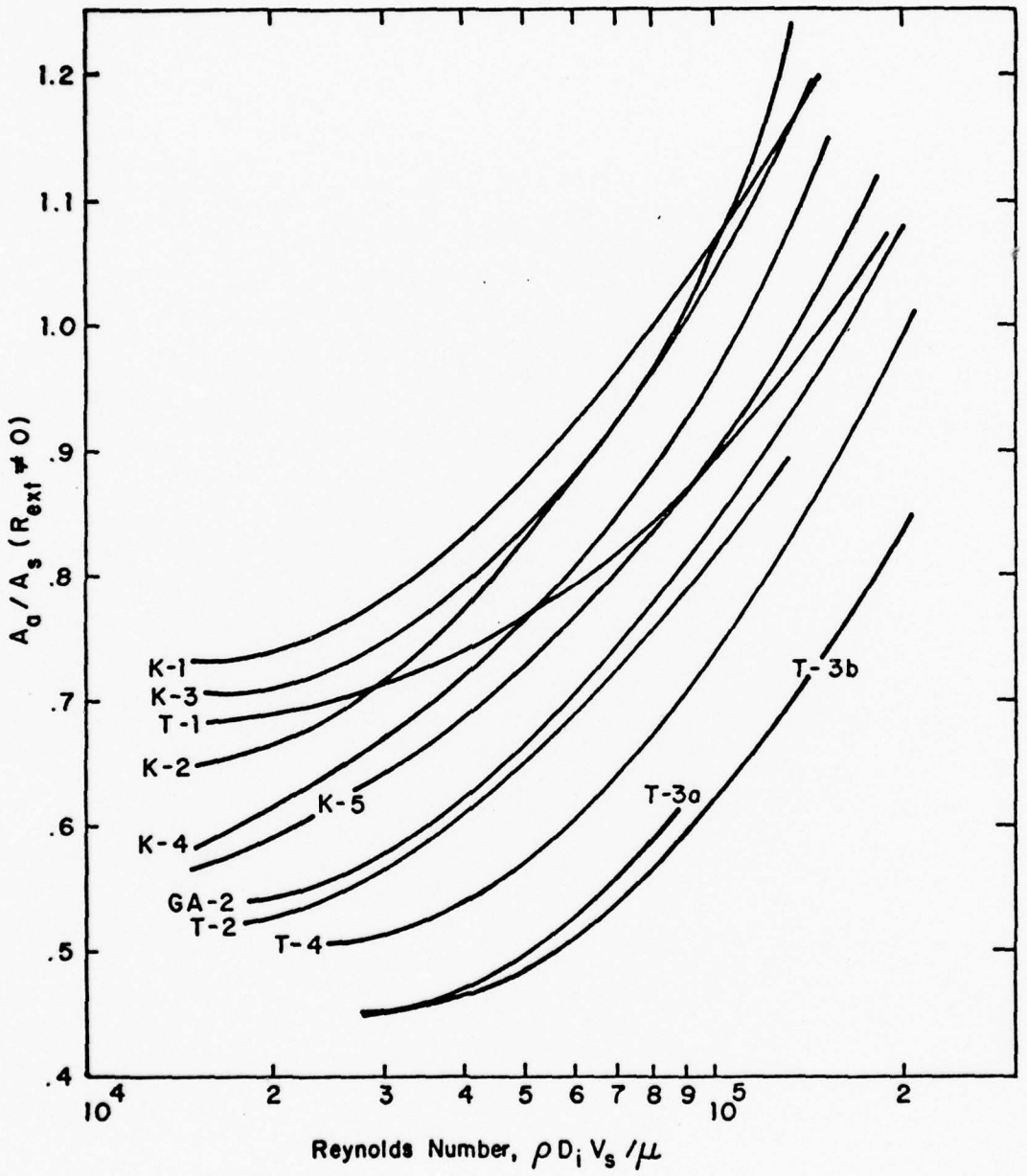


Figure 40. Augmented to Smooth Tube Surface Area Ratio ($R_{ext} \neq 0$) Versus Reynolds Number.

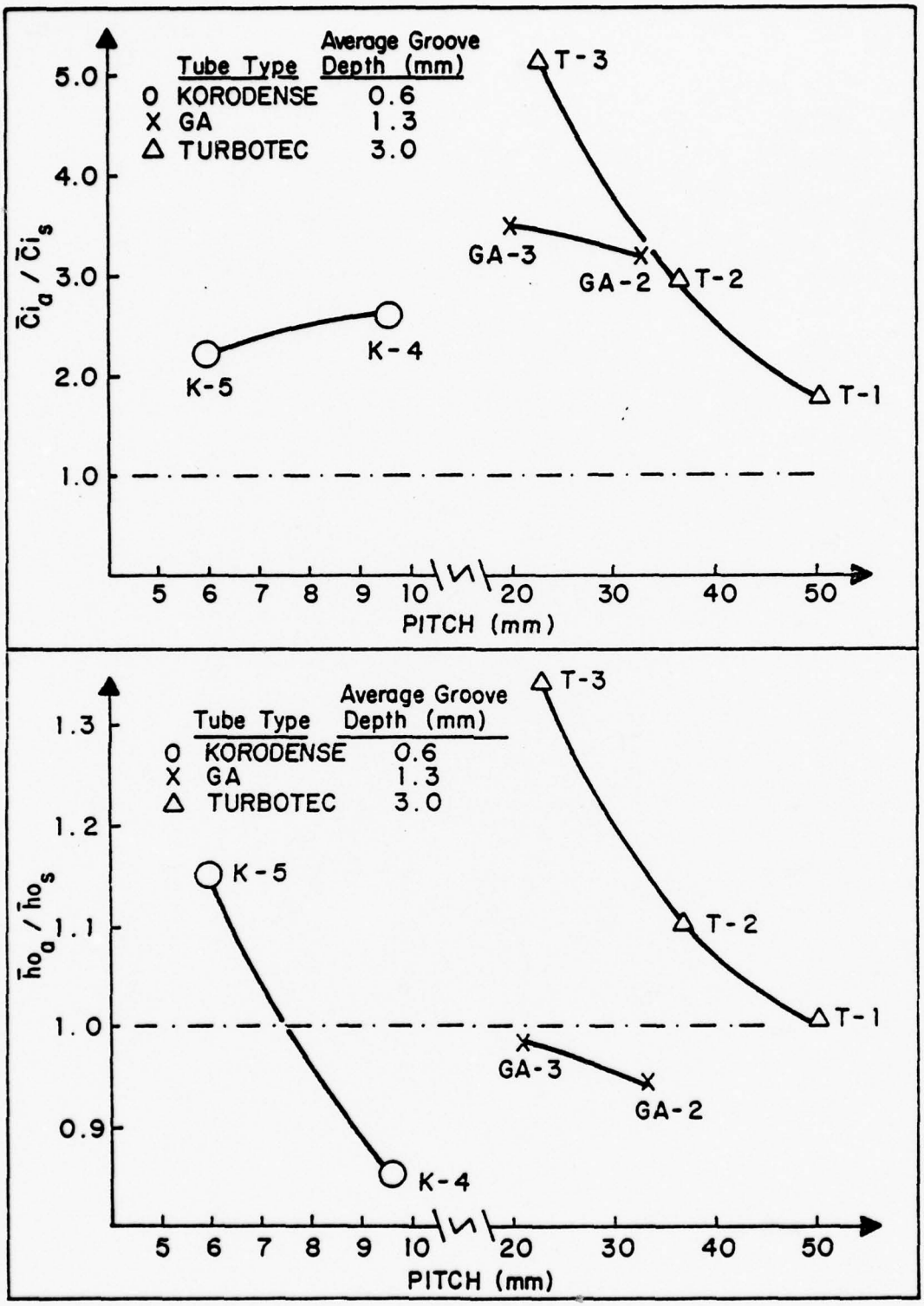


Figure 41. Comparative Effect of Tube Pitch (Helix Angle) on Both Inside and Outside Heat Transfer Coefficients (for Constant Groove Depth)

APPENDIX A

OPERATING PROCEDURES

1. Light-off Procedure

   a. Boiler Operation

      (1) Energize main circuit breaker located in power panel P-2.

      (2) Turn key switch on--located on right side of main control board.

      (3) Energize circuit breaker on left side of main control panel by depressing start button.

      (4) Energize individual circuit breakers on left side of main control panel. The following list identifies each circuit breaker:

         (a) #1 - Feed pump

         (b) #2 - Outlets

         (c) #3 - Hot water heater (feedwater tank)

         (d) #4 - Condensate pump

         (e) #5 - Boiler

         (f) #6 - Cooling tower

         (g) #7 - Cooling water pump (only when using closed cooling water system)

      (5) Insure water level is up in the feedwater tank, and turn on switch to energize heater.

      (6) Turn on the switch to the feed pump to recirculate water in the feedwater tank.

(7) Energize instrumentation.

(a) Multichannel pyrometer.

(b) Autodata 9 recorder and amplifier.

(c) Program Autodata using following procedure:

SET TIME:

- all alarms and output switches off
- set date/time on thumbwheels (24 Hour clock)
- depress the STOP/ENTER switch
- set the DISPLAY switch to "time"
- lift the SET TIME switch to enter time.

ASSIGNING MULTIPLE CHANNELS:

- depress the STOP/ENTER switch
- check that all alarms and output switches are still off
- set the SCAN switch to "continuous"
- set the FIRST CHANNEL and LAST CHANNEL thumbwheels to 001
- set the DISPLAY switch to "all" and depress the SLOW switch
- lift the SCAN START switch to start scanning channel 1. To assign channel 1 depress and hold the AUTO and STD RES buttons for at least one scan
- set the LAST CHANNEL thumbwheels to 039 before setting the FIRST CHANNEL thumbwheels to 002

- depress the SKIP button to skip channels 2 through 39 (may have to depress the T/^{o}C button first to break unit out of automode)
- set the LAST CHANNEL thumbwheels to 052 before setting the FIRST CHANNEL thumbwheels to 040
- to assign channels 40 through 52 depress and hold the T/^{o}C and HI RES buttons for at least one complete scan

INTERVAL SCAN:

- set thumbwheels to interval desired between scans (usually one minute)
- depress the STOP/ENTER switch
- set the DISPLAY switch to "interval"
- depress the SET INTERVAL switch
- set the SCAN switch to "interval"
- set the FIRST CHANNEL thumbwheels to 001
- set the LAST CHANNEL thumbwheels to 052
- lift the SCAN START switch

Use the following as needed/desired:

- printer on/off
- SLOW switch
- single channel display

(8) Energize cold trap refrigeration unit, insure that flammable stowage locker exhaust fan is on, and start vacuum pump.

(9) After feedwater tank has reached a temperature of 60°C, insure water level in boiler is above low level mark and energize boiler.

(10) Open valve DS-1 (set rotameter to 15-20% flow)

b. House Steam Operation

Follow steps (1) through (4), (6) and (8) as outlined above for the boiler.

2. Operation

a. Cooling Water System

(1) Open valve CW-1; then open valve CW-2 one turn to prime the cooling water pump, keeping valves SW-3 and CW-4 closed.

(2) Energize cooling water pump (switch near pump), and close valve CW-2. Open valve CW-3 one turn until flow is established, then open valve CW-4 to purge air.

(3) Open valves CW-3 and CW-4 to obtain desired flow rates.

(4) Vent both sides of the 3.66 meter manometer.

(5) When using the house water supply remove plug from sump and open valve CW-2 with valve CW-1 closed. Follow step 3.

(6) Begin flow to secondary condenser (valve behind column next to boiler).

b. Steam System

(1) Boiler Operation

(a) When boiler has reached the desired pressure (approximately 20.7 kPa) open valve MS-1.

(b) Insure valves MS-6 and MS-5 are open.

(c) Open valve MS-3 to obtain desired steam flow rate to test condenser. Open valve MS-4 as necessary to maintain boiler pressure at desired level (34.5 kPa).

(2) House Steam

(a) Insure valve MS-1 is closed. Open valve MS-2.

(b) Follow steps (b) and (c) for boiler use.

c. Condensate and Feedwater System

(1) Using Boiler

(a) To collect drains in test condenser hotwell operate with valve C-1 closed. After test run has been completed, open valve and condensate will drain into secondary condenser.

(b) The condensate pump is operated intermittently, when level in secondary condenser dictates. When pump is secured, keep valve C-2 closed. When pump is required, start pump and then open valve C-2. In this mode keep valve C-3 closed.

(c) While feed pump is running (continuous operation) valve FW-1 must be fully open and valve FW-2 must be throttled so that a

positive flow is insured. Valve FW-3 is a solenoid valve which is actuated by the boiler controls.

(d) When boiler is energized, valve FW-4 must be fully open.

(e) Make-up is added to the system through the top of the feedwater tank by removing anode.

(2) Using House Steam

(a) Follow step (a) for using boiler.

(b) To pump condensate from secondary condenser hotwell, start pump, and open valve C-3. In this mode keep valve C-2 closed.

(c) Delete steps (c) through (e) for using boiler.

3. Securing System

a. Using Boiler

(1) Close valves MS-3 and MS-4. Secure power to boiler and then close MS-1.

(2) Close valve DS-1 and drain desuperheater hotwell.

(3) Pump condensate from secondary condenser hotwell to feedwater tank. Secure valve C-2.

(4) Secure vacuum pump and refrigeration unit.

(5) Secure power to heater (switches on side and stand).

(6) Secure flow to secondary condenser.

(7) Bottom blow boiler to remove deposits. Repeat twice, blowing from high water mark to low water mark each time.

(8) Secure cooling water pump or close valve CW-2 when using house water supply. Close valves CW-3 and CW-4.

(9) Secure instrumentation.

(10) Secure power to feed pump.

(11) De-energize individual circuit breakers.

(12) De-energize circuit breaker on control panel; depress stop button. Turn key switch off.

b. Using House Steam

(1) Close valve MS-2.

(2) Pump condensate into return line; close valve C-3.

(3) Follow steps (4) through (6), (9) and (10) as outlined for procedure using boiler.

4. Secondary Systems

a. Vacuum System

Vacuum is established by a mechanical vacuum pump and is controlled by a vacuum regulator mounted on instrument board mounted by test condenser. The vacuum pump is separated from the condenser system by a refrigerated cold trap to prevent moisture from entering the pump.

b. Desuperheater

Valve DS-1 controls flow of feedwater (60^{o}C) to spray nozzles. Optimum flow level is between 15 and 20 percent flow on rotameter. Condensate is collected in a small tank below desuperheater so the mass flow rate can be determined.

5. Safety Devices

a. Emergency Power Shut-Off

To secure all power to the system in an emergency, depress the red button on the right of the main control panel next to the key switch.

b. Boiler

(1) The mercury switches mounted on the main control panel secure power to the heating elements of the boiler when the steam pressure exceeds 172.4 kPa. Power is restored to the heating elements when the pressure drops to approximately 103.4 kPa.

(2) A low water level limit switch is contained within the boiler, and when the water level inside the boiler drops below a preset level, power is secured to the boiler and will not be restored until the water level is above this preset height.

(3) The relief valve mounted on the boiler is set to lift at 206.8 kPa.

APPENDIX B

SAMPLE CALCULATIONS

A sample calculation is performed here to illustrate how the data reduction program [11] progresses to the results. The KORODENSE, copper-nickel-MHT Tube (K-2), run number 12 at 50 percent flow on the high flow rotameter was selected at random to perform this analysis. This tube and run number are the same as that used for the error analysis in Appendix C.

Section 2 of this appendix corresponds to the calculations performed for plain end inside diameter. The water property calculations are shown in section 1.

INPUT PARAMETERS

Tube	KORODENSE, CuNi-MHT, Tube K-2
Run Number	12
Tube Inside Diameter, Plain End (D_i)	0.01339 m
Tube Outside Diameter, (D_o)	0.01588 m
Overall Tube Length (L)	1.22 m
Enhanced Section Lenght (L_{TS})	0.9144 m
Enhanced Section Cross Sectional Flow Area,* (Ac)	0.0001316 m^2
Outside Nominal Surface Area, (A_n)	0.045604 m^2
Tube Thermal Conductivity, (k_w)	44.652 W/m ^oC
Wall Resistance, (R_w)	30.315 x 10^{-6} m^2 ^oC/W

*This area, Ac, was determined by measuring the liquid volume contained within the enhanced section of each tube and dividing by the enhanced section length.

Cooling Water In, (Tc_i)	22.9 ^oC
Cooling Water Out, (Tc_o)	27.8 ^oC
Average Cooling Water Temperature (T_b,T_{br})	25.35 ^oC, 298.5 ^oK
Steam Vapor Temperature, (T_v)	67.6 ^oC
Tube Wall Temperature, (T_w)	314.0 ^oK
Tube Pressure Drop, (ΔP_m)	36.148 kPa
% Flow	50
Tube Inlet Contraction Factor	Kc } Ke + Kc = 0.030
Tube Outlet Expansion Factor	Ke }

Section 1, Water Properties

$$\mu = (4.134 \times 10^{-4}) \exp\{[(0.008291758)(298.5)+(2644.2189)/(298.5)] - 10.59252566\}$$

$$\mu = 8.6717 \times 10^{-4} \text{ kg/m·sec} = 3.1218 \text{ kg/m·hr}$$

$$k = 0.5565919 + (0.002174417)(25.35) - (0.70127 \times 10^{-5})(25.35)^2 - (2.0914 \times 10^{-10})(25.35)^3$$

$$k = 0.6072035 \text{ W/m·}^oC$$

$$\rho = 1004.44434 - (0.12673368)(25.35) - (0.0023913147)(25.35)^2$$

$$\rho = 999.695 \text{ kg/m}^3$$

$$c_p = 4.2377955 - (0.0018553514)(25.35) + (1.3948314 \times 10^{-5})(25.35)^2$$

$$c_p = 4.1997259 \text{ kJ/kg·}^oC$$

$$\dot{m} = \ell/m \times \rho = (35.582)(60)(0.001)(999.695)$$

$$\dot{m} = 2134.2688 \text{ kg/hr} = 0.59285 \text{ kg/sec}$$

$$Pr = \frac{\mu c_p}{k} = \frac{(8.6717 \times 10^{-4})(4.1997259 \times 10^{3})}{(0.6072035)}$$

$$Pr = 5.997$$

Section 2, Plain-End-Tube Reduction

1. Determination of cooling water velocity

$$v = \frac{4\dot{m}}{\rho\pi D_i^2} \qquad v_{TS} = \frac{\dot{m}}{\rho Ac} = v_a$$

$$v = \frac{(4)(2134.2688)}{(999.695)(\pi)(0.01339)^2} \qquad v_{TS} = \frac{(2134.2688)}{(999.695)(0.0001316)}$$

$$v = 15161.094 \text{ m/hr} \qquad v_{TS} = 16222.795 \text{ m/hr}$$

$$= 4.211 \text{ m/sec} \qquad = 4.506 \text{ m/sec}$$

2. Determination of Mass Flow Rate per Unit Area

$$G = \frac{4\dot{m}}{\pi D_i^2} = \rho v$$

$$= (999.695)(15161.094)$$

$$= 15,156,469. \text{ kg/m}^2 \text{ hr}$$

$$= 4210.13 \text{ kg/m}^2 \text{ sec}$$

3. Determination of Reynolds Number

$$Re = \frac{D_i G}{\mu_{H_2O}}$$

$$= \frac{(0.01339)(4210.13)}{(8.6717 \times 10^{-4})}$$

$$Re = 65,008.75$$

4. Determination of Overall Heat Transfer Coefficient

$$U_n = \frac{\dot{m} c_p}{A_n} \ln \left(\frac{T_v - Tc_i}{T_v - Tc_o}\right)$$

$$= \frac{(0.59285)(4.1997259 \times 10^3)}{(0.045604)} \ln \left(\frac{67.6 - 22.9}{67.6 - 27.8}\right)$$

$$= 6339.01 \text{ W/m}^2 \text{ }^\circ\text{C}$$

5. Determination of Corrected Overall Heat Transfer Coefficient

$$U_c = \frac{1}{\frac{1}{U_n} - R_w}$$

$$= \frac{1}{\frac{1}{6339.01} - 30.315 \times 10^{-6}}$$

$$= 7846.932 \text{ W/m}^2 \text{ }^\circ\text{C}$$

6. Determination of Friction Factor

$$f_s = \frac{0.046}{Re^{0.2}}$$

$$= \frac{0.046}{65008.75^{0.2}}$$

$$= 0.005014$$

$$\Delta P_s = \frac{4 f_s G^2 \left(\frac{L_s}{D_i}\right)}{\rho \, 2g_c}$$

$$= \frac{(4)(0.005014)(4210.13)^2 \left(\frac{0.3842}{0.01339}\right)}{(999.695)(2)}$$

$$= 5.103 \text{ kPa}$$

$$\Delta P_{exp/con} = \frac{\rho\, v_{TS}^2}{2g_c} \quad (Kc + Ke)$$

$$= \frac{(999.695)(4.506)^2}{(2)} \quad (0.030)$$

$$= 0.3045 \text{ kPa}$$

$$\Delta P_{TS} = \Delta P_m - \Delta P_s - \Delta P_{exp/con}$$

$$= 36.147502 - 5.102 - .3045$$

$$= 30.741 \text{ kPa}$$

$$f_a = \frac{\rho \Delta P_{TS} 2g_c}{4G^2 \left(\frac{L_{TS}}{D_i}\right)}$$

$$= \frac{(999.695)(30.741 \times 10^3)(2)}{(4)(4210.13)^2\left(\frac{0.9144}{0.01339}\right)}$$

$$= 0.0126943$$

7. Determination of Wilson Plot Parameters

(a) Ordinate

$$Y = \frac{1}{U_n}$$

$$= \frac{1}{6339.01} = 1.578 \times 10^{-4} \quad \frac{m^2\, {}^\circ C}{W}$$

(b) Abscissa

$$X = \frac{1}{Re^{0.8} Pr^{1/3}} \left(\frac{\mu}{\mu_w}\right)^{0.14}$$

$$\mu_w = (4.134 \times 10^{-4}) \exp\{[(0.008291758)(314.0) + (2644.2189)/(314.0)] - 10.59252566\}$$

$$= 6.368799 \times 10^{-4} \text{ kg/m·sec}$$

$$X = \frac{1}{(65008.75)^{0.8}(5.997)^{1/3}(\frac{8.6717}{6.368799})^{0.14}}$$

$$= 7.4395 \times 10^{-5}$$

8. Determination of Sieder Tate Coefficient

$C_i = \frac{D_o}{Mk}$, where M = slope of linear regression subroutine

M = 0.4726852, from linear regression subroutine

$$C_i = \frac{(0.01588)}{(0.4726852)(0.6072035)}$$

$C_i = 0.055328$

9. Determination of Inside Heat Transfer Coefficient

$$h_i = \frac{C_i}{D_i} k \, Re^{0.8} Pr^{1/3} (\frac{\mu}{\mu_w})^{0.14}$$

$$= (\frac{0.055328}{0.01339}) \, (0.6072035)(65008.75)^{0.8}(5.997)^{1/3} \, (\frac{8.6717}{6.368799})^{0.14}$$

$h_i = 33725.222 \ W/m^2 \ ^oC$

10. Determination of Outside Heat Transfer Coefficient

$$h_o = \frac{1}{\frac{1}{U_n} - R_w - \frac{D_o}{D_i h_i}}$$

$$= \frac{1}{1.577533 \times 10^{-4} - 30.315 \times 10^{-6} - \frac{(0.01588)}{(0.01339)(33725.222)}}$$

$h_o = 10837.413 \ W/m^2 \ ^oC$

11. Determination of Nusselt Number

$$Nu = \frac{h_i D_i}{k} = \frac{(33725.22)(.01339)}{(.6072035)}$$

$$= 743.706$$

12. Determination of Stanton Number

$$St = \frac{Nu}{RePr}$$

$$= \frac{(743.706)}{(65008.75)(5.997)}$$

$$= 1.90764 \times 10^{-3}$$

13. Determination of Performance Factor

$$TPF = \frac{2j}{f_a}$$

$$j = St\ Pr^{2/3} = (1.90764 \times 10^{-3})(5.997)^{2/3}$$

$$j = 6.2968 \times 10^{-3}$$

$$TPF = \frac{(2)(6.2969 \times 10^{-3})}{(0.0126943)}$$

$$TPF = 0.9921$$

14. Determination of Area Ratios

a. $R_{ext} = 0$

$$Re_s = \sqrt{\frac{0.027\ f_a\ Re_a^3}{0.046\ \ Nu_a/Pr^{1/3}\ (\mu/\mu_w)^{0.14}}}$$

$$= 74195.57$$

$$f_s = \frac{0.046}{Re_s^{0.2}}$$

$$= 0.00488295$$

$$\frac{A_a}{A_s} = \frac{Re_s^3 f_s}{Re_a^3 f_a}$$

$$= 0.579$$

14. b. $R_{ext} \neq 0$

Correction factors F_1, F_2 and F_3 were obtained from reference [23] and applied as outlined in reference [22].

F_1 = 1.0 (fouling correction)

F_2 = 0.9 (material correction for 90-10 copper-nickel)

F_3 = 1.02 (temperature correction from coolant inlet temperature of 23.2°C to 21.1°C)

C' = 2883 (from III.B.5.(b)(2))

$C = F_1 F_2 F_3 C' = 2595$

$U_a = U_n/F_3 = 6214.72 \text{ W/m}^2 \text{ °C}$

$$v_s = [\frac{f_a v_a^3 C}{0.046 U_a}(\frac{\rho D_i}{\mu})^{1/5}]^{1/2.3}$$

$$= 5.89 \text{ m/s}$$

$$U_s = C (v_s)^{0.5}$$

$$= 6297.9 \text{ W/m}^2 \text{ °C}$$

$$\frac{A_a}{A_s} = \frac{U_s}{U_a} = \frac{6297.9}{6214.72}$$

$$= 1.013$$

APPENDIX C

ERROR ANALYSIS

The basic equations used in this section are reproduced from Reilly [11]. The general form of the Kline and McClintock [27] "second order" equation is used to compute the probable error in the results. For some resultant, R, which is a function of primary variables X_1, X_2, ... X_n, the probable error in R, δR is given by:

$$\delta R = [(\frac{\delta R}{\delta X_1} \delta X_1)^2 + (\frac{\delta R}{\delta X_2} \delta X_2)^2 + \ldots + (\frac{\delta R}{\delta X_n} \delta X_n)^2]^{1/2} \qquad (C\text{-}1)$$

where δX_1, δX_2, ..., δX_n is the probable error in each of the measured variables.

C.1. Uncertainty in Overall Heat Transfer Coefficient, U_n

The overall heat transfer coefficient is given by equation (4), in Chapter III as:

$$U_n = \frac{\dot{m} c_p}{A_n} \ln [\frac{T_v - Tc_i}{T_v - Tc_o}] \quad . \qquad (4)$$

By applying equation (C-1) to equation (4), the following equation results:

$$\frac{\delta U_n}{U_n} = \left[\left(\frac{\delta A_n}{A_n}\right)^2 + \left(\frac{\delta c_p}{c_p}\right)^2 + \left(\frac{\delta \dot{m}}{\dot{m}}\right)^2 + \left(\frac{\delta T_v\,(Tc_i - Tc_o)}{(T_v - Tc_i)(T_v - Tc_o)\ln\frac{T_v - Tc_i}{T_v - Tc_o}}\right)^2\right.$$

$$\left. + \left(\frac{\delta Tc_i}{(T_v - Tc_i)\ln\frac{T_v - Tc_i}{T_v - Tc_o}}\right)^2 + \left(\frac{\delta Tc_o}{(T_v - Tc_o)\ln\frac{T_v - Tc_i}{T_v - Tc_o}}\right)^2\right]^{1/2}$$

(C-2)

The following are the values assigned to the variables.

$\delta c_p = 0.0042$ kj/kg ^oC

$\delta \dot{m} = 0.01\ \dot{m}$ kg/sec

$\delta_{T_v} = 1.0\ ^oC$

$\delta Tc_o = 0.1\ ^oC$

$\delta Tc_i = 0.1\ ^oC$

$\delta A_n = 0.00074\ m^2$

For Run 12 at 50 Percent Flow

$$\frac{\delta U_n}{U_n} = \left[\left(\frac{.00074}{.045604}\right)^2 + \left(\frac{.0042}{4.19973}\right)^2 + \left(\frac{.01\ \dot{m}}{\dot{m}}\right)^2 + \left(\frac{(1.0)(-4.9)}{(44.7)(39.8)\ln(1.123)}\right)^2\right.$$

$$\left. + 2 + \left(\frac{(0.1)}{(39.8)\ln(1.123)}\right)^2\right]^{1/2}$$

$$\frac{\delta U_n}{U_n} = .051$$

$\therefore U_n,\ 50\% = 6339 \pm 326\ W/m^2\ ^oC$

C.2. Uncertainty in Inside Heat Transfer Coefficient, h_i

The probable error in the inside heat transfer coefficient is given by:

$$\frac{\delta h_i}{h_i} = \left[\left(\frac{\delta k}{k}\right)^2 + \left(\frac{\delta D_i}{D_i}\right)^2 + \left(\frac{0.8\delta Re}{Re}\right)^2 + \left(\frac{0.333\delta Pr}{Pr}\right)^2 + \left(\frac{\delta C_i}{C_i}\right)^2 + \left(\frac{0.14\delta(\mu/\mu_w)}{\mu/\mu_w}\right)^2\right]^{1/2}, \quad \text{(C-3)}$$

where:

$\delta k = 0.030$ W/m °C,

$\delta D_i = 0.00051$ m,

$\delta Pr = 0.10$, and

$\delta\left(\frac{\mu}{\mu_w}\right) = 0.050$.

The probable error in the Reynolds number is given by:

$$\frac{\delta Re}{Re} = \left[\left(\frac{\delta G}{G}\right)^2 + \left(\frac{\delta \mu}{\mu}\right)^2 + \left(\frac{\delta D_i}{D_i}\right)^2\right]^{1/2}, \quad \text{(C-4)}$$

where,

$$\frac{\delta G}{G} = \left[\left(\frac{0.01\dot{m}}{\dot{m}}\right)^2 + \left(2\frac{\delta D_i}{D_i}\right)^2\right]^{1/2}, \quad \text{(C-5)}$$

$$\frac{\delta G}{G} = \left[(.01)^2 + \left(\frac{.00013}{.01339}\right)^2\right]^{1/2} = 0.013 .$$

Since $\delta\mu = 0.15$ kg/m·hr, then

$$\frac{\delta Re}{Re} = \left[(.013)^2 + \left(\frac{0.15}{3.1218}\right)^2 + \left(\frac{.00051}{.01339}\right)^2\right]^{1/2} = 0.05$$

$\therefore Re_{50\%} = 65008 \pm 3245$

The probable error in the coefficient C_i is given by:

$$\frac{\delta C_i}{C_i} = \left[\left(\frac{\delta D_o}{D_o}\right)^2 + \left(\frac{\delta slope}{slope}\right)^2 + \left(\frac{\delta k}{k}\right)^2\right]^{1/2} , \qquad (C\text{-}6)$$

where:

δD_o = 0.00025 m,

δk = 0.03 W/m·°C, and

$\delta slope$ = 0.065 slope.

$$\frac{\delta C_i}{C_i} = \left[\left(\frac{0.00025}{.01588}\right)^2 + (.065)^2 + \left(\frac{0.03}{.6072035}\right)^2\right]^{1/2}$$

$$\frac{\delta C_i}{C_i} = 0.082$$

$$\therefore C_{i,50\%} = 0.053 \pm .004$$

Using the above information, the probable error in the inside heat transfer coefficient can be calculated as:

$$\frac{\delta h_i}{h_i} = \left[\left(\frac{.030}{.6072035}\right)^2 + \left(\frac{0.00051}{.01339}\right)^2 + (.082)^2 + (0.8 \times 0.05)^2 + \left(\frac{.333 \times 0.1}{5.997}\right)^2 + \left(\frac{.14 \times 0.05}{1.361591}\right)^2\right]^{1/2}$$

$$\frac{\delta h_i}{h_i} = 0.096$$

$$\therefore h_{i,50\%} = 33725 \pm 3238 \text{ W/m}^2 \text{ °C}$$

C.3 The Uncertainty in the Outside Heat Transfer Coefficient, h_o

The probable error in the outside heat transfer coefficient is given by:

$$\frac{\delta h_o}{h_o} = \left\{ \left[\frac{\delta U_n}{U_n^2 \left(\frac{1}{U_n} - R_w - \frac{D_o}{D_i h_i}\right)} \right]^2 + \left[\frac{\delta R_w}{\left(\frac{1}{U_n} - R_w - \frac{D_o}{D_i h_i}\right)} \right]^2 + \left[\frac{\left(\frac{D_o}{D_i h_i}\right)\left(\frac{\delta h_i}{h_i}\right)}{\frac{1}{U_n} - R_w - \frac{D_o}{D_i h_i}} \right]^2 \right\}^{1/2}, \qquad \text{(C-7)}$$

where:

$$\frac{\delta U_n}{U_n} = .051,$$

$$\delta R_w = 1.54 \times 10^{-6} \text{ m}^2 \text{ }^\circ\text{C/W, and}$$

$$\frac{\delta h_i}{h_i} = 0.096$$

also, $\frac{1}{U_n} - R_w - \frac{D_o}{D_i h_i} = 9.2273 \times 10^{-5} \text{ m}^2 \text{ }^\circ\text{C/W.}$

With this information:

$$\frac{\delta h_o}{h_o} = \left\{ \left[\frac{.051}{(6339.01)(9.2273 \times 10^{-5})} \right]^2 + \left[\frac{1.54 \times 10^{-6}}{9.2273 \times 10^{-5}} \right]^2 + \left[\frac{(.01588)(.096)}{(.01339)(33725)(9.2273 \times 10^{-5})} \right]^2 \right\}^{1/2}$$

$$\frac{\delta h_o}{h_o} = .096$$

$$\therefore h_o = 10837 \pm 1041 \text{ W/m}^2 \text{ }^\circ\text{C}$$

C.4 Uncertainty in Tube Performance Factor, 2j/f

Since the Colburn Analogy defines j as St $Pr^{2/3}$, the probable error in the Tube Performance Factor 2j/f is given by:

$$\frac{\delta TPF}{TPF} = \left[\left(\frac{\delta St}{St}\right)^2 + \left(\frac{2}{3}\frac{\delta Pr}{Pr}\right)^2 + \left(\frac{\delta f_a}{f_a}\right)^2\right]^{1/2}, \qquad \text{(C-8)}$$

where

$$\frac{\delta St}{St} = \left[\left(\frac{\delta Nu}{Nu}\right)^2 + \left(\frac{\delta Re}{Re}\right)^2 + \left(\frac{\delta Pr}{Pr}\right)^2\right]^{1/2}, \qquad \text{(C-9)}$$

$$\frac{\delta Nu}{Nu} = \left[\left(\frac{\delta h_i}{h_i}\right)^2 + \left(\frac{\delta D_i}{D_i}\right)^2 + \left(\frac{\delta k}{k}\right)^2\right]^{1/2}, \text{ and} \qquad \text{(C-10)}$$

$$\frac{\delta f_a}{f_a} = \left[\left(\frac{\delta \Delta P_{TS}}{\Delta P_{TS}}\right)^2 + \left(2\,\frac{\delta G}{G}\right)^2 + \left(\frac{\delta L_{TS}}{L_{TS}}\right)^2 + \left(\frac{\delta \rho}{\rho}\right)^2 + \left(\frac{\delta D_i}{D_i}\right)^2\right]^{1/2}. \qquad \text{(C-11)}$$

Assuming $\delta\Delta P_{TS} = .02\ \Delta P_{TS}$, $\delta\rho = 0.1\rho$, and $\delta L_{TS} = .0013$ m, the following numerical values result:

$$\frac{\delta f_a}{f_a} = \left[(.02)^2 + (2 \times .013)^2 + \left(\frac{.0013}{.9144}\right)^2 + (.01)^2 + \left(\frac{.000051}{.01339}\right)^2\right]^{1/2}$$

$$\frac{\delta f_a}{f_a} = 0.03$$

$$\frac{\delta Nu}{Nu} = \left[(.096)^2 + \left(\frac{.000051}{.01339}\right)^2 + \left(\frac{.030}{.6072035}\right)^2\right]^{1/2}$$

$$\frac{\delta Nu}{Nu} = 0.11$$

$$\frac{\delta St}{St} = \left[(0.11)^2 + (.05)^2 + \left(\frac{0.10}{5.997}\right)^2\right]^{1/2}$$

$$\frac{\delta St}{St} = 0.12$$

$$\frac{\delta TPF}{TPF} = \left[(0.12)^2 + \left(\frac{2}{3} \times \frac{0.10}{5.997}\right)^2 + (0.03)^2\right]^{1/2}$$

$$\frac{\delta TPF}{TPF} = 0.124$$

$\therefore TPF_{50\%} = 0.992 \pm 0.123$

C. 5 Uncertainty in the Area Ratios

C. 5. 1 $R_{ext} = 0$

Using Equation (24) the probable error in the area ratio ($R_{ext} = 0$) is given by:

$$\frac{\delta(A_a/A_s)}{(A_a/A_s)} = \left[\left(\frac{\delta Nu_s}{Nu_s}\right)^2 + \left(\frac{\delta Nu_a}{Nu_a}\right)^2\right]^{1/2} \qquad \text{(C-12)}$$

where

$$\frac{\delta Nu_a}{Nu_a} = .11$$

In addition, from equation (26),

$$\frac{\delta Re_s}{Re_s} = \left[\left(\frac{1}{2}\frac{\delta f_a}{f_a}\right)^2 + \left(\frac{3}{2}\frac{\delta Re_a}{Re_a}\right)^2 + \left(\frac{1}{6}\frac{\delta Pr}{Pr}\right)^2 + \left(0.07\frac{\delta(\mu/\mu_w)}{(\mu/\mu_w)}\right)^2 + \left(\frac{1}{2}\frac{\delta Nu_a}{Nu_a}\right)^2\right]^{1/2}$$

$$\therefore \frac{\delta Re_s}{Re_s} = \left[\left(\frac{1}{2}\{.03\}\right)^2 + \left(\frac{3}{2} \times 0.05\right)^2 + \left(\frac{1}{6} \times \frac{0.10}{5.997}\right)^2 + \left(0.07 \times \frac{0.050}{1.361591}\right)^2 + \left(\frac{1}{2} \times 0.11\right)^2\right]^{1/2}$$

$$\frac{\delta Re_s}{Re_s} = 0.094$$

and using equation (25)

$$\frac{\delta Nu_s}{Nu_s} = \left[\left(0.8\frac{\delta Re_s}{Re_s}\right)^2 + \left(\frac{1}{3} \times \frac{\delta Pr}{Pr}\right)^2 + \left(.14 \times \frac{\delta(\mu/\mu_w)}{(\mu/\mu_w)}\right)^2\right]^{1/2} \quad \text{(C-13)}$$

$$\frac{\delta Nu_s}{Nu_s} = \left[(.8 \times .094)^2 + \left(\frac{1}{3} \times \frac{.10}{5.997}\right)^2 + \left(.14 \times \frac{.15}{1.36159}\right)^2\right]^{1/2}$$

$$\frac{\delta Nu_s}{Nu_s} = .075$$

$$\frac{\delta(A_a/A_s)}{(A_a/A_s)} = [(.075)^2 + (0.11)^2\ ]^{1/2} = .13$$

$$\therefore A_a/A_{s(R_{ext}=0)50\%} = 0.57 \pm 0.07$$

C. 5. 2 $R_{ext} \neq 0$

From equation (29), the probable error in the Area Ratio ($R_{ext} \neq 0$) is given by:

$$\frac{\delta(A_a/A_s)}{(A_a/A_s)} = [(\frac{\delta U_s}{U_s})^2 + (\frac{\delta U_a}{U_a})^2\ ]^{1/2} \qquad \text{(C-14)}$$

where:

$$\frac{\delta U_a}{U_a} = .051$$

and from equation (30)

$$\frac{\delta U_s}{U_s} = \frac{1}{2}\frac{\delta v_s}{v_s} \ . \qquad \text{(C-15)}$$

Equation (27) can be used as follows:

$$\frac{\delta v_s}{v_s} = [(\frac{\delta Re_s}{Re_s})^2 + (\frac{\delta D_i}{D_i})^2 + (\frac{\delta \rho}{\rho})^2 + (\frac{\delta \mu}{\mu})^2]^{1/2} \qquad \text{(C-16)}$$

$$\frac{\delta v_s}{v_s} = \left[(.094)^2 + \left(\frac{.000051}{.01339}\right)^2 + (.01)^2 + \left(\frac{.15}{3.1218}\right)^2\right]^{1/2}$$

$$\frac{\delta v_s}{v_s} = .11 ,$$

and

$$\frac{\delta(A_a/A_s)}{(A_a/A_s)} = \left[\left(\frac{1}{2} \times .11\right)^2 + (.051)^2\right]^{1/2} = .075$$

$$\therefore A_a/A_{s_{(R_{ext} \neq 0)50\%}} = 1.013 \pm .076$$

BIBLIOGRAPHY

1. Search, H. T., A Feasibility Study of Heat Transfer Improvement in Marine Steam Condensers, MSME, Naval Postgraduate School, Monterey, CA December 1977.

2. Bergles, A. E., Enhancement of Heat Transfer, Keynote paper presented at the Sixth International Heat Transfer Conference, Toronto, Canada, 7-11 August 1978.

3. Palen, J., Cham, B., and Taborek, J., Comparison of Condensation of Steam on Plain and Turbotec Spirally Grooved Tubes in a Baffled Shell-and-Tube Condenser, Heat Transfer Research, Inc., Report 2439-300/6, January 1971.

4. Young, E. H., Withers, J. G., and Lampert, W. B., Heat Transfer Characteristics of Corrugated Tubes in Steam Condensing Applications, AIChE Paper No. 3, August 11, 1975.

5. Catchpole, J. P., Drew, B. C. H., "Evaluation of Some Shaped Tubes for Steam Condensers," Steam Turbine Condenser, NEL Report No. 619, pp 68-82, August, 1976.

6. Newson, I. H., Hodgson, T. K., "The Development of Enhanced Heat Transfer Condenser Tubing," 4th International Symposium on Fresh Water From the Sea, Vol. 1, pp 69-94, 1973.

7. Combs, S. K., An Experimental Study of Heat Transfer Enhancement for Ammonia Condensing on Vertical Fluted Tubes, Oak Ridge National Laboratory, Report ORNL-5356, January, 1978.

8. Combs, S. K., Mailen, G. S., Murphy, R. W., Condensation of Refrigerants on Vertical Fluted Tubes, Oak Ridge National Laboratory, Report ORNL/TM-5848, August, 1978.

9. Beck, A. C., A Test Facility to Measure Heat Transfer Performance of Advanced Condenser Tubes, MSME, Naval Postgraduate School, Monterey, CA, January 1977.

10. Pence, D. T., An Experimental Study of Steam Condensation on a Single Horizontal Tube, MSME, Naval Postgraduate School, Monterey, CA, March 1978.

11. Reilly, D. J., An Experimental Investigation of Enhanced Heat Transfer on Horizontal Condenser Tubes, MSME, Naval Postgraduate School, Monterey, CA, March, 1978.

12. Metals Handbook, 8th ed., v. 2, p 665, American Society for Metals, 1964.

13. Acurex Autodata, Autodata Nine Technical Manual.

14. Brundrett, E., "Modified Hydraulic Diameter for Turbulent Flow," Proceedings of NATO Advanced Studies Institute on Turbulent Forced Convection in Channels, Istanbul, July 1978.

15. Holman, J. P., Heat Transfer, 4th ed., McGraw-Hill, 1976.

16. Wilson, E. E., A Basis for Rational Design of Heat Transfer Apparatus, paper presented at the Spring Meeting of the Society of Mechanical Engineers, Buffalo, NY, June 1935.

17. Briggs, D. E., and Young, E. H., "Modified Wilson Plot Techniques for Obtaining Heat Transfer Correlations for Shell and Tube Heat Exchangers," Heat Transfer-Philadelphia, v. 65, No. 92, pp 35-45, 1969.

18. Subroutine, NPS COMPUTER FACILITY, LEAST SQUARES POLYNOMINAL FITTING, LSQPL2, Programmed By D. E. Harrison, November 1969.

19. Kays, W. M., and London, A. L., Compact Heat Exchangers, pp 92-97, 2nd ed., McGraw-Hill, 1964.

20. Knudsen, J. G., and Katz, D. L., Fluid Dynamics and Heat Transfer, pp 332-335, McGraw-Hill, 1958.

21. Bergles, A. E. and Jensen, M. K., Enhanced Single-Phase Heat Transfer for Ocean Thermal Energy Conversion Systems, Report HTL-13 ISU-ERI-AMES-77314, ERI Project 1278, April 1977.

22. Department of the Navy, Bureau of Ships, Design Data Sheet DDS 4601-1, 15 OCT 1953.

23. Standards for Steam Surface Condensers, 6th ed., Heat Exchange Institute, NY, 1970.

24. Reynolds, O., Transactions of the Royal Society, 174A:935, London, 1883.

25. Colburn, A. P., Trans. AIChE, 29:174, 1933.

26. Cunningham, J., Milne, H. K., The Effect of Helix Angle on the Performance of Roped Tubes, paper presented at Sixth International Heat Transfer Conference, Toronto, Canada, 7-11 August, 1978.

27. Kline, S. J., McClintock, F. A., "Describing Uncertainties In Single Sample Experiments," Mechanical Engineering, v. 74, pp 3-8, January 1953.

INITIAL DISTRIBUTION LIST

		No. Copies
1.	Defense Documentation Center Cameron Station Alexandria, Virginia 22314	2
2.	Library, Code 0142 Naval Postgraduate School Monterey, California 93940	2
3.	Department Chairman, Code 69 Department of Mechanical Engineering Naval Postgraduate School Monterey, California 93940	2
4.	Office of Research Administration, Code 012A Naval Postgraduate School Monterey, California 93940	1
5.	Professor Paul J. Marto, Code 69Mx Department of Mechanical Engineering Naval Postgraduate School Monterey, California 93940	20
6.	LT James Fenner 1081 Debolt Road Utica, Ohio 43080	4
7.	CDR W. W. Baline, USN Naval Sea Systems Command (033) (acting) 2221 Jefferson Davis Highway, CP#6 Arlington, Virginia 20360	1
8.	Mr. Charles Miller Naval Sea Systems Command (0331) 2221 Jefferson Davis Highway, CP#6 Arlington, Virginia 20360	2
9.	Mr. Frank Ventriglio Naval Sea Systems Command (0331) 2221 Jefferson Davis Highway, CP#6 Arlington, Virginia 20360	1
10.	Dr. Earl Quandt Naval Ship Research & Development Center Annapolis Laboratory Annapolis, Maryland 21402	1
11.	Mr. J. W. Murrin Naval Sea Systems Command (0331) 2221 Jefferson Davis Highway, CP#6 Arlington, Virginia 20360	1

12. CAPT R. E. Greer, USN — 1
Naval Sea Systems Command (PMS-301)
2221 Jefferson Davis Highway, CP#6
Arlington, Virginia 20360

13. CDR D. W. Barns, USN — 1
Naval Sea Systems Command (PMS-301.B)
2221 Jefferson Davis Highway, CP#6
Arlington, Virginia 20360

14. Mr. Walter Aerni — 1
Naval Ship Engineering Center (6145)
Washington, D. C. 20360

15. Mr. Wayne L. Adamson — 1
Naval Ship Research & Development Center(2761)
Annapolis, Maryland 21402

16. Mr. Gil Carlton — 1
Naval Ship Engineering Center (6723)
Philadelphia, Pennsylvania 19112

17. Dr. David Eissenberg — 1
Oak Ridge National Laboratory
Post Office Box Y
Oak Ridge, Tennessee 37830

18. Miss Eleanor J. Macnair — 1
Ship Department
Ministry of Defence
Director - General Ships, Block B
Foxhill, Bath, Somerset
ENGLAND

19. Mr. Kurt Bredehorst — 1
NAVSEC 6147D
Department of the Navy
Hyattsville, Maryland 02782

20. Professor Kenneth J. Bell — 1
School of Chemical Engineering
Oklahoma State University
Stillwater, Oklahoma 74074

21. Professor A. E. Bergles — 1
Department of Mechanical Engineering
Iowa State University
Ames, IA 50010

22. Professor James G. Knudsen — 1
Engineering Experimental Station
Oregon State University
Covell Hall-219
Corvallis, Oregon 97331

23. Dr. Ken Read — 1
OTEC Branch
Division of Solar Energy
Department of Energy
Washington, D. C. 20545

24. Dr. A. L. London — 1
4020 Amaranta Avenue
Palo Alto, California 94306

25. Mr. Norman F. Sather — 1
Argonne National Laboratory
9700 S. Cass Avenue
Argonne, Illinois 60439

26. Dr. Jeff Horowitz — 1
Argonne National Laboratory
9700 S. Cass Avenue
Argonne, Illinois 60439

27. Mr. J. B. Henderson — 2
Market Development Manager
Wolverine Tube Division
Universal Oil Products Incorporated
Post Office Box 2202
Decatur, Alabama 35602

28. Mr. M. K. Ellingsworth — 1
Office of Naval Research
800 N. Quincy Street
Arlington, Virginia 22217

29. Mr. R. Muench — 1
David W. Taylor Naval Ship
Research and Development Center
Annapolis Laboratory
Annapolis, Maryland 21402

30. Mr. W. Thielbar — 1
Naval Weapons Center
China Lake, California 93555

31. CAPT Bress (Code 03) — 1
Naval Sea Systems Command
Washington, D. C. 20362

32. Mr. John Michele — 1
Oak Ridge National Laboratory
Oak Ridge, Tennessee 37830

33. Mr. Robert W. Perkins — 2
Spiral Tubing Corporation
533 John Downey Drive
New Britian, Connecticut 06051

34. Mr. Jack S. Yampolsky — 2
Senior Technical Advisor
Advanced Projects Division
General Atomic Company
Post Office Box 81608
San Diego, California 92138

35. Dr. Win Aung — 1
Division of Engineering, National Science Foundation
1800 "G" Street NW
Washington, D. C. 20550

36. Mr. John W. Ward — 1
Marine Division
Westinghouse Electric Corporation
Hendy Avenue
Sunnyvale, California 94088